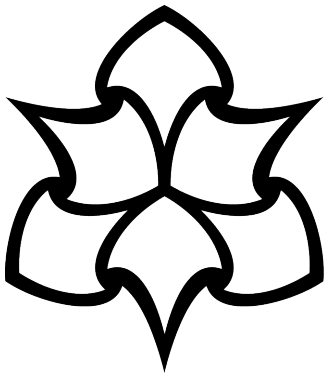

SIGNALLING MECHANISMS ASSOCIATED WITH CYCLIN-DEPENDENT KINASE 5 ACTIVITIES DURING ANGIOGENESIS

A Thesis Submitted in Partial Fulfilment of the Requirements of Manchester Metropolitan University for the Degree of Doctor of Philosophy

Kamela Ali

School of Healthcare Science

Manchester Metropolitan University

June 2017

Table of contents

List of figures

List of tables

Abstract

Stroke is one of the major causes of death and disability in developing countries. It takes place when the blood supply to a fraction of the brain is abruptly interrupted or severely reduced by, for instance, a blood clot. This is known as an ischaemic stroke. A number of studies indicate that deregulation of a set of cell cycle kinases has been implicated in neural death following an ischaemic insult and in neurodegenerative disorders. Overall the cyclin-dependent kinase 5 (Cdk5) and its two activators; the p35/p25 proteins, have been highlighted as critical players in neural survival, and potential mediators of angiogenesis. Hence, a detailed understanding of the mechanisms involving them in the pathogenesis of stroke can provide a platform for therapeutic intervention and potentially enable adoption of strategies to prevent the disease. The aim of the study was to identify key regulatory factors associated with Cdk5 signalling pathway during angiogenesis in a human brain microvascular endothelial cell line (hBMECs).

Two cell clones of hBMECs were generated by stable transfection; overexpression of wild-type human Cdk5 and CIP (Cdk5 inhibitory peptide). Cdk5 and p35 protein co-localisation were detected by Immunofluorescence analysis.

The findings suggest that the ratio of p35/p25 is altered in favour of p25 by hypoxia. It was able to cleave p35 into a p25, which reduce the migration. The overexpression of Cdk5 increased the ratios of p35/p25 under hypoxic condition. Activation of p35/Cdk5 signalling occurred at the expense of p25-Cdk5, therefore, may have a protective role against endothelial cells apoptosis in hypoxia and

positively contribute to preserving cell motility and the proper spatial and temporal control of cytoskeletal dynamics, which is essential for sprout formation (angiogenesis). Here it is shown that the protective roles of CIP are mediated through the down-regulation of HSP-70 and active caspase-3 and up-regulation of the phospho-extracellular signal-regulated kinase (p-ERK). CIP was able to protect hBMECs against apoptosis, and to allow angiogenesis to continue effectively during hypoxia. Therefore, it may be considered a potential future protector therapeutic after stroke and other brain injury.

Declaration

I hereby declare that this work has been composed by myself, and has not been accepted for any degree before and is not currently being submitted in candidature for any degree other than the degree of Doctor of Philosophy of the Manchester Metropolitan University.

KAMELA ALI

Acknowledgment

No project such as can be carried out by only one individual. I have many thanks and acknowledgement. Special thanks to almighty God who is the source and origin of all knowledge.

I must express my heartiest gratitude to the worthy and kind supervisor, Prof Mark Slevin for his dynamic supervision, constructive criticism and affectionate behaviour through this study. His wide knowledge and logical way of thinking have been of great value for me and his intensive and creative comments have helped me step by step throughout this project.

I would like to express my deep gratitude and respect to Dr Donghui Liu an excellent study adviser who helped me learn several laboratory techniques, and providing quotes for ordering laboratory materials. His outstanding attitude and vast knowledge helped me to carry on my laboratory work.

I am also forever grateful to Dr Jie Qi and Dr Alessandra Boussoti for their approachability; optimism and fortitude have been invaluable. Thank you for your practical support and insight. Their wisdom and generosity will not be forgotten.

Special thanks to Dr Ayman M. Mahmoud from Faculty of Science, Beni-Suef University, Egypt, for his support and help during my study.

I would like to extend my greatest thanks to my colleagues and to my friends Ali Shukur, Asima Farooq, Sally Merzha, Deina Alshammari, Abdulmannan Fadel, Sarah Al-dabbagh and Yasmin Zeinolabediny at the School of Healthcare Science who shared great research ideas during my time at Manchester Metropolitan

University. And many thanks to Ruth Shepherd for her kind help on proofreading of my thesis.

Finally, I acknowledge the people that mean the most to me. My special children, Mohammed, Tasneem, Isra, Ahmed and Yusra for their patience, unfailing love and support during my pursuit of PhD. Especially my late husband, Ali, may God give him mercy, for making the completion of my PhD possible, and encouraging me to continue during his illness. My sincere deepest gratitude to all my family and in-laws for their support and encouragement through this work. Special thanks to my father for his prayers and support throughout.

Dedication

Dedicated to my husband, Dr Ali Elabani, beloved mother Rahma, father in law, Gheith and youngest brother in law, Abdul-Hakeem. May God rest your souls.

Publications (Papers):

1. Bosutti A, Qi J, Pennucci R, Bolton D, Matou S, **Ali K,** Tsai L H, Krupinski J, Petcu E B, Montaner J, Al Baradie R and Slevin M. 2013. Targeting p35/Cdk5 signalling via CIP-peptide promotes angiogenesis in hypoxia. *PloS one*, *8*(9), p.e75538.
2. Liu D, Slevin M, Ashworth J, **Ali K**, Fadel M, Li C, Guo B, Kumar P, Bernabeu C, Kumar S. Overexpression of CD105 inhibits map kinase pathway activation in rat myoblasts". (Revising) Cell Biology International**,** 2017
3. Liu D, **Ali K**, Ashworth J, Li C, Guo B, Bernabeu C, Kumar S, Kumar P, Slevin M. "Overexpression of CD105 promotes protein kinase C pathway in L6E9 cells" (Manuscript is in preparation) 2017.
4. Liu D, Zhang M, Liu Y, Ahmed N, Ashworth J, Xu X, Sun Y, **Ali K**, Slevin M. "Determination of the endothelial protective effects of the bioactive components of aged garlic extracts - as a main-line preventative clinical medicine against the development of atherosclerosis and cardiovascular disease". (Manuscript is in preparation) 2017.
5. **Ali K,** Liu D, Degens H, Slevin M. "Determination of the endothelial protective effects of CDK5 overexpression on stroke". (Manuscript is in preparation) 2017.
6. Alshammari D, **Ali K**, Krupinski J, Abudawood M, Ali Aljohi, Al-Baradie R, Petcu EB, Justicia C, Planas A, Liu D, Slevin M. "Citicoline Modulates Angiogenesis and Improving Survival of Vascular/Human Brain Microvessel Endothelial Cells Under Stroke". (Manuscript is in preparation) 2017.

Conferences (Posters):

- Bosutti, A., **Ali K.,** Bolton, D., Qi, J., Pennucci, R., Matou, S., Seth L., Tsai, L.H.,Karl Peter Giese, Degens H., Kumar S., Krupinski, J., Montaner, J. and Slevin M. Modulation of p35/Cdk5 signalling rectifies defective hBMECs migration produced by *in vitro* simulation of ischaemic stroke. Physiological Society 2013.

Abbreviation List

AMPA	α-amino-3-hydroxy-5-methyl-4-isoxazolepropionic acid
APAF-1	Apoptotic Protease Activating Factor -1
APS	ammonium persulphate
ATP	Adenosine Triphosphate
BDNF	Brain-Derived Neurotrophic Factor
BSA	Bovine Serum Albumin
Ca^{2+}	Calcium
CBF	Cerebral blood flow
CDK5	Cyclin-Dependent Kinase5
CNS	Central nervous system
CT	Computerised Tomography
DAPT	N-[N-(3,5-Difluorophenacetyl)-L-alanyl]-S-phenylglycine t-butyl ester
DMSO	Dimethyl sulfoxide
DNA	Deoxyribonucleic acid
EBM-2	Endothelial cell basal medium-2
EC	Endothelial cell
EDTA	Ethylenediaminetetraacetic acid
EGTA	Ethylene glycol-bis(β-aminoethyl ether)-N,N,N',N'-tetraacetic acid
ERK1/2	phospho-Extracellular-signal regulated kinase 1/2
FBS	Foetal Bovine Serum
FGF-2	Fibroblast Growth Factor-2
HB-EGF	Heparin-binding EGF-like growth factor
hBMEC	Human Brain Microvessel endothelial cell line

HIF	Hypoxia-inducible factor
HRP	Horseradish Peroxidase
HSP	Heat Shock Protein
ICAM	Intracellular Adhesion Molecule
IGF	Insulin-like Growth Factor
IL	Interleukin
IL-RA	Interleukin receptor antagonist
LTD	long-term depression
LTP	long-termpotentiation
MAPK	Mitogen-Activated Protein Kinase
MCP-1	Monocyte Chemoattractant Protein-1.
MRI	Magnetic Resonance Imaging
mRNA	Messenger RNA
NF-H	Neurofilament heavy chain
NGF	Nerve Growth Factor
NMDA	N-Methyl-D-Aspartate
PI	Propidium Iodide
PI3K	Phosphoinositide3-Kinase
PAK1	P21- Activated Kinase
PBS	Phosphate Buffered Saline
ROS	Reactive Oxygen Species
Rpm	Round per minute
SD	Standard deviation
SDS	Sodium dodecyl sulphate
SDS-PAGE	SDS-polyacrylamide gel electrophoresis

SPM	Serum Poor Medium
TBS	Tris Buffered Saline
TBS–T	Tris Buffered Saline – Tween
TEMED	N,N,N‟,N‟ tetramethylethylenediamine
TNFα	Tumour necrosis factor α
TNFRs	Tumour necrosis death factor receptors
tPA	Tissue plasminogen activator
TUNEL	Terminal deoxynucleotidyl transferase-mediated up biotin Nick End Labelling
VEGF	Vascular endothelial growth factor

List of Units

%	Percentage
µg	Microgram
µL	Microliter
µm	Micrometre
bp	Base pair
cm	Centimetre
Da	Dalton
h	Hour
g	Gram
k	Kilo
L	Litre
M	Molar
mg	Milgram
min	Minute
ml	Millilitre
mm	Millimetre
mM	Millimolar
ng	Nanogram
°C	Degree Celsius
RPM	Revolutions per minute
Sec	Second

Chapter 1 Introduction

1.1 Stroke

Stroke is defined as a severe onset focal neurological event involving a vascular cause. It is the second highest cause of mortality around the world accounting for 9% of deaths. The current 5.7 million stroke deaths are expected to increase to 7.8 million by 2030 with 87% of all stroke mortalities occurring in low- and middle-income countries. Stroke mortality accounts for almost 50% of the total disease burden over the past ten years. The 30% increase in the number of patients suffering a first-ever stroke in the UK between 1983 and 2023 may be related to the ageing population and changes in cardiovascular disease risk factor profiles (Bornstein, 2009). This will increase the demand for specialised stroke medical facilities and costs to the healthcare authorities. Clinical and biomedical research can improve survival after stroke and decrease disabilities through medical interventions (Williams et al., 2010). However, patients could survive with a reduced quality of life depending on the severity of their condition. There are a number of risk factors that are responsible for initiating the first stroke. These factors are categorised according to whether they are: (1) unmodifiable; (2) well recorded and modifiable, and (3) less well recorded modifiable. Unmodifiable risk factors include age, gender, family history, low birth weight and ethnicity. Modifiable risk factors include: cardiovascular disease, coronary heart disease, heart failure, peripheral arterial disease, hypertension, tobacco smoking, diabetes mellitus, asymptomatic carotid stenosis, atrial fibrillation, sickle cell anaemia, dyslipidaemia, high total cholesterol, low high-density lipoprotein cholesterol, dietary factors (sodium intake >2300 mg, potassium intake <4,700 mg), obesity, lack of physical exercise and postmenopausal hormone

replacement therapy. Less well recorded modifiable risk factors include: metabolic syndrome, alcohol abuse, hyperhomocysteinaemia, drug abuse, hypercoagulability, oral contraceptive use, inflammatory processes, migraine, high lipoprotein (a), high lipoprotein-associated phospholipase A2 and sleep apnoea (Johannes Binder, 2012). Hypertension characterised by an increase in blood pressure (BP) above 115/75 mmHg, is regarded as one of the most important risk factors leading to stroke with a higher prevalence in women at an older age, which accounts for 60% of all stroke events (Gorgui et al., 2014). This is possibly due to women having a longer life expectancy than men do. Diabetes is another major risk factor accounting for 10-20% of all strokes (Sun et al., 2017), in particular, ischaemic strokes. The disease is part of a group of metabolic disorders characterised by hyperglycaemia. The abnormalities in insulin secretion, insulin action, or both that underline diabetes, leads to chronic hyperglycaemia, which is associated with long-term damage, dysfunction, and failure of various organs – particularly the eyes, kidneys, nerves, heart and blood vessels. Diabetes is also associated with hypertension and high blood cholesterol levels, increasing the risk of vascular disease. There are increasing cases of obesity and type II diabetes worldwide and hence the increasing incidence of strokes.

The cause and location of the stroke determine its type, for instance, haemorrhagic stroke, ischaemic stroke, lacunar stroke, embolic stroke, young stroke, thrombotic stroke, spinal cord stroke, venous stroke, brain-stem stroke and cerebellar stroke (Ackerley et al., 2003). There are two main types of stroke (Figure1.1): haemorrhagic and ischaemic. Haemorrhagic stroke is characterised by a ruptured

vessel inside the skull leading to bleeding into the brain or the surrounding fluid. The occlusion of the blood supply to the brain is termed ischaemia stroke, where the insufficient blood supply to a region of the brain causes abnormal functioning of that brain tissue. Four out of every five cerebral strokes are ischaemic (Caplan, 2010).The cause of ischaemic stroke is subdivided into three categories: thrombosis, embolism and decreased systemic perfusion. Thrombosis is defined as a process where an obstruction of the blood supply occurs due to a localised occlusion within one or multiple blood vessels. The lumen of the vessel is narrowed or occluded by a change in the vessel wall or by the formation of a clot. Embolism involves the formation of material originating from the aorta, carotid, and vertebral arteries or, from systemic veins in a different location within the vascular system blocking the lumen of an artery and preventing blood flow. The blockage of the artery is not caused by a localised process originating within the blocked artery, and hence is transient and may continue for hours or days before moving distally. The final category decreased perfusion, can arise from low systemic perfusion pressure due to cardiac pump failure (e.g. myocardial infarction or arrhythmia, and systemic hypotension) and as a result of blood loss or hypovolaemia, restricting the blood flow to the brain tissue (Caplan, 2009).

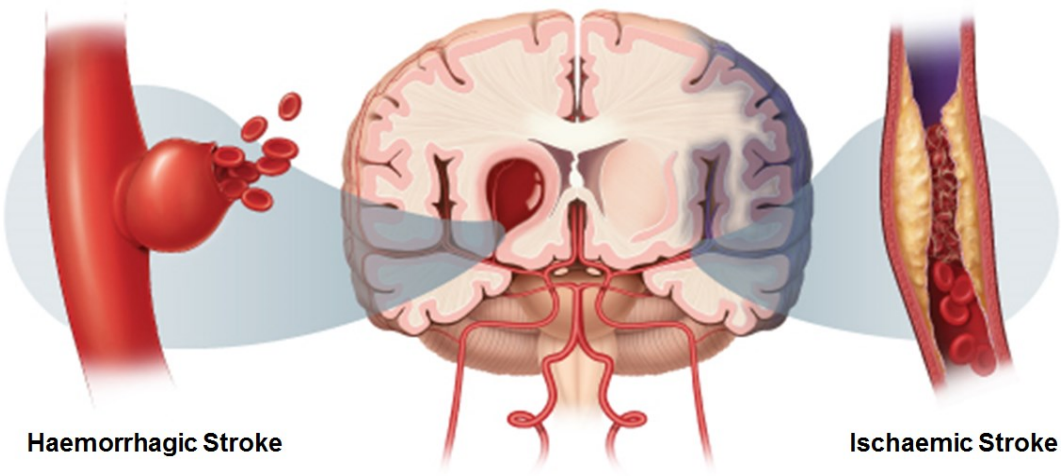

Figure 1-1 A representation of the two major types of stroke

Adapted from http://fescenter.org/clinical-programs/current-clinical-trials/stroke-programs.

Intracerebral haemorrhage caused by unmanaged high blood pressure and cerebral amyloid angiopathy is characterised by a spontaneous rupture of small vessels, which accounts for approximately 80% of haemorrhagic strokes. In the elderly, cerebral amyloid angiopathy results from damage caused by the brain deposition of a molecule known as damage β-amyloid protein in the small and medium-sized blood vessels (Brunner et al., 2010). Subarachnoid haemorrhage is caused by a weakening of the arterial wall and is characterised by a rupture in an intracranial aneurysm, which accounts for about 20% of haemorrhagic strokes. Headache is a more common symptom of haemorrhagic stroke compared to ischaemic stroke. Other symptoms of haemorrhagic stroke include early loss of consciousness, vomiting and severely elevated blood pressure (Popp, 2011).

Ischaemic stroke and haemorrhagic stroke have similar symptoms, and it may be difficult to distinguish between the two types. It is also difficult to distinguish between hypoglycaemia, stroke because hypoglycaemia can produce focal neurological symptoms that resemble those of stroke. However, hypoglycaemia should be ruled out in all cases of suspected stroke, especially in known diabetics. Brain tumours and other intracranial masses (such as subdural haematomas) and stroke as hypoglycaemia can cause transient neurological deficits and other stroke-like symptoms. The location of the stroke can predict the pattern of associated symptoms. The ischaemic stroke has been associated with the absence of function such as loss of a single eye vision in an entire hemifield, numbness in part of the body, weakness or paralysis on one side of the body. Intracerebral haemorrhage has been shown to be associated with more severe neurological dysfunction, including weakness, numbness, vision loss, diplopia, dysarthria, gait disorder, vertigo, aphasia, or unconsciousness. The symptoms become worse when a small bleed (2 cm in diameter) increases in size in the first few hours of stroke (Alway and Cole, 2009).

The diagnosis of acute stroke includes history taking, clinical examination, acute brain and cardiovascular imaging and basic laboratory tests. Brain imaging, Computerised tomographic (CT) or Magnetic resonance imaging (MRI) are considered reliable techniques to differentiate between ischaemic stroke and intracerebral haemorrhage. CT can be utilised to detect early abnormalities following a large ischaemic stroke involving the cortex or basal ganglia within 1-3 hours, whereas longer periods (12-24 hours) are required to visualise small and brainstem

strokes. MRI has a higher resolution, faster appearance of abnormalities and improved brain-stern imaging over CT for the detection of acute stroke, while perfusion-CT has been used for early ischaemic attack and reliably differentiates between reversible and irreversible ischaemia (Fisher, 2009). The management of acute stroke involves rehabilitation, avoidance of adverse outcomes in the sub-acute setting and administration of intravenous tissue plasminogen activator (tPA). The limited treatment window (3 hours) of tPA requires early patient arrival and early detection (Goldstein, 2011).

1.2 Pathophysiology of Acute Ischaemic Stroke

Ischaemic stroke is a heterogeneous disorder caused by one of two pathogenic mechanisms: 1) atherosclerotic disease of large or small vessels and 2) embolism. Different areas of the brain may have varying susceptibilities to ischaemic injury (Aronowski et al., 1999). Atherosclerosis in small vessels (lacunar infarct) accounts for up to 25% of all ischaemic strokes (Shi and Wardlaw, 2016). Cerebral ischaemia or infarction is characterised by an impaired cerebral blood flow (CBF) resulting from an obstruction of the blood flow in a main cerebral vessel (often the middle cerebral artery). leading to the local deprivation of both oxygen and glucose is leads to a central core of dead and irreversibly damaged neurons within minutes of ischaemic onset (Kaufmann et al., 1999). The volume of the brain infarct is determined by the area of the ischaemic penumbra. This is a region of viable ischaemic tissue perfused with over 20-25% of regular blood flow to maintain function and morphologic integrity

(10-12ml/100g/min) around the infarcted core, where electrical activity is not lost (Olsen et al., 1983; Heiss, 2000). In contrast, the core is hypoperfused at less than 18-20ml/100g/min and is at risk of dying within several hours (Gusev and Skvortsova, 2003a). The normal brain tissue that immediately surrounds the ischaemic tissue is less likely to die, as it is perfused at only slightly below the minimal normal rate of 60ml/100g/min.

While the ischaemic core suffers irreversible loss of ion homeostasis, the insult in the penumbra is either milder or of shorter duration, because of sub-optimal blood flow in arterioles, capillaries and collateral vessels. These neurones in the penumbra are unable to maintain normal function but can be saved if reperfusion is achieved in time. However, if the blood flow drops below the critical level (10-15ml/100g/min), they do not return to normal, leading to the cessation of their activity, primary neuronal death and expansion of the infarct zone. In the ischaemic penumbra (continued ischaemia), the activation of several death pathways leads to secondary neuronal death and tissue necrosis promoting the stabilisation of the clinical deficits. Thus maintaining a minimal blood flow through e.g. thrombolytic treatment to the infarcted core and penumbra can preserve the cellular energy haemostasis and decrease the final infarct volume (Belayev et al., 2012).

Brain ischaemia involves changes in signalling, signal transduction, metabolism, and gene regulation/expression at a cellular level. Cerebral ischaemia involves the obstruction of cerebral blood flow regularly resulting in a reduction in ATP availability, rapid failure of membrane ionic pumps and loss of homeostasis, the

release of excitotoxic neurotransmitters (glutamate), and the consequent neuronal calcium ion excess that activates a series of highly detrimental enzymatic cascades within 1 or 2 hours. The formation of free radicals such as Nitric oxide (NO) can cause cellular injury through the degeneration of cytoskeletal proteins, loss of cellular membrane integrity and deoxyribonucleic acid (DNA) degradation. These events lead to apoptotic or necrotic death. Brain injury leads to the upregulation of neurodestructive, and pro-inflammatory (I-1B, TNFα) gene expression. This leads to excitotoxicity, peri-infarct depolarisation, inflammation and apoptosis causing damage within the ischaemic penumbra, which plays a critical role in the pathophysiology of stroke (Dirnagl et al., 1999) and ischaemic neuronal death (Gillardon et al., 1999). A more in-depth understanding of the cellular and molecular mechanisms that promote recovery or prevent acute stroke is required to prevent delayed ischaemic neuronal death. One way is to enhance the activity of endogenous neuroprotective mechanisms to inhibit toxic pathways, inflammation and apoptosis. It is the balance between these pathways that determines the fate of the tissue at risk.

1.3 Excitotoxicity

Glutamate plays a vital role in a) the processing of events occurring in regular sequence and b) neuronal plasticity. It is released from presynaptic terminals to allow Na^+ and Ca^{2+} influx through N-methyl-D-Aspartate (NMDA), α-amino-3-hydroxy-5-methyl-4-isoxazole propionic acid (AMPA) and/or kainate receptors

leading to membrane depolarisation; an increased and/or additional activation of receptors due to uncontrolled release of glutamate in ischaemic areas results in neuronal death (glutamate excitotoxicity). The glutamate-calcium cascade is initiated by the interaction of glutamate with the NMDA receptor (permeable to Ca^{2+}, Na^{+}, K^{+} and H^{+}), which induces a calcium-mediated focal hypoxic-ischaemic necrotic lesion (Gwag et al., 2002) and the formation of brain infarction (Gusev and Skvortsova, 2003b).The activation of NMDA receptors (Koh et al., 1990) and calcium influx can cause neuronal death after focal cerebral ischaemia that is accompanied by temporary (30-60 min) elevation of extracellular glutamate (Liu et al., 2009), while Na^{+} influx contributes to the swelling of neuronal cell bodies (Zhang, 2016). Since an energy-dependent mechanism is responsible for the export of Ca^{2+} from the cytoplasm (100nM, 1/10,000 of that in the extracellular matrix) to the extracellular compartment in neurons (Wright, 2013), energy failure in the ischaemic brain during hypoxia, results in passive efflux of K^{+} from cells, enhancing Ca^{2+} entry and its release into neurons (Gusev and Skvortsova, 2003b). The resulting elevated levels of intracellular cytoplasmic Ca^{2+} lead to oxidative stress (Leker and Shohami, 2002) and glutamate excitotoxicity of biochemical processes resulting in further injury (Budd, 1998) (Figure 1.2). DNA, lipids and protein damage can be secondary to Ca^{2+} dependent effector protein activity due to prolonged elevation of Ca^{2+} levels. These include; endonucleases, phospholipases, lipases, protein kinases and proteases that may cause damage.

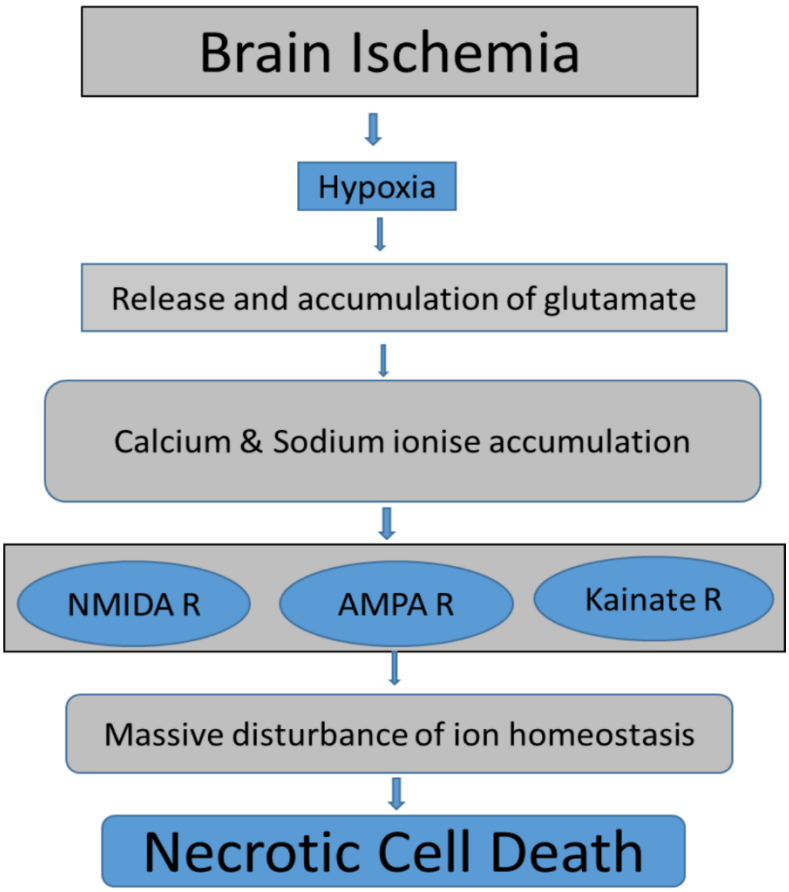

Figure 1-2 Schematic model of cell death caused by excitotoxicity

The schematic flow chart demonstrates the excitotoxic cell death scheme in ischemic brain injury and basic mechanisms of glutamate-calcium cascade through which excitotoxicity results in necrotic cell death after ischemic stroke.

1.4 Inflammation

The inflammatory response in cerebral ischaemia is characterised by the activation and release of cytokines, chemokines, endothelial-leukocyte adhesion molecules and proteolytic enzymes, exacerbating tissue damage for several days after the

onset of symptoms (Shukla et al., 2017). Following acute focal ischaemia, pro-inflammatory cytokines such as tumour necrosis factor α (TNFα) and interleukins IL-6 and IL-1 (Kim et al., 2014) are produced by astrocytes, microglia, leukocytes and endothelial cells (Lakhan et al., 2009) and lead to a local inflammation in the brain lesion and subsequently inflammation causes more damage and increases the infarct volume (Gusev and Skvortsova, 2003b). Peripherally cytokines derived from phagocytes, T-lymphocytes, natural killer cells and polymorphonuclear leukocytes can exacerbate central nervous system inflammation and gliosis (Barber et al., 2003). Shortly after an ischaemic attack, inflammatory intermediaries are upregulated in the presence of damaged tissue. Due to their role in brain tissue damage, pro-inflammatory cytokines expressed within the first 2 hours after the onset of ischaemia remain significantly elevated for several days after stroke onset (Jin et al., 2010). This presence of proinflammatory cytokines during an acute stroke has deleterious effects on the outcome of cerebral ischaemia; including cerebral infarction (Fassbender et al., 1994; Tarkowski et al., 1995; Vila et al., 2000) and increased cardiovascular risk (Zhou et al., 2013). For instance; brain ischaemia has been suggested to be associated with the expression of a number of inflammatory cytokines (IL-1 and TNFα) and chemokines [IL-8, monocyte chemoattractant protein-1 (MCP-1), β-chemokine Regulated upon Activation, Normal T-cell Expressed and Secreted (RANTES) and interferon-γ-inducible Protein, and up-regulation of adhesion molecules [intercellular adhesion molecule-1 (CAMI) selectins], which maintain leukocyte recruitment to the vascular endothelium (Feuerstein et al., 1998; Ramesh et al., 2013). The expression of chemokines is

upregulated in the ischaemic territory. These chemokines aid the infiltration of inflammatory cytokines into the ischaemic sites (Mirabelli-Badenier et al., 2011). Cytokines such as TNFα and IL-1β have involved in the propagation and maintenance of the brain inflammatory response to injury acting as a chemoattractant to leukocytes. Thus, the chronic exposure of damaged brain tissue to TNFα and IL-1β may promote neuronal survival. Given both potential deleterious and beneficial effect of elevated cytokines and associated inflammation, the net effect of inflammation during stroke still needs to be established.

Adhesion molecules such as CD11/CD18 integrins, ICAM1ELAM1, P-selectin and tissue matrix metalloproteinases (MMPs) have been shown to be expressed early after the insult (Kim et al., 2014) and act to facilitate penetration of leukocytes through the blood-brain barrier (Pantoni et al., 1998; Del Zoppo et al., 2000). Thus, the suppression of postischaemic inflammation through antibodies against adhesion molecules neutrophil depletants, inhibitors of proinflammatory cytokines, and anti-inflammatory cytokines (Clark and Zivin, 1997; Spera et al., 1998; Dietrich et al., 1999; Ooboshi et al., 2005) may provide therapeutic strategies for acute stroke patients. In response to continued proinflammatory cytokine production, lymphocytes and monocytes/macrophages act to secrete anti-inflammatory cytokines such as IL-10 and IL- 4 in a feedback loop to block and inhibit inflammatory cytokine production (Tedgui and Mallat, 2001). These anti-inflammatory cytokines may have neuroprotective effects in reducing the infarct volume following the ischaemic attack (Bonaventura et al., 2016) (Figure 1.3).

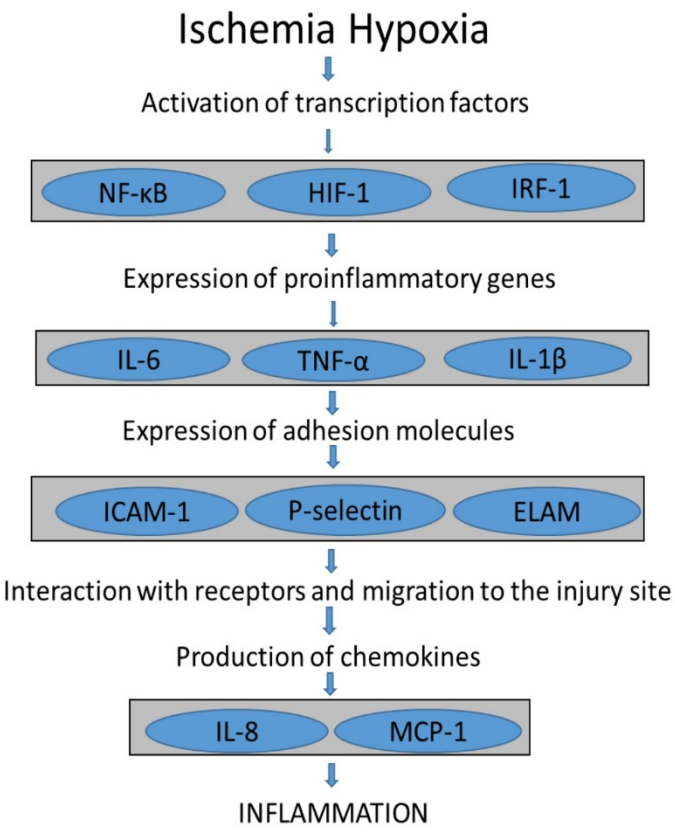

Figure 1-3 Schematic diagram illuminate the cytokines interacted during inflammation

Inflammatory pathways associated with acute ischemic stroke, which stimulates expression of nuclear transcription factors. Subsequent synthesis of pro-inflammatory cytokines and chemokines, together with adhesion molecules expression, cause migration of leukocytes and lymphocytes to the infarcted area resulting in inflammation.

1.5 Apoptosis

Apoptosis or programmed cell death is an energy-dependent biochemical mechanism through which cell death occurs. It is a highly cell-specific process, and it may be induced in damaged cells where the damage is beyond repair (Rastogi and Sinha, 2010). Hence, it is involved in normal cell turnover, proper development and functioning of the defence system, hormone-dependent atrophy, embryonic development and cell death caused by chemicals. Disruption in the process of apoptosis may lead to diseases such as ischaemic damage (Figure1. 4), autoimmune disorders and various types of cancer (Elmore, 2007).In apoptosis, the extrinsic pathway is mediated by a sub-group of tumour necrosis death factor receptors (TNFRs) a superfamily that includes TNFR, Fas and TRAIL (Portt et al., 2011). Upon activation via death signals, the latter receptors form the death-inducing signalling complex (DISC) activate caspase 8, which in turn activates caspase 3. The stimulation of death receptors can also activate the intrinsic apoptotic pathway, controlled by members of the BCL-2 family. This occurs when caspase 8 cleaves BID to t-BID, that then interacts with BAX within the mitochondria leading to the leakage of cytochrome c and via the formation of the apoptosome to activation of caspase 9 (Chiong et al., 2011). Both extrinsic and intrinsic pathways, resulting in the same outcome; the activation of a cascade of proteolytic enzymes, members of the caspase family (Sprick and Walczak, 2004).

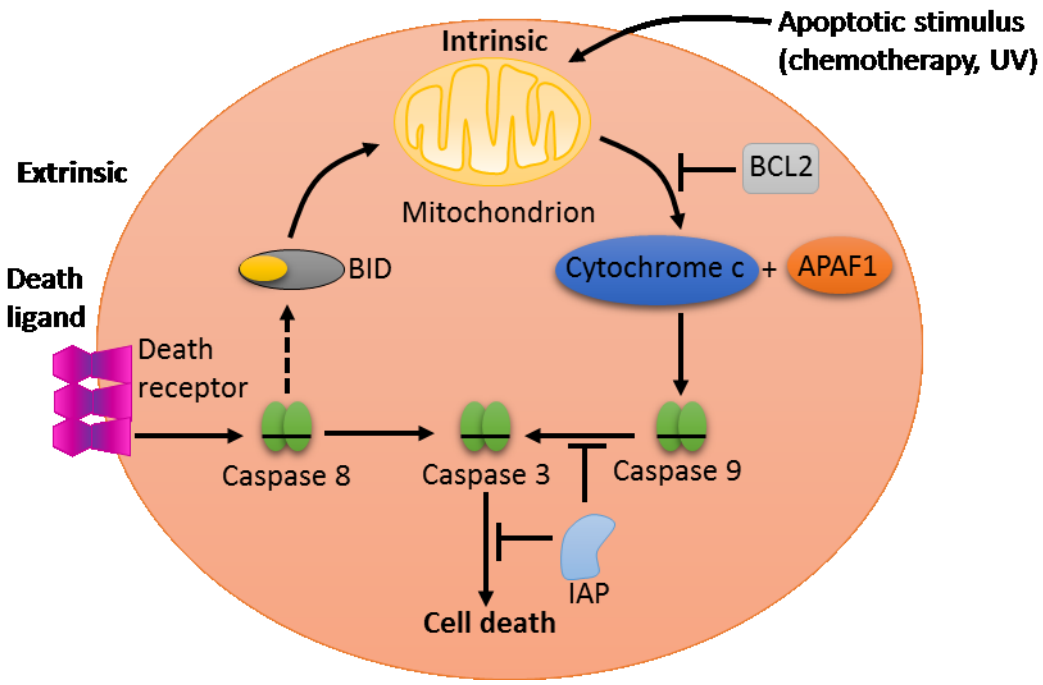

Figure 1-4 A representation of the two major apoptotic pathways; the extrinsic and the intrinsic pathway

The death-receptors activate the extrinsic pathway that acts through caspase 8 or the mitochondrial intrinsic pathway. The intrinsic pathway activates caspase-activating complex (which includes cytochrome c and apoptosis-activating factor 1, APAF1) that acts on caspase 9, which in turn activates caspase 3. These pathways are regulated by BCL2 and the inhibitor of apoptosis IAP protein families, respectively. BCL2 proteins are believed to regulate the mitochondrial permeability promoting BID and cytochrome c release (Andersen et al., 2005).

1.6 Apoptosis after Stroke

Ischaemia-induced programmed cell death was suggested to occur in neurones (D'amelio et al., 2010), vascular endothelial cells and non-neuronal cells that constitute the ischaemic core. The restricted blood flow after cerebral ischaemia is a key factor leading to the disruption of the blood-brain barrier integrity, the

regulation of arterial tone and apoptosis (Hu et al., 2017). The mechanism of apoptosis is thought to be mediated via caspase-3 and several other caspase family members, which have been reported to be activated in astrocytes and microglia after middle cerebral artery occlusion (Chen et al., 1997; Krupinski et al., 2000). Following cerebral ischaemia, the caspases cause the breakage of DNA strands within the border zone of astrocytes in infarcted tissue (Chen et al., 2011) leading to apoptosis. For instance, evidence suggests that the mechanism of apoptosis in cerebral endothelial cells of basilar arteries after subarachnoid haemorrhage involves TNFR1 and the caspase-8 and caspase-3 pathways. This was mainly colocalised DNA fragmentation and either caspase-3, caspase-8 or TNFR1 (Zhou et al., 2004). Another mechanism of apoptotic death after stroke may involve the generation of ROS e.g. due to blood reperfusion after stroke (Shirley et al., 2014; Kalogeris et al., 2014). Reactive oxygen species (ROS) may react with vascular endothelium-derived nitric oxide to form the highly toxic peroxynitrite radical initiating the process of apoptosis in vascular cells after ischaemic stroke (Rodríguez-Yáñez et al., 2006). One approach to improving neuron survival after stroke may involve the use of SMND-309, a novel neuroprotective metabolite of salvianolic acid, which can prevent neuronal cell death via the activation of the PI3K/Akt/CREB-signalling pathway (Wang et al., 2016).

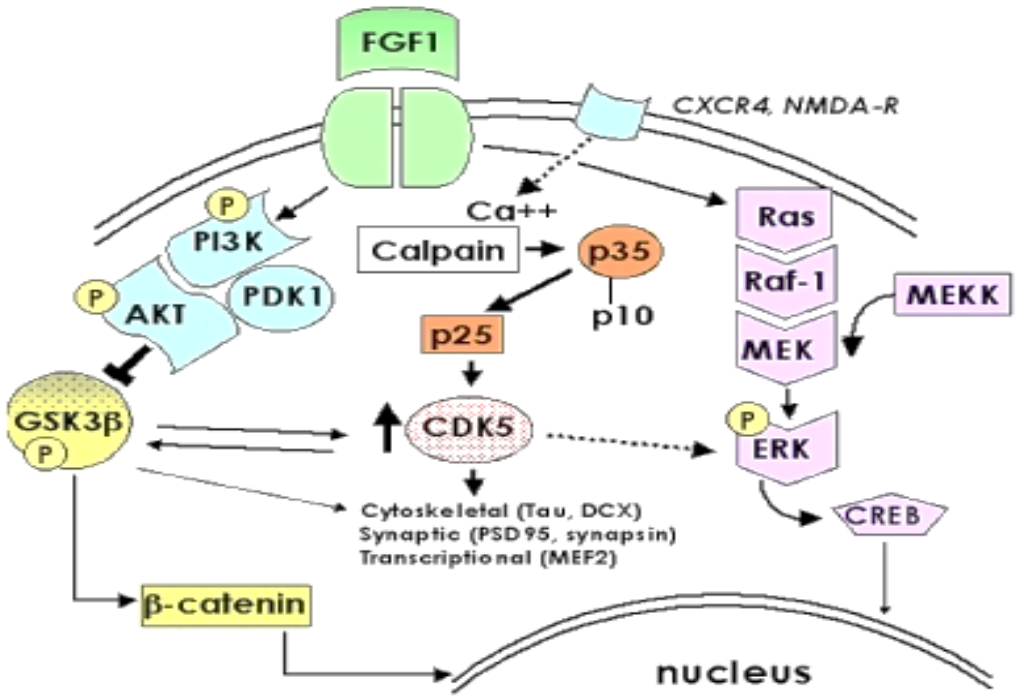

Figure 1-5 A schematic diagram represents the CDK5 signalling pathways

Schematic diagram showing the role of PI3K signalling pathways via receptor interactions, resulting in the downstream disruption of processes involved in regulating CDK5 integrity. PI3K is upstream of cdk5/p35, and its activation can lead to an increase in p35 protein levels, and some other factors might ameliorate these effects by antagonising the activation of PI3K by cellular neurotoxins. PI3K and CDK5 share several downstream targets (e.g. Tau), and simultaneous activation of both of these pathways may exacerbate the neurotoxic effects of proteins involved in stroke. Adapted from Crews et al (Crews et al., 2009).

1.7 Neuroprotection

Some mediators induced in the peri-lesional zones contribute to cellular death, while others such as heat shock proteins (HSPs), anti-inflammatory cytokines and endogenous anti-oxidants may counteract ischaemic damage and improve neuronal repair. The targeting of these survival-promoting mechanisms could be used in the

development of new therapeutic strategies. The expression or upregulation of HSPs such as HSP70, HSP72 and HSP27 can be triggered by various harmful stresses including ischaemia within 1-2 hours and then downregulated after 1-2 days (Sharp et al., 2013). They can act to prevent the aggregation of denatured proteins by allowing their refolding to the correct tertiary structures preventing protein denaturation (Leker and Shohami, 2002). Studies have indicated that anti-inflammatory cytokines, such as IL-1 receptor antagonist (IL-1 ra) and IL-10, may protect against ischaemic damage by inhibiting the production of pro-inflammatory cytokines (Kim et al., 2014; Wang et al., 2015). Neuroprotective growth factors increase after 1-3 hours after stroke, with a peak at 12 hours, and complete downregulation by 2-3 days (Chodobski et al., 2011). They induce signal transduction pathways leading to multiple transcription factors of genes involved in neuronal cell survival and proliferation.

A number of growth factors such as Nerve growth factor (NGF), Brain-derived neurotrophic factor (BDNF), fibroblast growth factor (FGF) and Transforming growth factor (TGF) are induced early after brain lesions. It has been suggested that these have a protective role in preventing apoptotic death (Leker and Shohami, 2002). They interfere with the apoptotic pathways through the PI3K/Akt, Ras/Mitogen-activated protein kinases (MAPKs), or both (Mendoza et al., 2011). The activation of glutamate receptors leads to the production and release of BDNF, which signals through the PI3K/Akt or Ras/MAPK pathway. PI3K activates the serine-threonine kinase Akt, which is translocated to the nucleus, where it phosphorylates to inactivate its target. Neurotrophins and other growth factors such as PI3K/Akt-

activated kinases promote cell survival by phosphorylating and inactivating the pro-apoptotic factor BAD via the Ras MAPK signalling pathway (Morrison et al., 2003).

1.8 Angiogenesis

Angiogenesis or neovascularisation is the process of generation of new blood vessels from a pre-existent vascular system. Revascularisation and reperfusion events can determine tissue survival and patient recovery after stroke. Angiogenesis plays a key role in allowing neuronal reorganisation and survival after stroke (Slevin et al., 2006). Angiogenesis involves the new vessel formation from endothelial cell (EC) sprouts, emanating from pre-existing vessels using angiogenic and anti-angiogenic factors that act to drive the recruitment, migration, proliferation and differentiation of ECs (Munoz-Chapuli et al., 2004). Angiogenesis is controlled spatially and temporally by focal adhesions and activation of cytoskeletal organisers, which regulate cellular mechanical forces and plasticity during migration, sprouting and cell differentiation (Avraham et al., 2003). During pathological processes, angiogenesis aid tumour growth, metastasis, inflammation and ocular disease (Mehta and Dhalla, 2013). The process of angiogenesis is initiated by endothelial cells, which line all blood vessels and constitute virtually the entirety of capillaries (Auerbach et al., 2003). Endothelial cells initially proliferate, selectively break down the basement membrane and adjacent extracellular matrix, migrate to the site and begin tube formation. Following tube formation, endothelial cells go through tissue-specific alterations to produce functionally distinct vessels (Figure 1.6).

Angiogenesis can occur at the embryonic level, where endothelial cell precursors (angioblasts) differentiate and associate to form primitive vessels in a process called vasculogenesis (Hoeben et al., 2004). Vasculogenesis is the *de novo* formation of a vascular network during embryonic development and growth. Angiogenesis or arteriogenesis can also occur in pre-existing vascular networks, where it is involved in the remodelling of pre-existing arterial vessels to form arteries. During arteriogenesis, ECs respond to angiogenic stimuli such as chemokines or growth factors, and increases in the diameter of vessels are mediated by the increased stress that is induced by elevated pressure rates in arteries, leading to thicker arterial walls. The balance between the activating and inhibiting signals of angiogenesis including cytokines, hormones, endothelial cell migration, circulating progenitor cells and destabilisation of the vessel wall, the basal lamina, the interstitial matrix, and chemical signals from cancer cells, regulate the latter process (Multhoff et al., 2014).

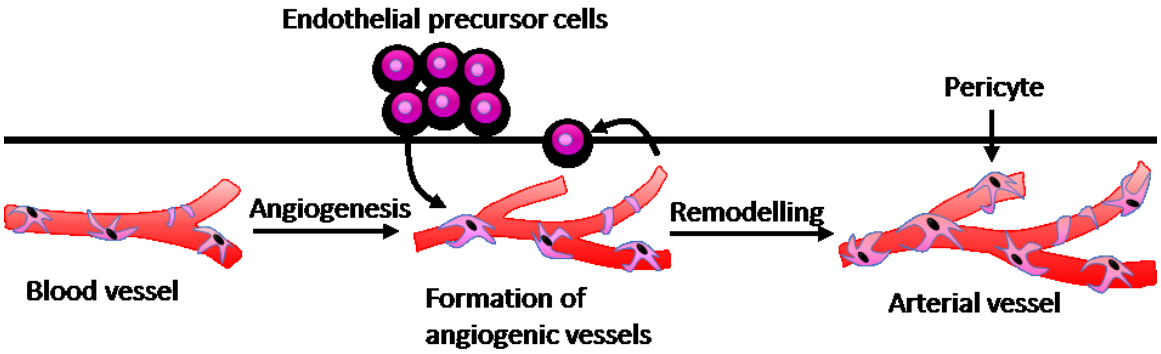

Figure 1-6 The formation of the arterial network

Angiogenesis by pericytes and vascular smooth muscle cells (Cao, 2010).

During ischaemia, angiogenic factors, such as FGF and VEGF, (Losordo and Dimmeler, 2004) are upregulated are mobilised to induce vascular growth. These factors act on endothelial cells to stimulate proliferation, migration and tube formation and make endothelial cells less sensitive to the induction of apoptosis. (Mehta and Dhalla, 2013). Angiogenesis can also occur in response to ischaemia in non-CNS tissues. A number of disorders can activate endogenous angiogenesis: including myocardial infarction and limb, hence, drugs that enhance angiogenesis can reduce injury in ischaemia. The regulatory mechanisms in the brain that trigger angiogenesis may involve hypoxia-inducible factor (HIF) pathways.

Even though the VEGF-induced angiogenesis results in vessels that are haemorrhagic, aggravating inflammatory responses in the recovering area surrounding an ischaemic event (Baeten and Akassoglou, 2011; Obermeier et al., 2013). The formation of these new blood vessels in areas surrounding the stroke site has been shown to be associated with longer survival in stroke patients, suggesting the benefits of angiogenesis for the ischaemic brain.

1.8.1 Mechanisms of Angiogenesis after Stroke

Angiogenesis is described as the growth of new blood vessels and as a key occurs during both physiological and pathological conditions (Carmeliet et al., 2001; Collen et al., 2001; Conway et al., 2001). Angiogenesis is vital for the development of new microvessels after stroke (Slevin and Krupinski, 2009). In the acute phase after stroke, thrombolytic reperfusion with recombinant tissue plasminogen activator is used in fewer than 5% of ischaemic stroke patients worldwide. Treatments involving

rehabilitation contribute in small part to recovering chronic ischaemia patients (Shuaib and Hussain, 2008). Mechanisms that promote neurogenesis and angiogenesis may provide a novel target for brain repair (Greenberg and Jin, 2005; Zhang et al., 2005; Chopp et al., 2008). Neurovascular remodelling is a key component in strokes. The collaboration between growth factors, adhesion molecule modifiers and cellular therapies may provide the optimal approach for promoting angiogenesis in the brain (Ma et al., 2012).

1.8.2 Cdk5

Cyclin-dependent kinase 5 (Cdk5) is a proline-directed serine/threonine kinase that is highly expressed in neuronal cells in the central nervous system (Kanungo et al., 2009). Unlike other Cdks, Cdk5 is not active in cell cycle regulation but is involved in a wide range of neuronal functions, including nervous system development, neuronal differentiation and survival (Chappell et al., 2011; Chillakuri et al., 2012). Under physiological conditions, Cdk5 activity is primarily restricted to postmitotic neurons and involved in the modulation of signalling pathways that control neurite outgrowth, neuronal cell adhesion, neuronal migration (Contreras-Vallejos et al., 2012), neural cytoskeletal organisation and synaptic activity and neuronal survival (Liebl et al., 2010; Chappell et al., 2011; Chillakuri et al., 2012; Yin et al., 2012). In instances where Cdk5 is degraded, it leads to neuron cell death under normal as well as pathological conditions (Ikeda et al., 2000; Rajdev et al., 2000; Glading et al., 2002; Potthoff et al., 2007; Kanungo et al., 2009) either directly or in an indirect

manner. On the other hand, in the presence of various neurotoxic insults, including brain ischemia and oxidative stress, Cdk5 is hyperactivated with potentially fatal consequences in respect to neuron cells (Ikeda et al., 2000; Rajdev et al., 2000; Glading et al., 2002; Liebl et al., 2010) emphasising that appropriate control of Cdk5 activity is crucial for normal cellular homeostasis (Kanungo et al., 2009). Evidence demonstrates that a crucial determinant of Cdk5 activation is the protein-protein interactions with its two regulatory partners p35 and p25 (Kanungo et al., 2009). The increase in intracellular calcium in a neuronal cell undergoing apoptosis (due to physical pressure and/or lack of blood supply) induces the production and release of calpain to the surrounding tissue (Walker and Tesco, 2013). The activation of calpain was demonstrated to increase the cleavage of p35 into p25 peptide in the endothelial cells of the ruptured blood vessel. The increase in the p25/p35 ratio was suggested to lead to the hyperactivation of Cdk5 (Glading et al., 2002; Liebl et al., 2010). This may play a role in the process of neo-blood vessel generation at a later stage. Conversely, an inhibition of p35 cleavage can confer neuron protection (Zhang et al., 2012), thus, further demonstrating the role of p25 as a marker for neuronal damage (Figure 1.7).

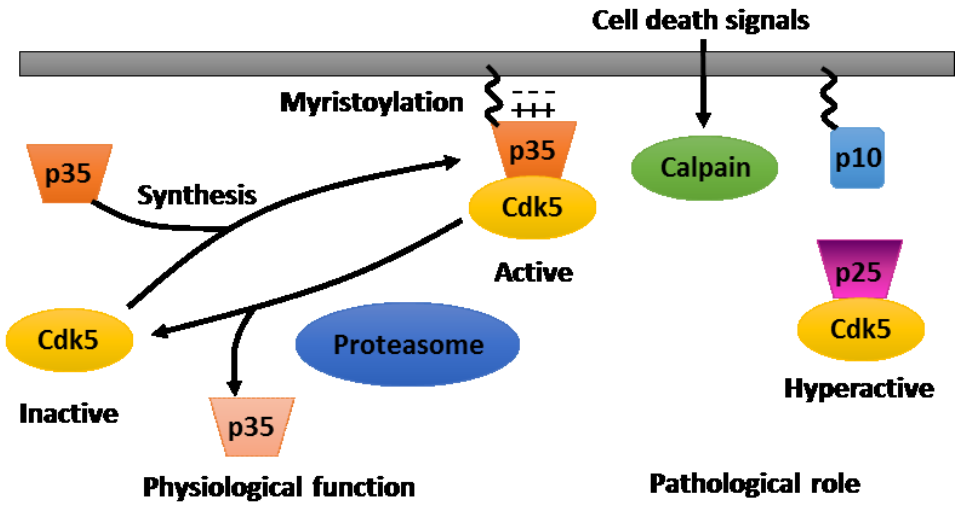

Figure 1-7 Activation mechanism of Cdk5

Cdk5 possesses an inactive catalytic subunit, which can become activated by the p35 Cdk5 activator. Upon activation, Cdk5 is recruited to membranes via p35 association with the myristoylation of its N-terminal region. The p35 protein has a short life span due to its susceptibility to proteasomal degradation. Under conditions of neuronal stress or death, calpain is activated, where it cleaves p35 into a p25 C-terminal fragment. p25 has a longer half-life, and it acts via the phosphorylation of membrane proteins making cdk5 hyperactive. p10 (a cleaved product of p35) is regarded as a Cdk5-specific inhibitor (Kimura et al., 2014).

Because of its philological activity, Cdk5 may be a potential drug target to treat brain injury. The currently available Cdk5 inhibitors have a poor selectivity and specificity as they inhibit off-target Cdks with equal or higher potency causing serious side effects. Developing Cdk5-specific inhibitors such as p10 (the cleaved product of p35), which selectively abrogate the interaction of Cdk5 with p25, but not with p35, may prevent neurotoxicity and increase the likelihood of neural survival (Zhang et al., 2012). Likewise, it has been shown that Cdk5 inhibitory peptide (CIP), a 125 amino acid fragment of p25 (Zheng et al., 2002), is effective in inhibiting the

hyperactivation of Cdk5–p25 *in vivo* (Sundaram et al., 2013) resulting in a subsequent reduction in the neurodegenerative pathologies caused by deregulation of Cdk5-p25 without compromising normal neurodevelopment.

1.8.3 p35

p35 is regarded as a Cdk5 activator that forms a tertiary structure that is similar to the cyclin-box fold domain, although the primary sequence of p35 is distinct from that of cyclins (Liu et al., 2017). The Cdk5-p35 complex has a ternary structure similar to the complex between Cdk2 and cyclin A (Cdk2–cyclin-A) (Tarricone et al., 2001). p35 is a membrane-anchored protein containing an N-terminal domain encompassing the p10 component and a C-terminal domain containing p25 with a short half-life ($t_{1/2}$=20-30 minutes). The p25 domain is responsible for binding Cdk5 leading to its activation, while the p10 domain contains the myristoylated region that is used to guide cdk5 to the plasma membrane. The p10 domain also contains a signal for p35 degradation through the ubiquitin-proteosome pathway. p35 is rapidly degraded in neurons bearing Cdk5 activity (Wei et al., 2005). The active form of Cdk5 also autoinhibits its activity through p35 phosphorylation specifically at amino acid residues Ser8 and Thr138 (hereafter S8 and T138, respectively). The phosphorylation events of p35 are differentially regulated and have different consequences (Kamei et al., 2007). The phosphorylation level of S8 is constant during development, whereas T138 phosphorylation is highest in the foetal brain but not so in the adult brain. Since both sites are phosphorylated by Cdk5, the

differential phosphorylation levels are believed to be due to dephosphorylation of T138 in the adult brain by protein phosphatase 1 (PP1) or protein phosphatase 2A (PP2A) (Kamei et al., 2007).

1.8.4 P25

p25, the truncated form of p35, is known as a neuron-specific activator of Cdk5 (Shah and Lahiri, 2014). It is generated from p35 under neurotoxic conditions, such as exposure to excitotoxicity, ischaemia and oxidative stress (Patrick et al., 1999; Sahlgren et al., 2006). Neurotoxin insults disrupt intracellular Ca^{2+}homeostasis in neurons, thereby activating calpain, which in turn cleaves p35 into p25 (Lee et al., 2000). The ability of p25 to activate or hyperphosphorylate Cdk5 may be attributed to the prolonged half-life of p25 compared to p35 (Zhang et al., 2013) and the resistance to ubiquitin-mediated proteolysis. The modification of Cdk5 may disrupt its normal physiological function and lead to the damage of the brain cells leading to neuronal toxicity. The Cdk5-induced neurotoxicity may have also been promoted by the ability of the Cdk5-p25 complex to translocate from the plasma membrane to the cytosol and the nucleus allowing the access of Cdk5-p25 to a variety of targets as opposed to the Cdk5-p35 complex, which localises primarily to the perinuclear region and the plasma membrane with minimal distribution in the nucleus (Fu et al., 2006; Asada et al., 2008).

Targets for the Cdk5-p25 complex include; GM130, peroxiredoxin 1, peroxiredoxin 2, lamin A, lamin B1, Cdc25A, Cdc25B and Cdc25C (Sun et al., 2008; Sun et al.,

2009; Chang et al., 2010; Chang et al., 2011; Chang et al., 2012). The phosphorylation of GM130 by the Cdk5-p25 complex may cause abnormal Golgi fragmentation leading to the phosphorylation of peroxiredoxins (Sun et al., 2008) and hence oxidative stress. The latter mechanism triggers the phosphorylation of lamins, Cdc25A, Cdc25B and Cdc25C resulting in the dispersion of the nuclear envelope and abnormal activation of the cell cycle (Chang et al., 2011; Chang et al., 2012). Under physiological conditions, Cdk5 also act via the phosphorylation of neurofilament heavy chain (NF-H) at its tail domain on Lys-Ser-Pro motifs. This aids the assembly of neurofilaments within the axon, resulting in axonal support and neurite outgrowth (Wang et al., 2012). However, under neurotoxic conditions, Cdk5-p25 was shown to hyperphosphorylate tau, which aggregates in cell bodies to form neurofibrillary tangles in several neurological disorders. Thus, the Cdk5-p25 complex-mediated toxicity is caused by the hyperphosphorylation of its physiological targets, and phosphorylation of non-physiological targets (Bano and Nicotera, 2007).

1.8.5 CIP-Peptide Promotes Angiogenesis in hypoxia condition

Evidence suggests the neuronal cytoprotective role of a small natural peptide (CIP-peptide) under neurotoxic stress. CIP has been identified as a derivative of the p35 cleavage peptide, which selectively targets the Cdk5/p25-dependent pathway (Kesavapany et al., 2007). CIP's role(s) are thought to be mediated through the selective inhibition of Cdk5/p25 activity without affecting the Cdk5/p35 signalling

pathways. CIP's role is implicated in increased p35 localisation with actin fibres and therefore the stabilisation of the actin cytoskeleton. The latter phenomenon leads to increased recovery of cell spreading and the formation of stable neo-capillaries. Thus, the p35/Cdk5 signalling pathway may in part have an autoprotective role during *in vitro* angiogenesis. Hence, CIP may act as a vascular protector supporting tissue remodelling after ischaemic stroke (Kesavapany et al., 2007).

1.8.6 Brain Ischaemia and Calcium

The inability to clear excitatory amino acids can cause sustained gating of receptor-operated channels (Gillessen et al., 2013) with prolonged neuronal depolarisation leading to calcium overload and ultimately a neuronal loss in the ischaemic brain. Inflammatory response and necrotic cell death can be triggered by excitotoxic stimulation within ischaemic regions, depending on the intensity of the insult (Northington et al., 2011). For instance, glutamate overstimulation of glutamate-ionotropic receptors at synaptic and extra-synaptic sites causes prolonged neuronal depolarisation that triggers the deregulation of intracellular calcium and sodium ion homoeostasis. This leads to apoptosis and in severe cases (Carvajal et al., 2016), where there is a widespread excess glutamate may cause necrosis. Hence, treatments aimed at reducing ion imbalance by blocking the gating of ionotropic glutamate receptor and voltage-gated channels can reduce brain infarct (Li et al., 2014). Calpains cleave the sodium-calcium exchanger (NCX). The Ca^{2+} extruding systems such as sodium-calcium exchangers (NCXs) are important for the Ca^{2+}

efflux from neurons (Figure1.8). NCXs have been shown as fundamental players during ischemia (Pignataro et al., 2007; Pignataro et al., 2011) and neuronal degeneration (Sisalli et al., 2015). NCX3, in particular, has been shown to be essential in the maturation of dissociated neurons (Gomez-Villafuertes et al., 2005) and in the control of intracellular Ca^{2+} in skeletal muscle fibres (Sokolow et al., 2004). In response to an excitotoxic stimulus such as high glutamate concentrations, calpains act by cleaving one of the major isoforms (e.g. isoform 3) of the NCX or NCX3. The cleavage of NCX3 inhibits its capability to remove accumulated Ca^{2+} and precludes the possibility to restore Na^{+}/Ca^{2+} exchange leading to a massive Ca^{2+} overload (irreversible build-up of the intracellular Ca^{2+} concentration) and neuronal degeneration (Jin et al., 2014). In addition, caspases can affect the activity of the plasma membrane Ca^{2+} ATPase (PMCA), perhaps through the glutamate-mediated pathway, via its internalisation and cleavage (Andersen et al., 2016). The internalisation of PMCA contributes to the deregulation of Ca^{2+} and causes neuronal death. Hence, there is a link between calcium-dependent proteases, calcium overload and neuronal degeneration after an excitotoxic insult. The studies relating to calpains and caspases highlight the important role of Ca^{2+} transporters in neuronal demise (Pottorf et al., 2006) and provide potential pharmacological targets to prevent extensive neuronal demise during the stroke.

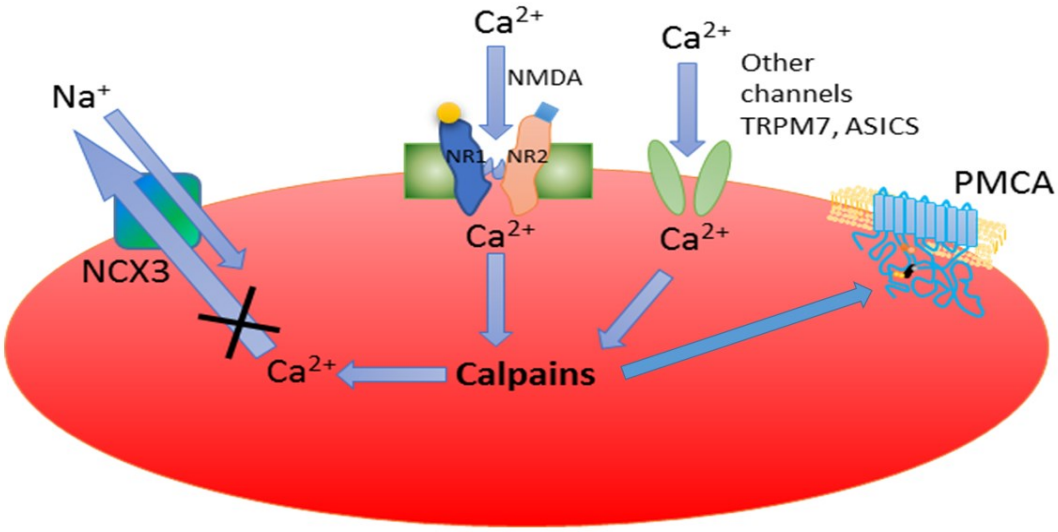

Figure 1-8 The Interaction between Calcium and Calpains – possible modulation effects

The entrance of Ca^{2+} by binding to NMDA and probably other channels initiates the increase in excitotoxic Ca^{2+}. Calpains are activated and cleave NCX3 prevents the restoration of Na^{+}/Ca^{2+} exchange, therefore this results in an irreversible accumulation of the intracellular Ca^{2+}concentration. Adapted from (Bano and Nicotera, 2007).

1.8.7 Gamma secretase inhibitor (DAPT)

Due to their shared roles in neuronal cell development and the phosphorylation, the relationship between Notch and CdK5 was established by the use of a Notch inhibitor, N-[N-(3,5-difluorophenacetyl)-1- alanyl]-S-phenylglycine t-butyl ester (DAPT) on Cdk5 expressing-cells (Kanungo et al., 2008). The use of roscovitine may inhibit the activity of Cdk5 activity in a different way to DAPT. Previous studies using 10 μM DAPT attenuated Cdk5 catalytic activity and reduced p35 bioavailability while upregulating Cdk5 expression at the transcriptional level. Also, the neuronal cytoskeletal proteins phospho-tau and phospho-neurofilament, normally

phosphorylated by Cdk5 showed a shift in their localisation from axons to cell bodies in DAPT-treated cells, suggesting a role for the Notch signalling and Cdk5 expression in regulating neuronal cytoskeletal protein dynamics. The action of DAPT was opposed by an over-expression of p35, which restored Cdk5 activity through direct interaction. Thus, DAPT action does not disrupt Cdk5 and p35 interaction and the latter is dependent on the levels of p35 within the cell, as well as its effects on regulating the expression of Cdk5 by inhibiting its activity (Tanaka et al., 2001; Joshi et al., 2014).

1.8.8 Signalling Pathway and Targets of Cdk5

Cdk5 has a role in the determination of the fate of neurons and ECs during the stroke. Cdk5 could be seen as a master switch controlling both neuronal survival and revascularisation. The action of Cdk5 is dependent upon its interaction with a number of substrates; namely the myocyte enhancer factor-2 (Mef2), caspase-3, Tau and p53 (Slevin and Krupinski, 2009; Slevin et al., 2015). Cdk5 has also been found in association with the cytoskeletal protein actin in ECs and potentially stimulates EC migration through its association with and/or activation of talin and Rac-1 (Liebl et al., 2010; Tripathi and Zelenka, 2010). The MEF2 proteins are members of the MCM1-agamous-deficiens-serum response factor (MADS) family of transcription factors. The alternatively spliced transcripts of vertebrate MEF2 proteins are encoded by four different genes including; MEF2A, B, C, and D and are regulated by posttranslational modification. They are a number of kinases that are responsible for up- or down-regulating the activity of Mef2 via phosphorylation. Mef2

exerts its regulatory effect through descending survival and death signals to the vasculature (Yin et al., 2012). Mef2 proteins are expressed in developing endothelial cells and are required for vascular survival, maintenance and development (Sacilotto et al., 2016).

1.8.9 Cdk5 in Stroke (role and mechanisms)

Stroke is considered as a primary cause of disability and/or death in developing countries. Strokes take place when the blood supply to a fraction of the brain is abruptly interrupted or severely reduced by, for instance, a blood clot. This phenomenon is referred to as an ischaemic stroke. A haemorrhagic stroke occurs when a blood vessel in the brain ruptures, spilling blood into the surrounding tissue, where the developing pressure, as well as the lack of blood supply, may cause the death of neurones. When the neurones within the brain no longer receive oxygen and nutrients from the blood, they die within a few minutes and may cause permanent disablement of body parts controlled by these brain regions. The matter is particularly problematic because brain cells once lost cannot be replaced (Caplan, 2009). The loss of brain cells is the result of an abnormal activation of multiple brain cell death pathways. In contrast, angiogenesis, vascular remodelling and neurogenesis are all essential processes for tissue recovery (Panickar et al., 2008; Slevin and Krupinski, 2009). Various studies have highlighted the significance of the process of microvascular angiogenesis for neurone replenishment and survival, displaying the latter as a potential target for therapies (Slevin and Krupinski, 2009).

Therefore, the characterisation of novel angiogenesis signalling proteins with potential therapeutic benefits is essential. Many lines of evidence indicate that deregulation of a set of cell cycle kinases has been implicated in neuronal death following ischaemic insult and neurodegenerative disorders (Liebl et al., 2010; Takacs et al., 2010). Cdk5 and its two activators (the p35/p25 peptides) are regarded as key mediators in neuronal survival through the activation of angiogenesis (Potthoff et al., 2007; Tripathi and Zelenka, 2010; Chillakuri et al., 2012; Yin et al., 2012).

In the presence of various neurotoxic insults, including brain ischemia and oxidative stress, Cdk5 is hyperactivated with potentially fatal consequences in respect to neurones (Ikeda et al., 2000; Rajdev et al., 2000; Glading et al., 2002; Liebl et al., 2010). On the other hand, lack of Cdk5 activity also leads to neuron cell death emphasising that appropriate control of Cdk5 activity is crucial for normal cellular homoeostasis. Evidence demonstrates that a crucial determinant of Cdk5 activation is the protein-protein interactions with its two regulatory partners p35 and p25 (Kanungo et al., 2009). The increase in intracellular calcium in neuronal cells undergoing apoptosis (due to physical pressure and/or lack of blood supply) induces the production and release of calpain to the surrounding tissue. The activation of calpain has been demonstrated to increase the cleavage of p35 into p25 peptide in the ECs of the ruptured blood vessel. The increase in p25 was suggested to lead to the hyperactivation of Cdk5 (Glading et al., 2002; Liebl et al., 2010), causing cell death by apoptosis.

In an *in vitro* experimental model of stroke (brain microvascular endothelial cells subjected to oxygen-glucose deficiency), the overexpression of Cdk5-wild type in the endothelium significantly protected ECs against damage resulting from stroke, whereas a dominant negative Cdk5 (Cdk5 kinase-inactive mutant), gave little or no protection (Panickar et al., 2008). This may suggest a role of wild-type Cdk5 in promoting new vascular generation leading to increased vessel formation and reperfusion, as well as the restoration of the blood supply, thereby protecting neurones from further damage *in vivo*. Nonetheless, little is known about its role in the latter in microvascular ECs under normal conditions. However, the effect of Cdk5 in contributing to neuronal death following ischaemia has also been evidenced, through different stimuli (Slevin and Krupinski, 2009). For instance, in the damaged areas that protrude into the peri-infracted region, the associated vessels overexpress Cdk5/p35 and were TUNEL-positive, indicative of EC-death of these microvessels (Potthoff et al., 2007). Recently, Liebl *et al*. reported that Cdk5 as a modulator of neuronal processes also regulated ECs migration and angiogenesis. After inhibition or knockout of Cdk5, the ECs motility and angiogenesis was blocked *in vitro* as well as *in vivo*, by a mechanism involving the Cdk5-Rac1 pathway (Liebl et al., 2010).

The pathway for Cdk5 activation involves an upstream excitotoxic signal transduction cascade induced by oxygen-glucose deficiency of hypoxia at the region of stroke-affected tissue (Mitsios et al., 2007). Hypoxic conditions lead to excessive activation of the calcium-activated cytosolic proteases (calpains), which act by cleaving p35 to the more stable p25 peptide leading into Cdk5 hyperactivation and

neurones and ECs apoptosis. On the other hand, the modulation of p35 and its binding with Cdk5 demonstrated a contribution to cytoprotection (Shi et al., 2012; Barros-Miñones et al., 2013). The nuclear translocation and/or up-regulation of Cdk5 and p35 in neurons and ECs and the subsequent Cdk5/p35 pathway is regarded as a key pathophysiological determinant of ECs survival and ultimately outcome after infarction (Mitsios et al., 2007; Bosutti et al., 2013) as well as being novel potential targets for cell protection and improved tissue remodelling after stroke (Slevin and Krupinski, 2009; Barros-Miñones et al., 2013). The use of inhibitors such as Roscovitine (Timsit and Menn, 2012; Bosutti et al., 2013) has been shown to affect the physiological function of Cdk5 and/or the regulation of synaptic plasticity (i.e. calpain inhibitors) (Koumura et al., 2008). Thus the side effects of Roscovitine can, therefore, compromise any therapeutic efficacy (Slevin and Krupinski, 2009). Therefore, it is essential to identify and characterise specific inhibitors for the Cdk5/p25 complex formation to re-generate Cdk5/p35 (Barros-Miñones et al., 2013) and enhance the re-vascularisation of the brain tissue after stroke (Slevin and Krupinski, 2009). The in-depth understanding and use of the neuronal cytoprotective natural small peptide (CIP-peptide) after neurotoxic stress may provide a therapeutic potential. CIP is a derived-p35 cleavage peptide that selectively targets Cdk5/p25 activity without affecting Cdk5/p35 signalling (Kesavapany et al., 2007).

Cdk5 has a role in promoting synaptic plasticity (Ohshima et al., 2005), learning and the formation of memories (Guan et al., 2011). Furthermore, Cdk5 has been demonstrated to be transiently upregulated under stress conditions and was shown

to facilitate context-dependent fear conditioning (Fischer et al., 2003). Likewise, an increase in Cdk5 activity, accelerated calpain-mediated degradation of the NMDA receptor subtype 2B (NR2B), leading to learning deficits (Sato et al., 2008). Taken together these findings suggest a role of Cdk5 in promoting long-term potentiation (LTP) and long-term depression (LTD), with an ability to counteract changes induced by LTP and LTD to maintain neuronal network stability; functioning as a homeostatic regulator of synaptic plasticity. However, these findings were contradicted by Hawasli *et al*., highlighting a negative role for Cdk5 in learning and memory formation when there is an initial loss of Cdk5 resulting in enhanced LTP, NMDA-receptor-mediated synaptic plasticity and enhanced performance in hippocampal behavioural learning tasks (Hawasli et al., 2007; Shah and Lahiri, 2014).

1.9 Aims, Objectives and Hypothesis

The aim of the study is to understand how Cdk5 regulates cell survival and angiogenesis in stroke. The role of the Cdk5-p35/p25 pathway in maintenance of the vascular bed and angiogenesis will be investigated in human brain microvascular endothelial cells (hBMECs) under mimicked stroke conditions.

The objectives were, therefore:

- To establish an effective *in vitro* hypoxia, that mimics a stroke, using hBMECs.

- To investigate the mechanism(s) that mediate cell attachment, spreading and migration and the levels of p35/p25 under hypoxia in Cdk5 over-expressing cells.
- Examine how tube formation, sprouting, angiogenesis and wound healing are affected by hypoxia and/or DAPT.
- Examine the impact of calcium treatment on CIP expressing and Cdk5-over-expressing hBMECs.
- To determine the impact of hypoxia on the expression of heat shock protein (HSP-70), ERK and caspase-3 in hBMECs.

Hypothesis:

The hypothesis of the current study is that Cdk5/p35 stimulates cell survival and angiogenesis in stroke.

Chapter 2 Materials and Methods

2.1 Materials

- Chromatography paper (Whatman Schleicher &ScuellInternational Ltd, England)
- Coverslips (Scientific laboratory supplier Ltd, SLS, UK)
- Cryovials (Nunc Corporation, Roskilde, Denmark)
- Eppendorf tube 0.5 ml, 1.5 ml and 2.0 ml (Nunc Corporation, Roskilde, Denmark)
- Nitrocellulose membrane (Schleicher & Schuell)
- Pipettes 0.5-10, 5-50, 50-200,100- 1000 µL (Scientific laboratory supplies Ltd)
- Sterile bijous (SLS, UK)
- Sterile plates 6-well, 24-well and 48-well (Nunc, Denmark)
- Sterile universal containers (SLS, UK)
- Superfrost slides (76x26) mm (Thermo Scientific, Germany)
- Tips (white, yellow and blue) (Thermo Scientific, Germany)
- Tissue culture plates (6-well, 12-well, 24-well, 48-well and 96-well) (Thermo Scientific, Germany)
- Tissue culture flasks (T-25, T-75) (SLS, UK)

2.2 Equipment

- Autoclave (Lab Impex Research, UK)
- Autovortex mixer SA1 (Stuart Scientific Co, UK)

- Axivoert fluorescence microscope (Zeiss, Oberkochen, Germany)
- Balancer (Sartorius analytic)
- Centrifuge (Mik20)
- CO_2 incubator (Lab Impex Research, UK)
- Electrophoresis unit mini-Protean® 3 (Bio-Rad, USA)
- Freezer -80C° (Juan Quality System, London, UK)
- G-box (Syngene, UK)
- ChemiDoc Touch Imaging System (Bio-rad Ltd, UK)
- Ice maker (Borolab Ltd, UK)
- Image J software analyser (Free online software)
- Laboratory fridge (SLS, UK)
- Laboratory pH/ temperature meter (Model AGB-75, UK)
- Laminar flow hood tissue culture grade (Walker safety cabinet Ltd, UK).
- Liquid nitrogen (BOC CryospeedThermolyne)
- Magnetic stirrer hot plate (Stuart Scientific CO., UK)
- Microscope (Nikon TMS)
- Modular incubator chamber (Billups-rothenberginc., USA)
- Nikon camera (Nikon Coolpix 4500)
- Pipettes 0.5-10,5-50,50-200,100-1000 (Scientific laboratory supplies Ltd, SLS)
- Power supply PS-251-2 (Sigma-Aldrich)
- Rotating shaker (Grant-bio PS0-300)
- Spectrophotometer (Pharmaxia Biotech).

- TC10™ Automated Cell Counter (Bio-Rad, USA)
- Trans-blot SD semi-dry transfer (Bio-Rad, USA)
- Ultra-low -80 freezer (Nuaire, USA)
- Water-bath (Grant instrument Ltd., UK)
- Hypoxic chamber (Grant instrument Ltd., UK)

2.3 Chemicals

- 1X Tris/Borate/EDTA (TBE) buffer, (Sigma, UK)
- 2-Propanol, for molecular biology, ≥ 99% (Sigma, UK)
- 40% Acrylamide/Bis solution (Bio-Rad Laboratories, UK)
- Ammonium persulphate (Sigma, UK)
- *Anti-Caspase 3, Active antibody produced in rabbit polyclonal (Sigma, UK).
- *Anti-Caspase 3 antibody produced in rabbit (Sigma, UK).
- *Anti-Phospho-Erk1/2 (E-4) mouse monoclonal antibody (Santa Crus Biotechnology).
- Bio-Rad protein assay kit (Bio-Rad Laboratories, Germany)
- Bis (N, N'-methylene bisacrylamide) (Sigma, UK)
- Blue wide range pre-stained protein ladder (Geneflow, UK)
- Bovine serum albumin, BSA (Sigma, UK)
- Bromophenol blue (Serva)
- Caspase 3, Active antibody produced in rabbit polyclonal (Sigma, UK)
- Distilled water (Millipore, UK)

- DMSO, Dimethyl sulfoxide (Sigma, UK)
- Ethanol (absolute for molecular biology) (Sigma, UK)
- EZ-ECL chemiluminescence detection kit for HRP (Biological industries, Israel)
- FBS- Brazilian Origin (Lonza, USA)
- Glycine (BDH, UK)
- Hydrochloric acid (Fisher Scientific, UK)
- Hydrogen peroxidase (Sigma, UK)
- Hypoxia gas (Boc Gases, UK)
- Isopropanol (Sigma, UK)
- Matrigel™ Basement Membrane Matrix 10 ml (BD, UK)
- Methanol (Fisher Scientific International, UK)
- Skimmed milk (Local store, UK)
- N, N, N', N'- tetramethylethylenediamine (TEMED) (Sigma, UK)
- Paraformaldehyde (Sigma, UK)
- Phosphate Buffer Saline, PBS (Lonza, USA)
- Phosphate Buffered Saline (Dulbecco A) tablets (Fisher Scientific, UK)
- Phosphate Buffered Saline (Dulbecco A) tablets (Fisher Scientific, UK)
- Polyclonal Goat Anti-mouse Immunoglobulin/Horseradish peroxidase, HRP (Dako, Denmark)
- Protease inhibitor cocktail (Sigma-Aldrich, UK)
- RIPA buffer (Sigma-Aldrich, UK)
- Sodium chloride (Sigma-Aldrich UK)

- Sodium Dodecyl Sulphate, SDS (BDH, UK)
- Sodium hydroxide (BDH, UK)
- Tris (hydroxylmethyl) methylamine (BDH, UK)
- Trypsin-EDTA 1X (Lonza, USA)
- Tween® 20 (Sigma, UK).

2.4 Required Buffers

2.4.1 Blocking buffer

1% (w/v) Bovine serum albumin (BSA) in TBS-Tween or 4% (w/v) of non-fat dry milk in TBS-Tween. TBS-Tween must be stored in the refrigerator at PH7.4

2.4.2 Electrode buffer

12.02 g Tris-base, 4g Sodium Dodecyl Sulphate (SDS), 57.68g glycine made up with 2 L of dH_2O.

2.4.3 Milk (required for the secondary antibodies)

5% (w/v) skimmed milk powder in TBS-Tween with pH adjusted to 7.4. Must be made fresh for each use.

2.4.4 Sample buffer (pH 6.8)

Tris-base 1.51 g, 20 ml glycerol mixed with 20 ml of d H_2O. Then add 4g of SDS, 3.6 ml of mercaptoethanol and 0.004 g bromophenol blue, and made up to 100 ml with dH_2O.

2.4.5 Separating buffer (pH 8.8)

Tris-base 36.3 g, and SDS 0.8 g dissolved in 250 ml of dH_2O.

2.4.6 Stacking buffer (pH 6.8)

Tris-base 15 g and SDS 1 g dissolved in 250 dH_2O.

2.4.7 Towbin buffer

Tris-base 1.51 g, glycine 7.2 g, SDS 0.167 g and 75 ml methanol then this combination was made up to 500 ml with dH_2O.

2.4.8 TBS-Tween buffer

Tris-buffered saline and Tween-20 (TBS-Tween pH 7.4): Tris-base 2.422 g, NaCl 16.36 g and 2 ml of Tween 20 mixed up to 2 L with dH_2O.

2.4.9 RIPA buffer

20 mM Tris-HCl (pH 7.5), 150 mM NaCl, 1 mM EDTA, 1 mM EGTA, 1% (v/v) Triton X-100, 1% (w/v) sodium deoxycholate, 2.5 mM sodium pyrophosphate, 1 mM Na_3VO_4, 1 mM β-glycerophosphate, 1 µg/ml leupeptin, 1 mM PMSF.

2.5 Cell Culture Medium

Endothelial basal medium-2 (EBM-2) supplemented with 2% (v/v) foetal bovine serum (FBS), Hydrocortisone, recombinant human Fibroblast Growth Factor B (rhFGF-B), recombinant human Vascular Endothelial Growth Factor (rhVEGF), Recombinant long Receptor Insulin-like Growth Factor-1(R3 IGF-1), Ascorbic Acid, recombinant human Epidermal Growth Factor (rhEGF) and Gentamicin sulphate Amphotericin-B (GA-100), were made up according to the supplier's recommendations.

2.6 Methods

2.6.1 Cell Line and Cell Clones

2.6.1.1 Human brain microvascular endothelial cell line

The Immortalised human brain microvascular endothelial cell line (hBMECs) (Haarmann et al., 2010) was used as the cell model for this study, which was kindly

provided by Prof Babette Weksler (Division of Haematology and Medical Oncology, Weill Medical College of Cornell University, New York).

All cell culture methods were carried out under sterile conditions.

2.6.1.2 Transfecting hBMEC and Selecting Cell Clones

Stable hBMECs overexpressing Cdk5 transfectants (OVCdk5) were generated by stable transfection of wild-type human Cdk5, (Cdk5-wt), which were obtained from pcDNA3-cdk5GFP expression vectors (Addgene, USA), using TransIT-2020 as transfection reagent (Mirus Bio LLC, Madison, USA). Cdk5 inhibitory peptide (CIP) was transferred with pcDNA-GFP-CIP. Non-transfected hBMECs was used as a control.

For the transfection, 2.5 µg of plasmids + 7.5 µL TransIT-2020 were added to 260 µL of EBM-2 medium containing 500 µg/ml of geneticin (G418, Invitrogen Life Science, UK) was used as a selective medium and incubated for 30 min at RT prior to being used. When the cell confluence reached about 90%, the DNA complex was added to cells and incubated for 24 hours.

For instance, the transfected cells were seeded in EGM-2 medium containing 500 µg/ml G418. After one week, G418 was changed to 300 µg/ml. Then after another week, G418 was reduced to 200 µg/ml. About one month after seeding, the drug medium was changed to normal EBM-2 medium. Transfection efficiency was defined by the presence of GFP fluorescence and Cdk5 protein levels in cells.

2.6.1.3 CIP Cloning and Stable Transfections

A modified EGFP-IRES vector containing the CIP sequence (Kesavapany et al., 2007), (pLV-CIP plasmids), was a kind gift from Prof Sashi Kesavapany, National University of Singapore. CIP peptide is comprised of 126 residues of p35 protein (accession number: AAH26347.1) spanning from aa 154 to aa 279. CIP-PCR products from pLV-CIPplasmid were obtained by polymerase chain reaction (PCR) (forward primer, TTA GGA TCC TTG CCT GGG TGA GTT TC and reverse primer, GTC GGA TCC TCA TGG GTC GGC ATT TAT C) and digested with Bacillus amyloliquefaciens (BamHI) (Invitrogen, UK) were then inserted by ligation into the pcDNA3-GFP expression vector. After positive cloning in DH5α, purified pcDNA3-CIP-GFP vectors were stably introduced by transfection into hBMECs using TransIT-2020 transfection reagent (Mirus Bio LLC, Madison, USA). EGM-2 medium containing 500 µg/ml G418 (Invitrogen Life Science, UK), was used as a selective media.

Positive hBMECs clones were detected by GFP fluorescent signals and by the level of CIP mRNA by RT-PCR. 18S rRNA (accession number: NM - 022551.2) was used as a housekeeping gene (forward primer, TAG AGG GAC AAG TGG CGT TC and reverse primer, TGT ACA AAG GGC AGG GACT T). Resistant clones were detected by GFP fluorescent signals under fluorescence microscopy, and the level of CIP mRNA confirmed by RT-PCR. (This work was done by Dr Jie Qi, School of Healthcare Science, Manchester Metropolitan University).

2.6.2 Thawing Cells

The thawing process was done in the quickest possible time to ensure that a high quantity of cells survived in the stressful procedure. When required, the cryovial containing frozen cells was taken out from liquid nitrogen and immediately defrosted by gently swirling in a water bath at 37°C. The pressure inside the vial was released inside a Laminar flow hood and the frozen cells were defrosted at 37°C water bath. Once defrosted, the cryovial was sprayed with 70% (v/v) ethanol and the contents were transferred into a flask [pre-coated with 0.1% (v/v) Poly-L-lysine solution] and maintained in a humidified 5% CO_2 atmosphere at 37°C. The medium was then replaced with fresh complete cell growth medium after 24 hours.

2.6.3 Cell Culture and Sub-Culture

Human brain microvascular endothelial cell line (hBMECs), CDK5 inhibitory peptides (CIP) and overexpressing Cdk5 transfected hBMECs (OVCdk5) were grown in EBM-2 medium supplemented with growth factors and 2% (v/v) FBS. Cells were seeded into T-25 flasks pre-coated with 0.1% (v/v) Poly-L-lysine solution and maintained in a dH_2O humidified 5% CO_2 atmosphere at 37°C. The cell growth medium was changed every three days, and when cells reached confluence, they were detached under the enzymatic activity of trypsin. Briefly, cell growth medium was discarded, and the cells were washed three times with 5-10 ml of warm PBS. Then, 2 ml of pre-warmed (1×) trypsin/EDTA at 37°C was added to cover the entire surface of the cell monolayers, and incubated for 5 mins in order to detach the cells

from the flasks. Following that, the action of the trypsin was blocked by adding an equal amount of fresh cell growth medium. After that, the cells in the suspension were collected in a universal tube and centrifuged at 300×g for 5 mins. The supernatant was discarded, and the cell pellet was re-suspended in fresh complete medium. The cells were seeded into fresh flasks or plates pre-coated with 0.1% (v/v) poly-L-lysine solution for further experimentation. Throughout the study, the cells used in all experiments were between passages 8 and 18. Cells were passaged when they had reached about 90% confluence.

2.6.4 Preparation of Freezing Medium

The freezing medium was prepared to contain 10% (v/v) dimethyl sulphoxide (DMSO) in FBS. Briefly, 1 ml of DMSO in 9 ml of cold FBS was mixed and kept at -20°C until use. The fresh freezing medium was prepared or defrosted shortly before use.

2.6.5 Freezing Cells

The trypsinised cells taken from the flask were centrifuged at 300×g for 5 minutes; the supernatant was then removed, and the cell pellet was re-suspended in 250 µL of complete medium with the addition of 750 µL of 10% (v/v) DMSO (freezing medium). One ml of the medium containing approximately 2.5×10^6 of cells was kept in a 1.5ml cryovial labelled with the cell passage, number and date. Cryovials

containing cells were kept at -20°C for 30 minutes. then the cryovial was transferred into a -80°C freezer overnight. After 24 hours, the cryovial was transferred to liquid nitrogen (-190°C) and the location was recorded.

2.6.6 Cell Counting

Following trypsinisation and centrifugation, 20 µL of the cell suspension was mixed with 20 µL of trypan blue and was then transferred into a haemocytometer chamber with 1×1×0.1 mm dimensions (covered with a coverslip) and visualised under a microscope with a 10× objective. The cell number was counted per each square of the haemocytometer using the formula illustrated in Figure 2.1 (number 1-5 squares) taking into consideration the dilution factor.

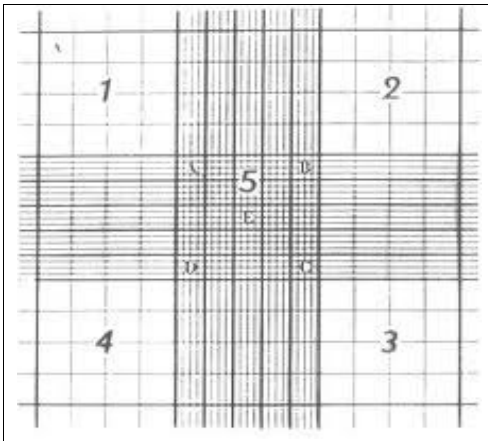

Cell number per mL = the average count per square × the dilution factor × 10^4.

Figure 2-1 The haemocytometer for counting cells with the equation used for the cell count

2.7 Angiogenesis Assays

2.7.1 Cell Migration (Wound Healing)

hBMECs, CIP expressing cells and OVCdk5 were seeded respectively at a concentration of 2×10^5 cells/ml in 500 µL of complete medium in each well of a poly-L-lysine pre-coated 24-well plates. After 24 hours of incubation at 37°C in 5% CO_2, the medium was replaced with serum poor medium [SPM, basal medium containing 0.5% (v/v) FBS]. Each well of the 24-well plates was washed with warm PBS three times and a wound was made using a sterile pipette tip. The wells then were washed carefully with warm PBS three times to remove any floating cells. Then calpain (0.1 µM) was added, and SPM [0.5% (v/v) FBS EBM-2] was applied to the cells, then the cells were incubated under hypoxic [1% (v/v) O_2] and normoxic conditions respectively for 24 hours.

Normal hBMECs, CIP expressing cells and OVCdk5 were incubated with FGF-2 (25 ng/ml) and γ-secretase (DAPT, inhibitor, at 10 mM) where appropriate. After 24 hours incubation, 50 µL of 4% (w/v) paraformaldehyde (PFA) was added to each well to fix the cells at room temperature (RT) for 15 mins. The medium was then removed, and the wells were washed with PBS. 100 µL of 100% ethanol was added to the cells and left for 5 mins. Then the ethanol was removed, and the wells were left to dry before staining the cells with methylene blue for 5 mins. The stain was removed, and the wells were washed with distilled water (dH_2O). Finally, the cells were examined under the microscope and pictures were taken. In this experiment, cells were treated in triplicate for each experimental condition and pictures of five areas of each well were taken. The picture analysis was performed using Image-J.

2.7.2 Tube-like Structure Formation in Matrigel™

The 96-well plate was coated with 50 µl of Matrigel™ and then put in an incubator at 37°C for 1 hour. hBMECs, CIP expressing cells and OVCdk5 (8×10^3 cells) were mixed respectively in 50µL of medium with various of conditions, and with or without DAPT inhibitor (10µg/ml), FGF-2 (25ng/ml). After 24 hours incubation, 4% (w/v) PFA was added to fix the endothelial tube-like structures in the well. Under an optical microscope, closed areas surrounded by endothelial tube-like structures were counted in 3-5 areas from each well.

2.7.3 Spheroid Sprouting Assay

After the initial trypsinisation stage, cells (6×10^5 cells/ml suspended in EBM-2 medium) were added to non-adhesive 96-well Greiner® plates (Sigma, UK) for suspension culture. Firstly, 6 ml of methylcellulose was made up with 30 ml of EBM-2 medium, from this 15 ml were added to 250 µL of the initial cell volume. The cells (150 µL/well) were then added to the 96-well plates and incubated in a 5% CO_2 incubator at 37 ºC for 24 hours.

In a separate bijou, 1.33 ml of collagen gel solution at (2 µg/ml) was added to 920 µL of EBM-2 medium and kept on ice. The spheroids were collected, added to 15 ml tubes and centrifuged at 400×g for 3 mins. When a clear pellet was distinguished, the supernatant was removed, and 250 µL methylcellulose gel was added. Before adding the spheroids in the 24-well plate, the collagen solution was neutralised by adding 150 µL 0.1 N NaOH. If the 0.1 N NaOH had been added early, the collagen

gel solution would have polymerised. The solution turned pink once resuspended. The spheroids were then added to the 24-well plates at 500 µL/well. Before adding the spheroids to the 24-well plates ensure the sterile tip was cut slightly from the tip to avoid damaging them. They were incubated at 37ºC, in 5% CO_2. After 24 hours, the spheroids were fixed with 4% (w/v) PFA for 15 min at room temperature and pictures were taken. Sprouting occurred from the spheroid core, and the sprout length was estimated with the software Image-J using five spheroids with similar sizes of the core of spheroid.

2.8 Hypoxia Studies

Hypoxia is defined as the reduction or lack of oxygen in organs, tissues, or cells. For an *in vitro* mimicked stroke condition, a hypoxia chamber was used in this study to provide a flow with different gas compositions as compared to normal atmospheric flow. The cell culture plates were placed in the hypoxic chamber (see appendices 7.3); also, a dish containing sterile water was placed in the chamber to provide adequate humidification of the cultures. The chamber was sealed airtight. All oxygen present in the chamber was removed by opening the gas tank at a flow rate of 20 litres per minute for about 5 mins feeling gas flowed out from another tube, which was linking in the chamber. Then quickly sealed off the out-tube with a clamp, then turned the gas flow down to 5 litres per min, and after this quickly turned off the gas flow and completely closed the chamber by closing both white clamps. The chamber was then put in a conventional incubator for the desired period.

2.9 Propidium iodide (PI) Staining

To study the protective effect of Cdk5 on ECs in hypoxia, glass coverslips were bathed in 100% ethanol for 10 - 20 min and left to air dry in a sterile environment. The coverslips were put in a 24-well plate and pre-coated with 500 µL of 0.1% (v/v) poly-L-lysine solution. After 10 min incubation, the coverslips were washed with PBS and the cells were grown in complete growth medium at a cell (hBMECs) concentration of 5×10^4 cells/ml. After a 24-hour incubation, the completed growth medium was removed and replaced with SPM containing 0.5% FBS and incubated for 24 hours in hypoxic (1% O_2) and normoxic conditions respectively. OVCdk5 and CIP expressing cells were also incubated in hypoxic conditions for 24 hours. One hour before the termination of the experiment, propidium iodide (PI, 10µg/ml) was added to each well as an indicator of DNA damage without removing the medium. After 1 hour incubation, the cells were washed three times with PBS, and one drop of Vectashield mounting medium with DAPI reagent was added on frosted glass slides. An average of three fields at ×40 of magnification was photographed per coverslip by using an Axiovert fluorescence microscope (Zeiss).

2.10 Protein Extraction

hBMECs, CIP expressing cells and OVCdk5 (8×10^5 cells/ml, 2 ml) were seeded respectively in complete medium in a 6-well plate. After 48 hour incubation, the medium was replaced with SPM containing 0.5% (v/v) FBS. Various conditions were applied to each well in addition to untreated cells, and then the cells were incubated

for 24 hours. Afterwards, the cells were washed with cold PBS and gently lysed on ice in 200 µL of ice-cold homogenised lysis (RIPA) buffer, with a protease inhibitor and a phosphatase inhibitor, pH 7.2. Then the cells were scraped, the lysate proteins were collected, and transferred into 0.5 ml microcentrifuge tubes and incubated on ice for 20 mins whilst being vortex mixed every 2 mins to make sure that the lysates were mixed properly. After that, the cell lysates were sonicated three times. The proteins were stored at -80°C until use.

2.11 Protein Estimation

The protein concentration was determined using the Bio-Rad protein assay. Briefly, BSA was used at 1mg/ml as a standard protein, and 10 µL of protein lysate was added and completed with 90 µL of dH_2O in a bijou tube. After that, 2 ml of Bio-Rad protein assay reagent (1:4 dilution) was added into each bijou tube. The absorbance of each sample was measured with a spectrophotometer at 595 nm.

The data outlining the reading of each protein sample and the standard curve required for protein estimation are shown below (Figure 2.2).

Table 2.1: The volume of BSA, dH_2O and Bio-Rad required to establish the standard curve.

BSA Standard (µg)	BSA volume added (1µg/µl)	Volume of dH_2O (µl)	Volume of diluted BioRad reagent (ml)
0	0	100	2
5	5	95	2
10	10	90	2
20	20	80	2
40	40	60	2

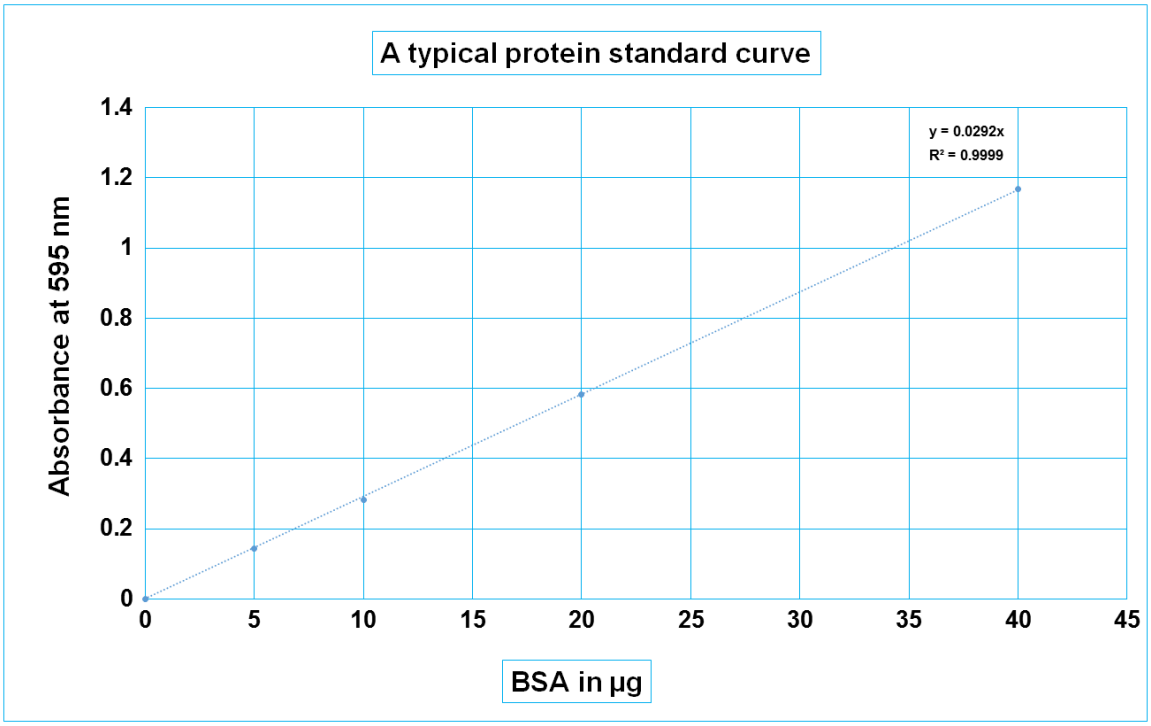

Figure 2-2 Standard curve for protein estimation

Absorbance of BSA (in µg) at 595 nm

2.12 Western Blotting

The acrylamide gel (12%) was prepared by mixing 3.3 ml of 40% bis-acrylamide with 4.2 ml distilled water (dH_2O) and 2.5 ml separating buffer in a universal tube. 100 µL of 10% (w/v) ammonium persulphate (APS) solution was added followed by 10 µL N, N, N', N'- tetramethylethylenediamine (TEMED). Few drops of isopropanol were added on top of the gel to remove the air bubbles and straight the surface of the gel, and the gel was left to polymerise for 20 mins. The isopropanol was removed after the gel polymerised and rinsed with dH_2O. dH_2O was removed by filter paper and then the stacking gel solution was prepared in a second universal tube by combining 1.45 ml of 40% bis-acrylamide with 6.1 ml dH_2O, and 2.5 ml stacking buffer. As before, 100 µL APS was added followed by 10 µL TEMED and the stacking gel was left to polymerise for a minimum of 20 mins. Slowly the combs, clamps, and gaskets were then removed taking care not to damage the wells and the gel plates were inserted into the electrophoresis chamber. The chamber was subsequently filled with electrode buffer [25 mM Tris, 192 mM glycine, 0.1% (v/v) SDS, pH 8.3]. A total of 400 ml electrode buffer was used to fill the tank, in the space between the two sets of glass plates. Take samples, sample buffers and molecular weight marker out of the freezer and defrost on ice. Equal measures of protein sample and sample buffer were mixed in an Eppendorf tube; the mixed samples were placed in boiling water for 15 mins. Molecular weight marker (5 µL) and the protein samples were gently loaded. Total protein (30 µg) was loaded into each well. Samples were separated by SDS-PAGE (12%) for~45 min at 65 V (when samples

were in the stacking gel) and switched to 200 V for separation until the dye, bromophenol blue, reached the bottom of the separation gel.

Table 2.2: Preparation of separating gel

Material	Volume
ddH_2O	4.2 ml
40% Acrylamide	3.3 ml
Separating buffer*	2.5 ml
10% APS	100 µL
TEMED	10 µL

*Preparation method as described above with a total volume of 10.11ml.

Table 2.3: Preparation of stacking gel

Material	Volume
ddH_2O	6.1 ml
40% Acrylamide	1.4 ml
Stacking buffer*	2.5 ml
10% APS	100 µL
TEMED	10 µL

* Preparation of the stacking gel as described as above with a total volume of 10.11ml.

2.12.1 Blotting

The nitrocellulose membranes (NCM) and 6 pieces of chromatography paper were soaked for 2 mins in Towbin buffer. The stacking gel was removed from the separating gel and discarded. The separating gel was sandwiched and assembled in an electro-blotter for each gel as follows: three pieces of blotting paper/NCM/gel/three pieces of blotting paper. Any air bubbles within the sandwiches were removed by rolling a clean 5 ml tip over the sandwich. Proteins were transferred onto the membrane at 45 mA per gel for one hour.

2.12.2 Blocking

Membranes were blocked with 1% (w/v) BSA in Tris-buffered saline (TBS) and Tween-20 buffer (TBS-T) for 1 hour at room temperature (RT) on a rotating shaker. The 1% (w/v) BSA was discarded, and the membranes were incubated separately in 10 ml of primary antibody solution (1:1000 dilution) at 4°C overnight on a rotating shaker. The following day, primary antibody solutions were transferred into labelled universal tubes and sodium azide was added to a final concentration of 0.02% (w/v) to prevent microbial contamination. The primary antibodies were then kept at 4°C and were used for up to one week. The membranes were washed five times with TBS-T for 10 min each at RT on a rotating shaker then were incubated for 1 hour at RT in 10 ml of goat anti-rabbit or rabbit anti-mouse horseradish peroxidase-conjugated (HRP) secondary antibody diluted in TBS-T containing 5% (w/v) skimmed milk powder (1:2000). After incubation, the secondary antibody solutions

were discarded, and the membranes were washed five times with TBS-T for 10 min each at RT on a rotating shaker.

2.12.3 Developing and Data Analysis

In a dark room, the membranes were immersed in enhanced chemiluminescence (ECL) solution. Chemiluminescence is a chemical reaction that generates energy in the form of light and fades over time. To prepare the ECL solution, an equal volume of solution-A and solution-B were mixed and put on the membrane in the darkroom for one minute, the excess reagent was then drained off, and the membranes were quickly wrapped in cellophane films and kept in a box. Then the membranes were taken to the G-Box or the ChemiDoc Touch Imaging System and were detected as chemiluminescent samples. The intensities of the bands on the membranes were quantified by Image-J analysis software. Day to day variations in luminescence could arise due to protein degradation or experimental errors. Therefore, loading controls were essential for proper interpretation of the Western blots and were used to normalise the levels of protein detected by confirming that the protein loading was the same across the gel. The expression levels of the loading control should not vary between the different sample lanes. The results were semi-quantitative and compared to the control. α-Tubulin was used as a loading control.

2.13 Confocal and Fluorescence Microscopical Analysis

Glass coverslips were bathed in 100% ethanol for 10-20 min and left to air dry in a sterile environment. The coverslips were put in a 24-well plate and pre-coated with 500 µL of 0.1 % (v/v) poly-L-lysine solution. After 30 min incubation, the coverslips were washed with PBS and the hBMECs were seeded in complete EBM-2 (2% FBS plus growth factors) medium. After fixing with 4% (w/v) PFA in PBS, cells were washed with PBS and permeabilised with 0.1% (v/v) Triton X-100 in PBS. After blocking with 1% (w/v) BSA in PBS incubations with primary antibodies against selected proteins were performed with conditions as recommended by the manufacturers, overnight at 4°C. Secondary antibodies Alexa Fluor 488 goat anti-rabbit IgG, Alexa Fluor 488 goat anti-mouse IgG, Alexa Fluor 568 anti-rabbit and Alexa Fluor 460 donkey anti-goat (Molecular Probes/Invitrogen) were incubated with conditions as recommended by the manufacturer. Rhodamine-phalloidin (Molecular Probes/Invitrogen) was used to stain filamentous actin (F-actin). Nuclei were stained with Hoechst 33258 solution (Sigma, UK). The coverslips were incubated for 2 hours at room temperature in the dark. The secondary antibodies were removed, and the coverslips were washed 5 times for 5 mins each with PBS in the dark. To mount coverslips, the edge was blotted on tissue paper to dry off excess liquid and cell side was placed down on the drop of mounting media (VECTASHIELD Mounting Medium with DAPI) on a glass slide. The coverslip was stabilised on a slide using nail polish and left to dry overnight before viewing. The images were captured using Axivoert fluorescence microscope. Samples without primary antibodies were used as negative controls. Confocal microscopy was performed with a Leica TCS SPE1000

system and the accompanying Leica Application Suite Advanced Fluorescence (LAS AF) software (Leica Microsystems Ltd, Milton Keynes, Bucks, UK). Images were acquired at 1024x1024 pixel resolution. Cells were pre-treated with roscovitine (50 μM) for 24 hours or the appropriate vehicle (DMSO) and then seeded on the plates. The signal of autofluorescence was tested, including a negative control antibody (IgG) staining, as well. In this experiment, cells were treated in triplicate for each experimental condition and pictures of five areas of each well were taken.

2.14 Statistical analysis

Statistical analysis was made by using the Microsoft Excel 2013 program. The results of each experiment determined as the mean ± standard deviation. Data shown were analysed for significance using Two-Way ANOVA test. Differences with p values ≤0.05 were considered statistically significant. Each experiment was repeated at least three times.

Statistical difference between more than two groups was determined using Two-way ANOVA and Bonferroni multiple comparison tests. Statistical significance was set at $p<0.05$.

Two-Way ANOVA test was used to assess the effects of various types of treatment on a different type of cells and to assess the interaction between treatments (FGF-2, DAPT, FGF-2 + DAPT) and type of cells (hBMEC, CIP and OVCdk5).

Western blot was repeated at least twice but there was no statistical analysis was performed here.

Statistical analysis and significance of data were determined using graph pad prism version (5). Graph pad software, San Diego, California, USA, www.graphpad.com.

No statistical analysis on Western blotting – too variable from one experiment to another.

Chapter 3 Results

3.1 The Transfection and Selection of Stable Expression Cell Clones

3.1.1 GFP-fluorescence Detection of CDK5 Inhibitor Peptide (CIP)

Before all the experiments, hBMEC cell lines were checked to confirm the transfection of CDK5 inhibitor peptide (CIP) by the expression of Green Fluorescent Protein (GFP) (Figure 3.1A), and that there were no fluorescent signals in hBMEC normal control cells (Figure 3.1B).

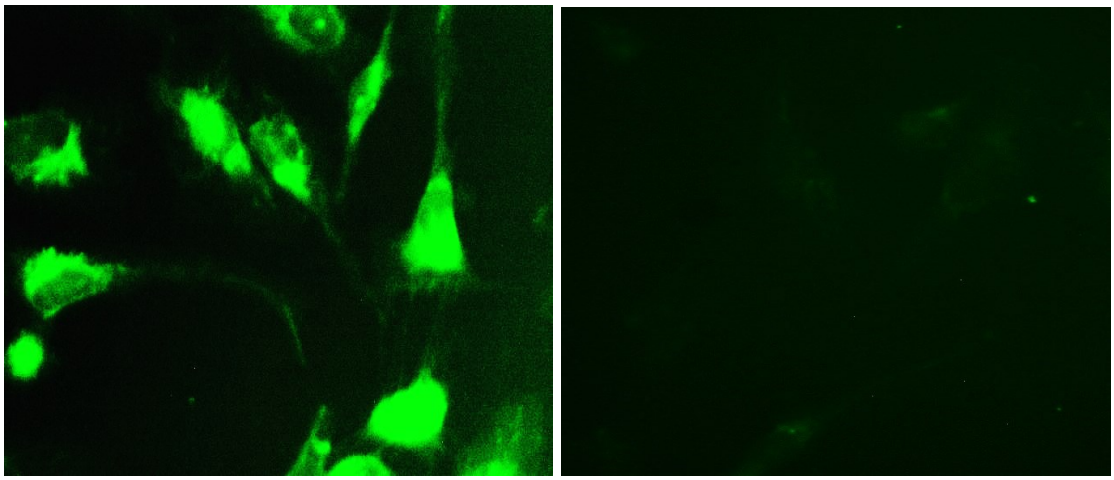

A: CIP B: hBMECs

Figure 3-1 Expression of GFP fluorescent marker in CIP-17 clones transfected with pcDNA-GFP

GFP Fluorescence images showing the successful transfection of CIP in stable hBMEC transfectants (A). There was no fluorescence in hBMEC normal control cells (B).

3.1.2 GFP-fluorescence Detection on OVCdk5 Transfectants

This was done to confirm that the transfection of the overexpressed CDK5 kinase (OVCdk5) in stable hBMEC transfectants was successful (Figure 3.2 A), but there was no fluorescence signal in hBMEC normal control cells (Figure 3.2 B).

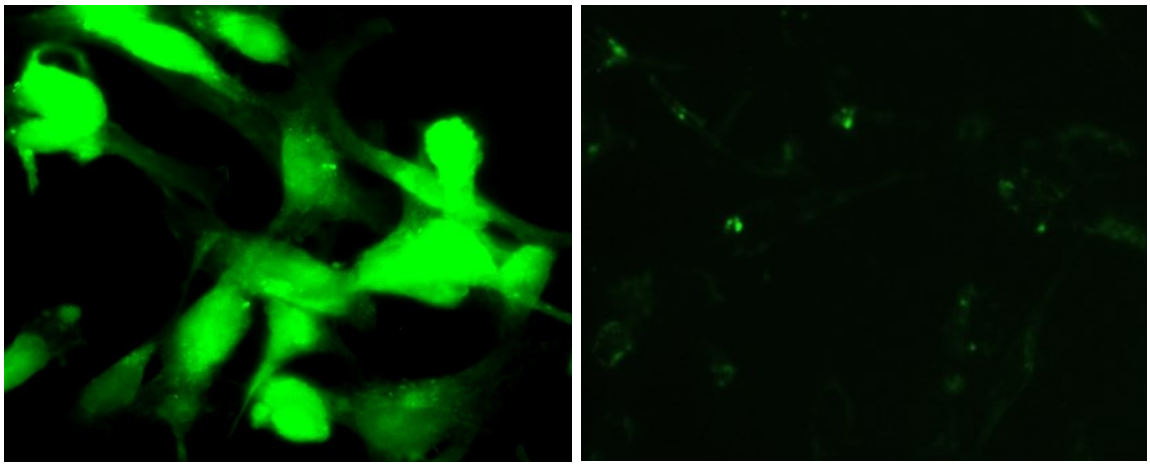

A: OVCdk5 B: hBMECs control

Figure 3-2 Expression of GFP marker in overexpressed Cdk5 clones transfected with pcDNA-GFP

GFP-fluorescence images shows the transfection of Cdk5 clones in hBMECs.

This experiment was performed to make sure that Cdk5 was expressed by stable OVCdk5 transfected hBMEC. Image (A) shows Cdk5 was expressed in OVCdk5-transfected hBMEC, and there are none fluorescence signals in normal hBMEC (B).

3.2 Cell Culture

3.2.1 Introduction

Endothelial cells (ECs) normally undergo angiogenesis that includes migration and tube formation. Our aim was to investigate whether this property is altered under hypoxic conditions.

3.2.2 Results

Hypoxia almost completely inhibited *in vitro* angiogenesis in hBMECs, as seen by the reduction in cell migration from scratched monolayer tubule-like structure formation and/or cell sprouting. Our study demonstrates that Cdk5 activation, through its major substrate p35, provides a key trigger for the initiation and maintenance of *in vitro* brain EC angiogenesis and that this interaction and signalling cascade are crucial for ensuring correct cytoskeletal organisation/dynamics. Our results also show that by introducing a natural inhibitor of the p25/Cdk5 complex formation, the CIP peptide (Kesavapany et al., 2007), we were able to alter the balance of p25/p35-Cdk5 signalling in favour of p35, and concomitantly significantly increase *in vitro* brain EC angiogenesis during normoxia. Most importantly, this also promoted cell survival and capillarisation in hypoxic conditions (Bosutti et al., 2013).

3.2.2.1 Hypoxia-Induced Cell-Damaging Effects in hBMECs

Propidium Iodide (PI) is usually excluded from surviving cells and used to identify dead cells in a population. Cells were observed using fluorescence microscopy with two filters, DAPI fluorescent filter and rhodamine filter with × 40 magnification. hBMECs considered apoptotic will display signs of apoptosis such as condensation of nuclear materials, incorporation of PI stain (colour in red**,** when PI staining) in the nucleus, disruption of cell cytoplasm and shrinkage of the cells. The normal cells appeared regular with round clear blue nuclei.

The representative results are shown in Figure 3.3 (image) and Figure 3.4 (graph). Hypoxia-induced cell-damaging effects in hBMECs showed increased PI stained nuclear inclusion (the arrows indicate the nuclei stained by PI, in red).

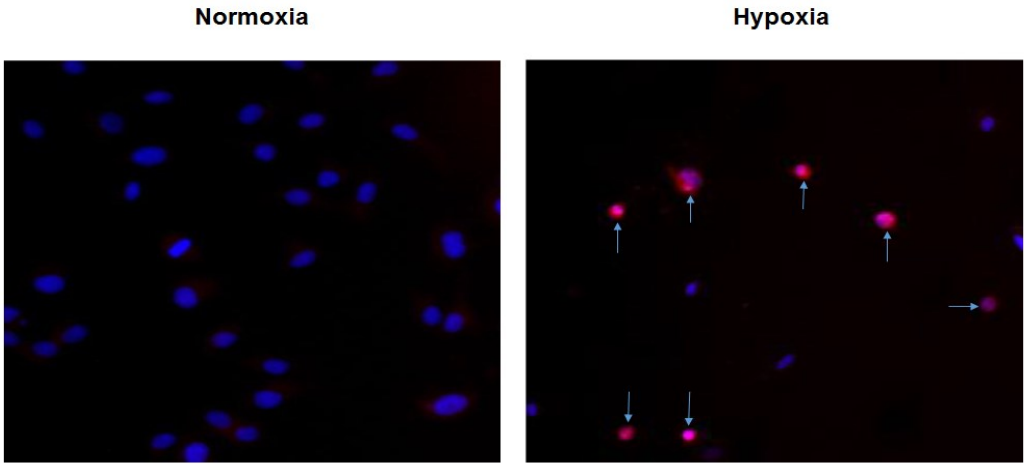

Figure 3-3 PI staining and the presence of PI in nucleus representative damage to the cell exposed to hypoxia

In this experiment, the efficiency of hypoxia was evidenced by the increased nuclear inclusion of PI. Surviving cells remained blue, but others became apoptotic and were stained red by PI (arrows, B).

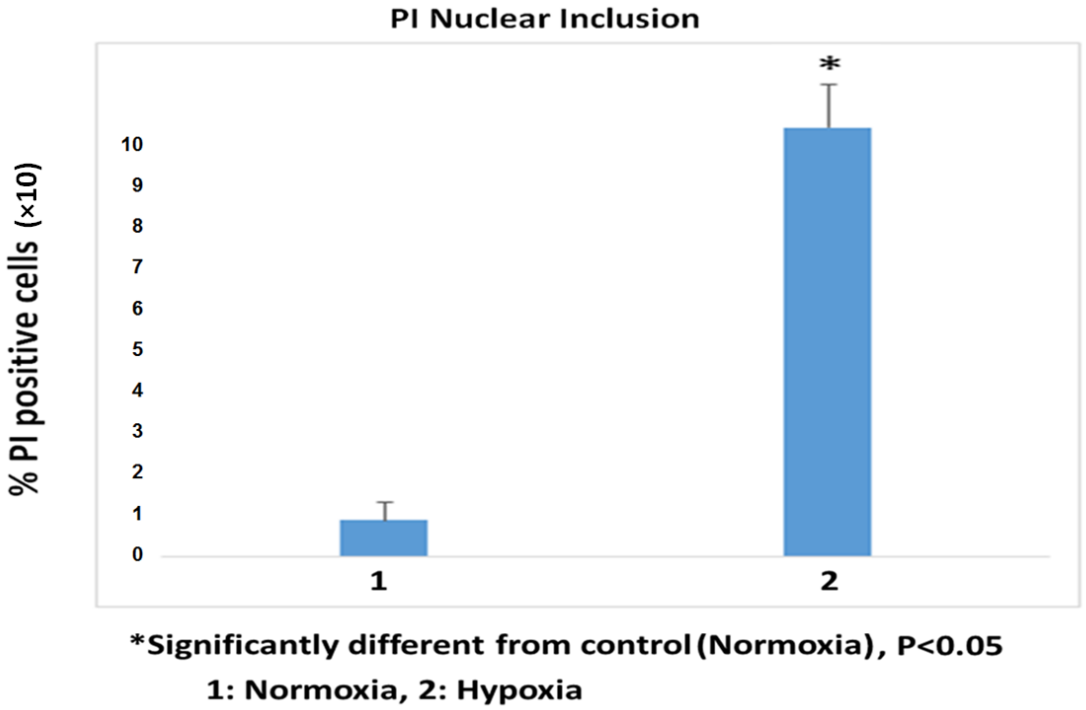

Figure 3-4 Bar chart indicates the significant difference from the normoxia control and hypoxia-induced cell-damaging in hBMECs

The percentage of hBMECs stained by PI was increased in hypoxia compared to normoxia. The bars represent the standard deviation.

PI staining showing a *significant increase (80%) in the number of PI-stained cells in hypoxia *vs.* normoxia, p <0.05. The experiments were performed in triplicate wells and repeated three times.

3.2.2.2 Cell Angiogenesis Assay

Previous work from our laboratory showed that Cdk5 can promote angiogenesis, hence our aim was to investigate the role of Cdk5 in promoting angiogenesis in normal versus stroke mimicking conditions (hypoxia) as well as the role of CIP in

reversing cellular apoptosis and allowing angiogenesis under hypoxia. To fulfil this aim, a series of experiments was conducted related to wound healing and tube formation in hBMECs, CIP-expressing cells and OVCdk5.

3.2.2.2.1 Cell Migration Assay

The scratch wound methods were applied to the hBMECs, Cdk5 kinase inhibitory peptide (CIP) and (OVCdk5) transfectants to compare the effects hypoxia. The images were taken using a camera under the microscope (Figure 3.5).

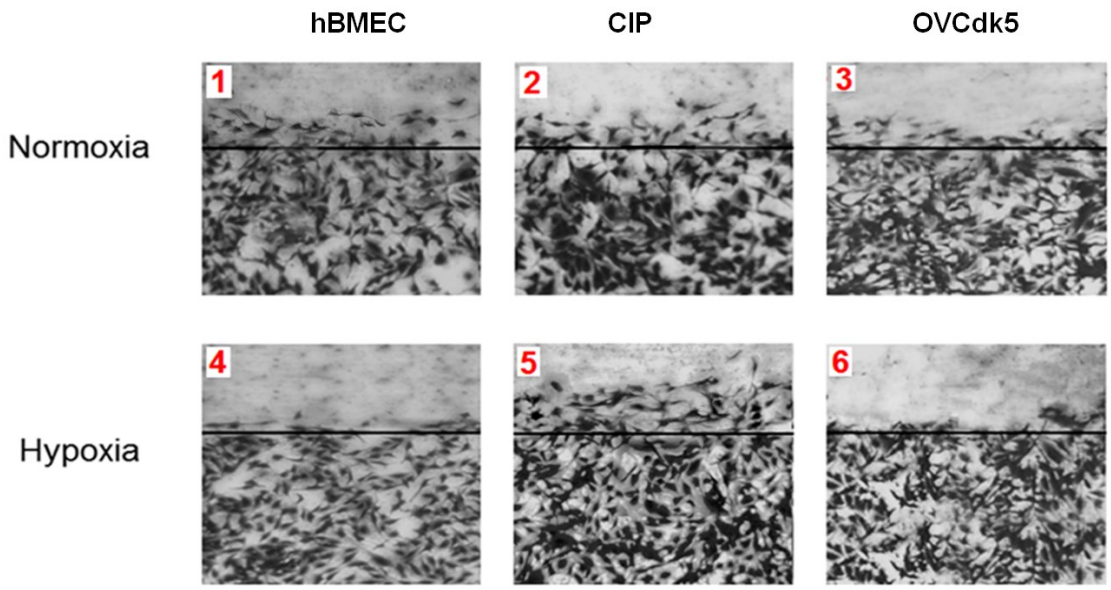

Figure 3-5 Cell migration assay on CIP- expressing cells and OVCdk5

1: hBMECs (normoxia), 2: CIP expressing cells (normoxia), 3: OVCdk5 (normoxia), 4: hBMECs (hypoxia), 5: CIP expressing cells (hypoxia) and 6: OVCdk5 (hypoxia).

Phase contrast images showed the impact of Cdk5 deregulation on cell migration under hypoxic conditions (1% O_2, 24 hours) compared to the normoxic condition (three views per well).

Cell migration assays were performed in hypoxia and normoxia, in hBMECs, CIP-expressing cells and overexpressing Cdk5 (OVCdk5). Hypoxia inhibited hBMECs migration, as seen by the reduction (number of cells in the wound area), Figure 3.5 (4, 6), but there were significantly more of cells in CIP-expressing cells, Figure 3.5 (5). Experiments were performed in triplicate wells and were repeated three times.

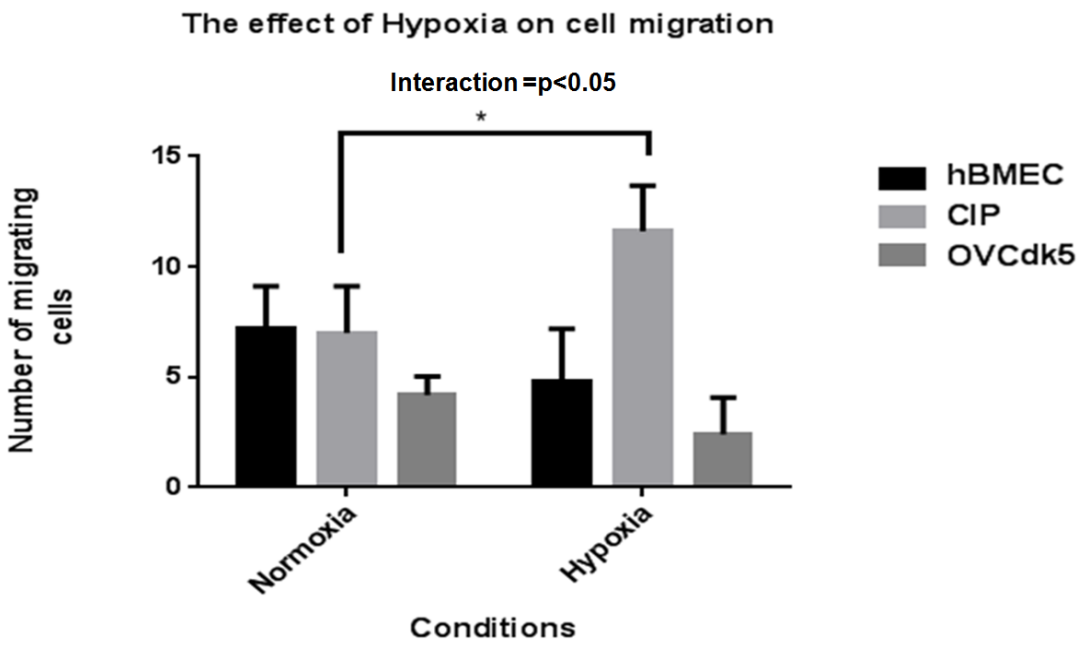

Figure 3-6. The effect of hypoxia on cell migration.

The effect of 24 hours incubation in hypoxia on the migration of hMBECs, CIP-expressing cells and OVCdk5 cells.

A * significant increase in the number of migrated CIP-expression cells in hypoxia *vs.* normoxia, p <0.05. Two-Way ANOVA test was used to assess the effects of hypoxia and normoxia on a different type of cells. The experiments were performed in triplicate wells and repeated three times.

3.2.2.2.2 Effects of DAPT on Cell Migration

The Cdk5 inhibition assay was performed during 24 hours of Cdk5 inhibition (cells treated with DAPT at 10μM), in normal hBMECs and OVCdk5. DAPT inhibited hBMECs migration, as seen by the reduction (in the number of cells in the wound

area, Figure 3.7 (3). DAPT also inhibited cell migration in OVCdk5, as seen by the number of cells that migrated to the wound area, Figure 3.7 (7). There was a large number of migrated cells (incubated with FGF-2) in the wounded area, Figure 3.7 (2, 6).

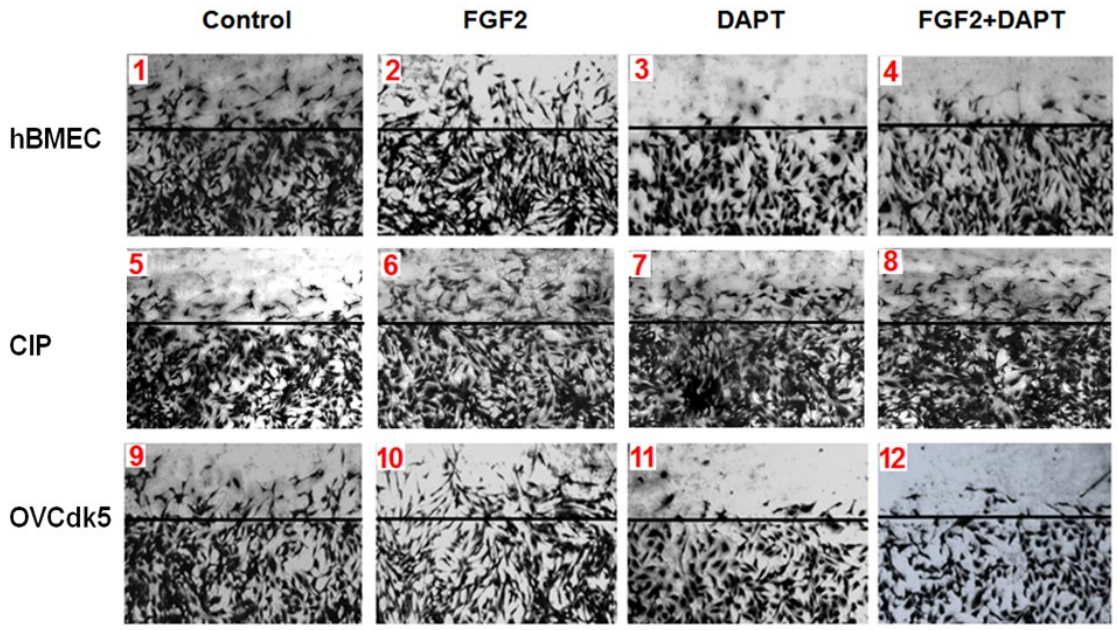

Figure 3-7 Effects of Cdk5 inhibition on cell migration

Top row-1: hBMECs control, 2: hBMECs positive control (FGF-2 25ng/ml), 3: hBMECs treated with DAPT (10μM) and 4: hBMECs treated with DAPT (10μM) plus FGF-2 (25ng/ml). In the middle- 5: CIP, 6: FGF2, 7: CIP + DAPT, 8: CIP+FGF2+DAPT. Lower panel – 9: OVCdk5 control, 10: OVCdk5 treated with FGF-2 25ng/ml, 11: OVCdk5 treated with DAPT (10μM) and 12: OVCdk5 treated with DAPT (10μM) together with FGF-2 (25ng/ml). The experiments were performed in triplicate wells and repeated three times.

Phase contrast images showing the impact of DAPT (Cdk5 inhibitor) on cell migration compared to normal hBMECs. DAPT inhibits cell migration, as seen by the number of cells migrated into the wound area (Figure 3.7-5). It can be seen from

the images that more cells had migrated into the wound area (both of the hBMECs and the OVCdk5 than the cells treated with DAPT. DAPT inhibits the effects of Cdk5 on cell activation. However, CIP did not produce the same level of response compared to OVCdk5, the reason could be the biological effect of CIP-expression is blocking apoptosis through Cdk5/p25 signalling pathway.

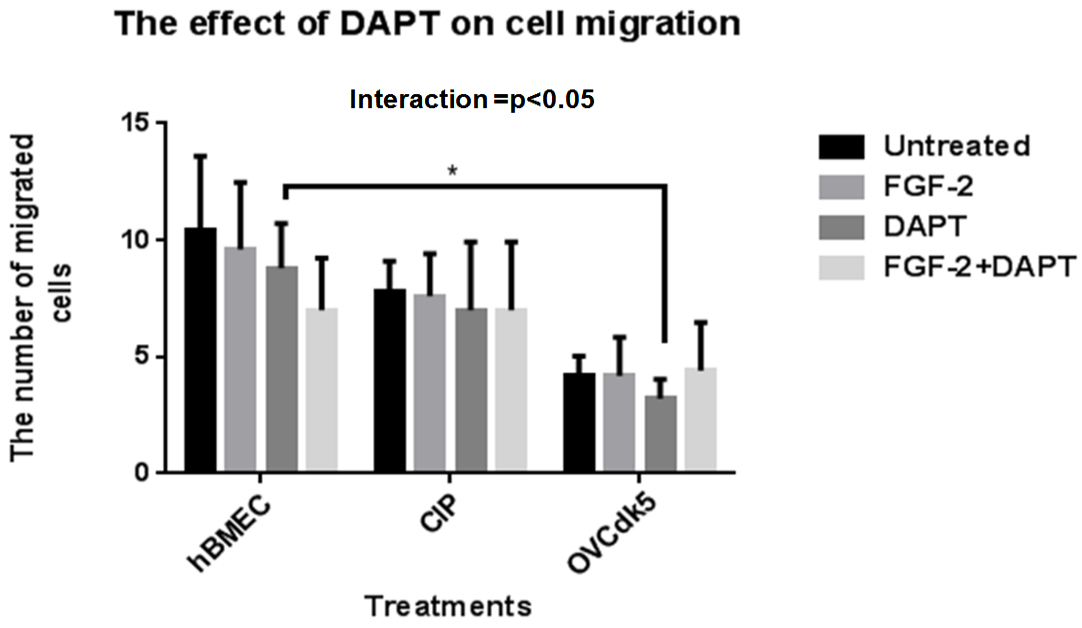

Figure 3-8 The effect of DAPT on cell migration.

The effect of Cdk5 inhibitor (DAPT) on hBMECs, CIP-expressing cells and OVCdk5 cell migration. After 24 hours incubation in hypoxia, DAPT is the same concentration (10μM).

A *significant effect of DAPT treatments was observed on OVCdk5 cells compared to hBMECs, $p<0.05$. Two-Way ANOVA test was used to assess the effects of various types of treatment on a different type of cells and to assess the interaction between treatments (FGF-2, DAPT, FGF-2 + DAPT) and type of cells (hBMEC, CIP

and OVCdk5). The experiments were performed in triplicate wells and repeated three times.

3.2.2.2.2 The Effects of Calpain on Cell Migration Assay

The effect of calpain on hBMEC migration assay was analysed after 24 hours, incubation under hypoxic condition compared to the normal condition. The images show significantly more cells in the wounded area under normal conditions (1 top left) than the cells treated with calpain (2 top right). There are decreased numbers of migrated cells (3 lower row left) compared to cells in hypoxia (4 lower row right).

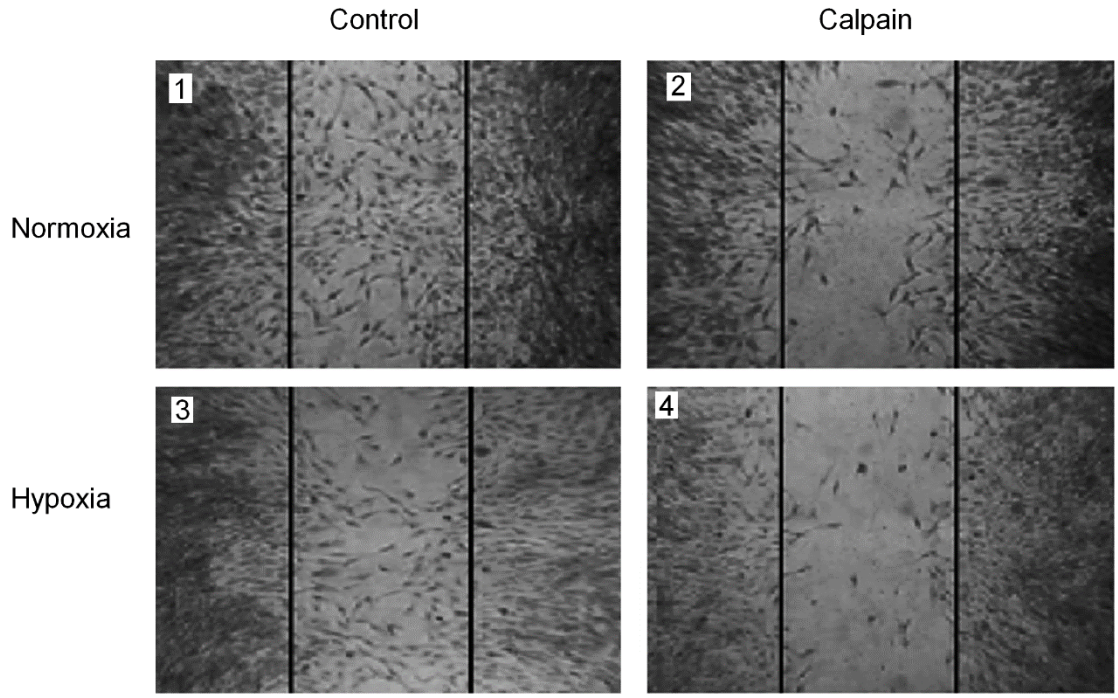

Figure 3-9 The effect of calpain on hBMECs migration assay

1: hBMECs (normoxia), 2: hBMECs treated with calpain (10μg/ml, normoxia), 3: hBMECs (hypoxia) and 4: hBMECs treated with calpain (10μg/ml, hypoxia).

Assays were performed over 24 hours, incubation, and the images were taken using a camera under the microscope (Figure 3.9).

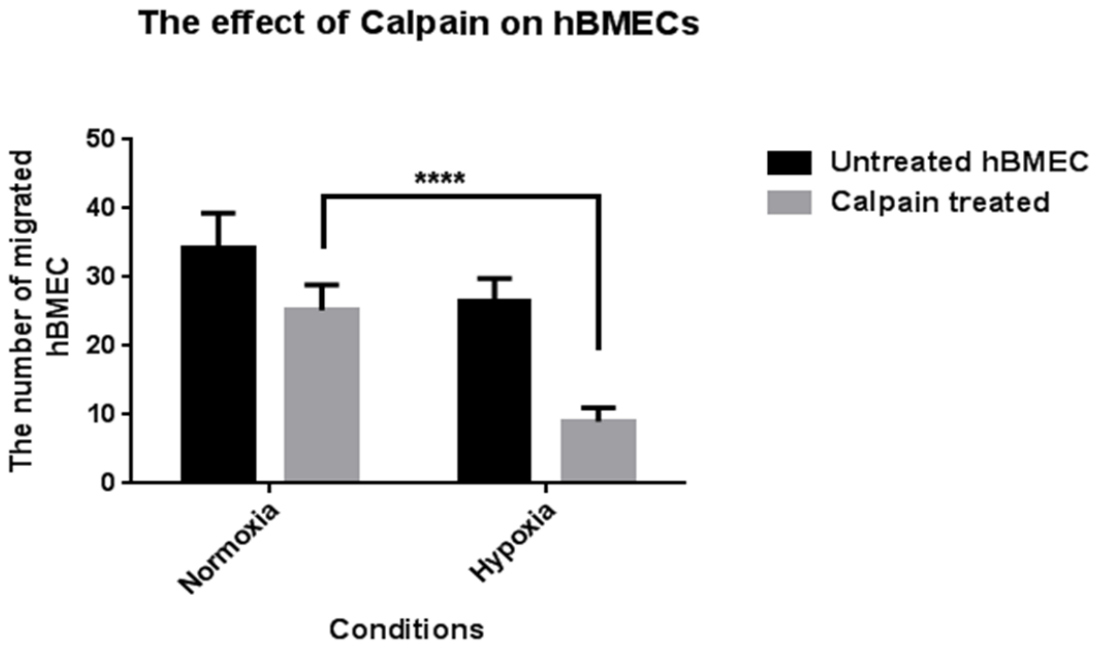

Figure 3-10 Bar chart representing the cell migrated numbers

The effect of 24 hours incubation calpain treatment on hBMEC, -cell migration compared to untreated cells.

Two-Way ANOVA test was used to assess the effects of hypoxia and normoxia on a different type of cells and to assess the interaction between them. It showed a ****significant decrease in the number of treated migrated cells ($p<0.0001$).

3.2.2.2.3 Effect of Hypoxia on Tube Formation

In order to investigate the consequences of hypoxia and Cdk5 deregulation on hBMECs tube formation, the assays were performed during 24 hours of the hypoxic and normoxic-control conditions, in hBMEC, CIP-expressing cells and OVCdk5. Hypoxia almost completely inhibited hBMECs forming tube-like structures, Figure 3.11 (4). The OVCdk5 and the CIP-expressing cells were still able to migrate to form new capillary structures under hypoxic condition, Figure 3.11 (5, 6).

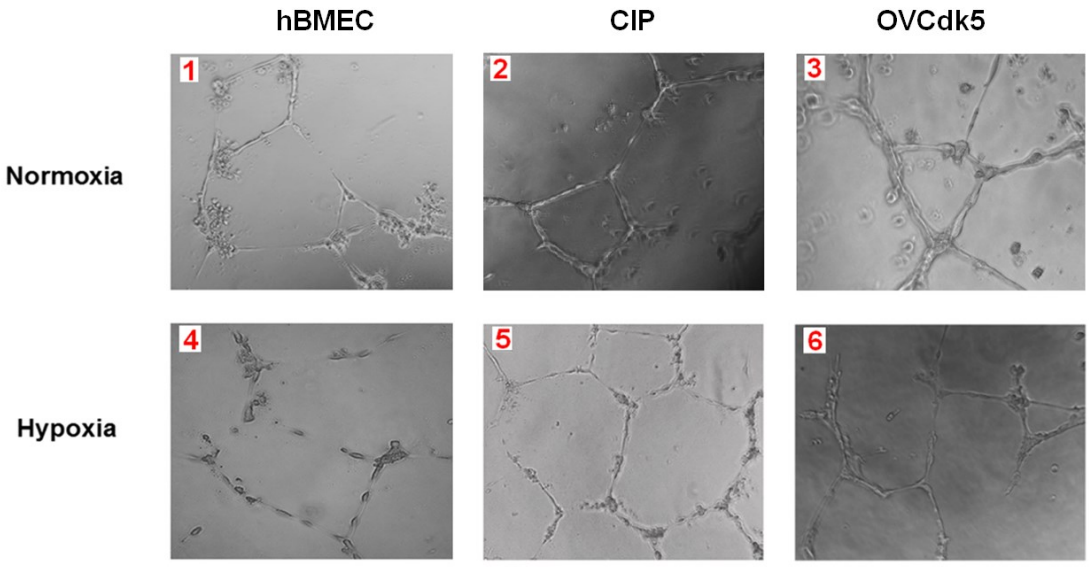

Figure 3-11 Phase contrast images showing the impact of Cdk5 deregulation on cell capillary tube formation under hypoxia (1% O2, 24 hours) compared to normoxic conditions

1: hBMECs (normoxia), 2: CIP-expressing cells (normoxia), 3: OVCdk5 (normoxia), 4: hBMECs (hypoxia), 5: CIP-expressing cells (hypoxia) and 6: OVCdk5 (hypoxia).

Phase contrast images showing the impact of hypoxia and Cdk5 deregulation on tube formation assay. In hBMECs, CIP-expressing cells and OVCdk5, hypoxia

almost completely inhibited tube formation in hBMECs, Figure 3.11 (4). CIP-expressing cells were still able to form tube-like structures under hypoxic conditions, Figure 3.11 (5).

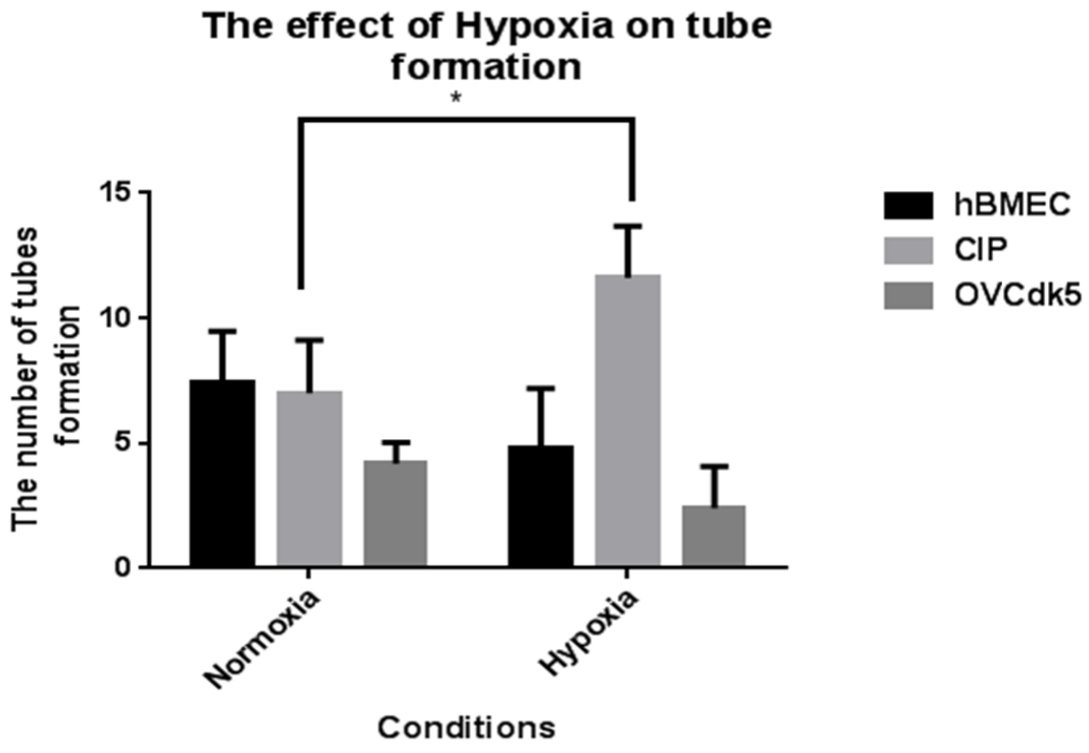

Figure 3-12 The effect of hypoxia on tube formation

The effect of 24 hours incubation in hypoxia on hMBEC, CIP-expressing cells and OVCdk5 tube formation compared to the normoxic condition.

Two-Way ANOVA test was used to assess the effects of hypoxia and normoxia on a different type of cells and to assess the interaction between them. It showed a *significant increase in the number of tube formation in CIP-expression cells in hypoxia vs normoxia ($p < 0.05$).

3.2.2.2.4 The Effect of DAPT on Tube Formation

Cdk5 inhibition in the tube formation assay was performed during 24 hours in normal hBMECs, CIP-expressing cells and OVCdk5 in the presence or absence of the inhibitor (DAPT; 10uM).

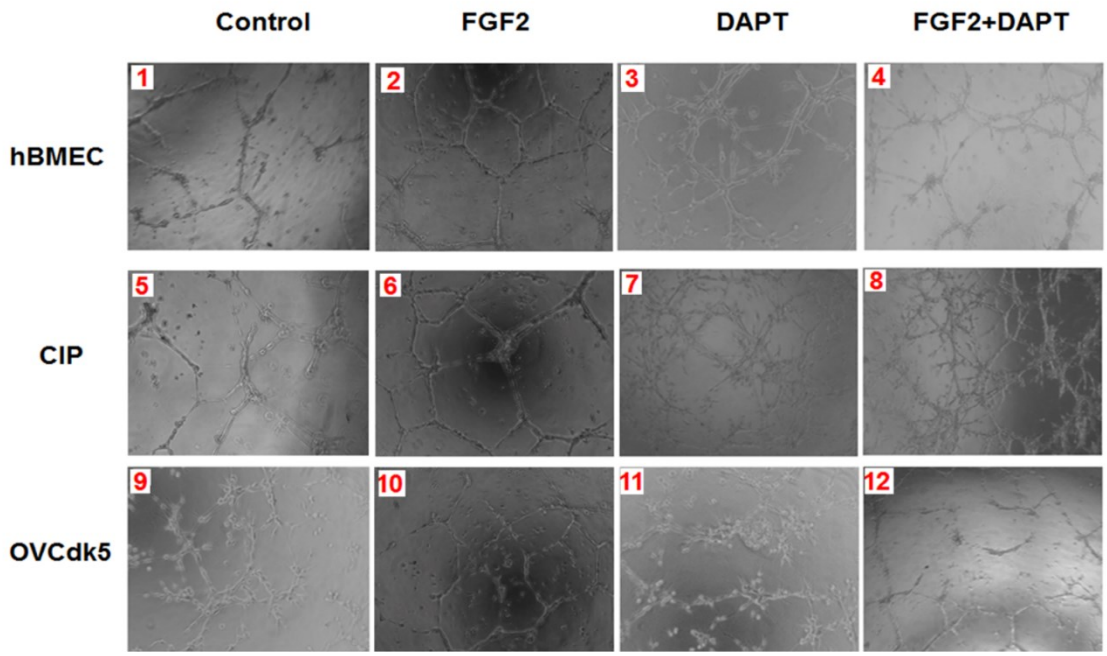

Figure 3-13 Images of tube formation assay on hBMECs CIP-expressing cells and OVCdk5

1: Normal hBMECs control, 2: hBMECs positive control (treated with FGF-2), 3: hBMECs treated with DAPT (10μM), 4: hBMECs treated with DAPT and FGF-2, 5: OVCdk5 control, 6: OVCdk5 treated with FGF-2, 7: OVCdk5 treated with DAPT and 8: OVCdk5 treated with DAPT and FGF-2. The experiments were performed in triplicate wells and repeated three times.

The capillary tube formation was inhibited in OVCdk5, as seen by the reduction in tubule-like structures. The cells were not able to migrate to form new capillary structures in the presence of DAPT, Figure 3.13 (11), CIP-expressing cells did not have the same response compared to OVCdk5, the reason could be the biological

effect of CIP-expression is blocking apoptosis through the Cdk5/p25 signalling pathway, Figure 3.13 (7).

Assays were performed during 24 hours of incubation with CDK5 inhibitor (DAPT; 10μM), in hBMECs, CIP-expressing cells and OVCdk5. DAPT inhibited OVCdk5 tube formation, as seen by the reduction in tubule-like structures, Figure 3.13 (11). The CIP-expressing cells were still maintained tube formation in the presence of DAPT, Figure 3.13 (7).

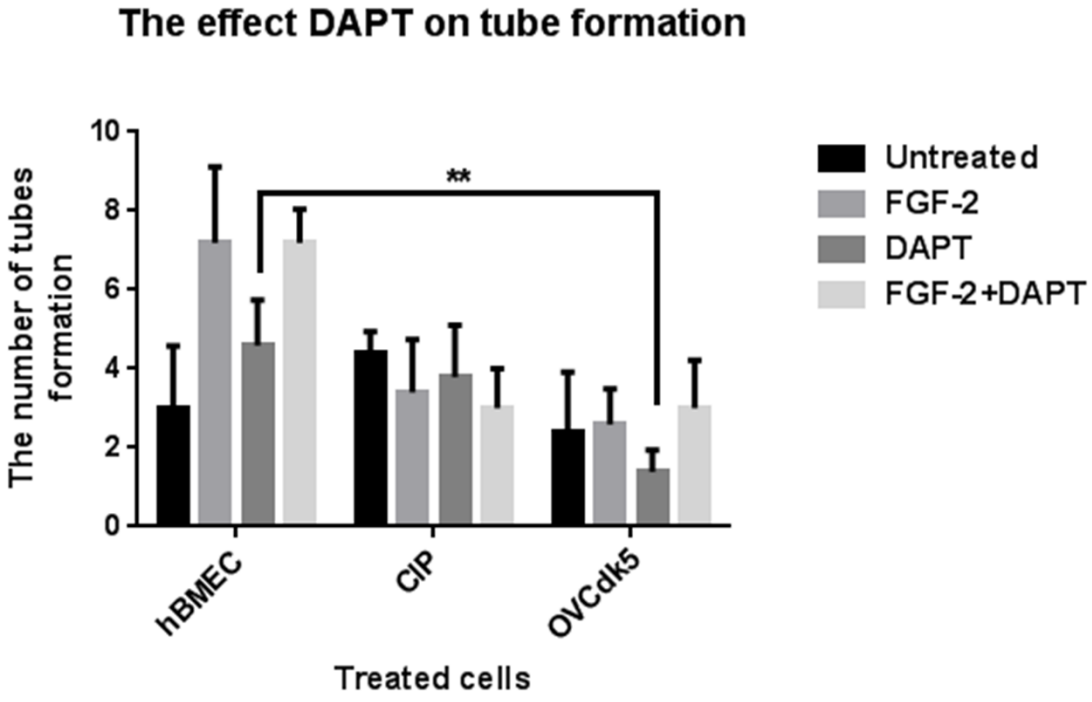

Figure 3-14 The effect of the DAPT on cells under hypoxia

The effect of DAPT on hBMECs, CIP-expressing cells and OVCdk5 tube formation after 24 hours incubation in hypoxia, DAPT was used at the same concentration (10μM).

Two-Way ANOVA test was used to assess the effects of various types of treatment on a different type of cells and to assess the interaction between treatments (FGF-

2, DAPT, FGF-2 + DAPT) and type of cells (hBMEC, CIP and OVCdk5). It showed a **significant effect of DAPT treatments was observed on OVCdk5 compared to hBMECs, $p<0.01$. The experiments were performed in triplicate wells and repeated three times.

3.2.2.2.5 hBMECs Spheroid Sprouting Assay

Sprouting occurred from the spheroid core, and the sprout length was estimated with the Image-J software (using five spheroids with similar spheroid core sizes for each condition). The methylcellulose gel was prepared prior to the experiment

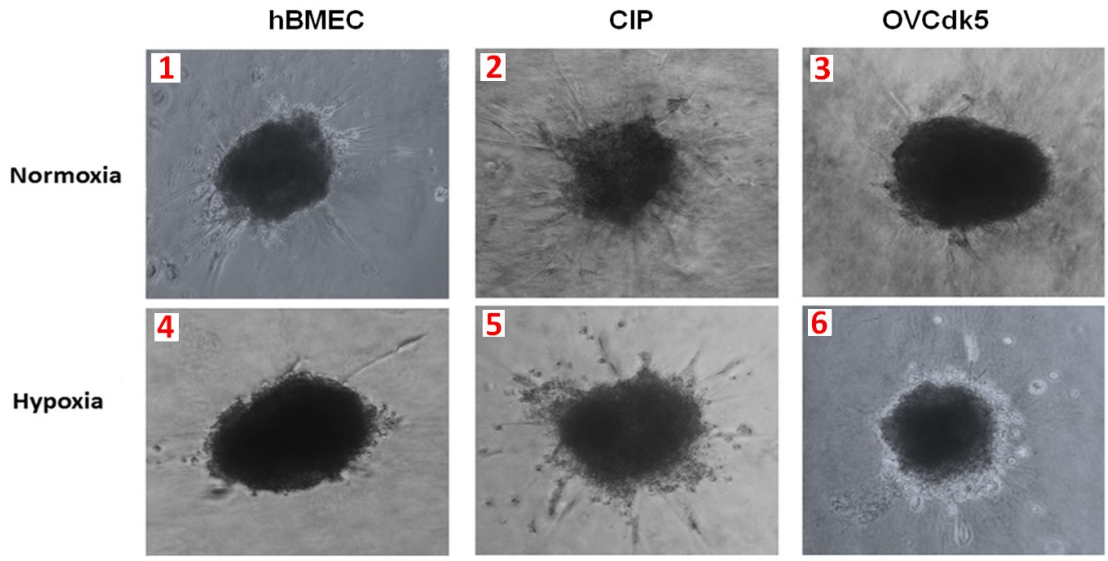

Figure 3-15 CIP expression cells support *in vitro* spheroid sprouting during hypoxia

1: hBMECs (normoxia), 2: CIP-expressing cells (normoxia), 3: OVCdk5 (normoxia), 4: hBMECs (hypoxia), 5: CIP-expressing cells (hypoxia) and 6: OVCdk5 (hypoxia).

Phase contrast images showing the impact of Cdk5 deregulation on spheroid cell sprouting under hypoxic (1% O_2, 24 hours) compared to normoxic conditions. The image (Fig 3-15) shows that there were fewer sprouts from hBMECs (4) compared to CIP-expressing cells (5), but there were no sprouts from OVCdk5 (6) under hypoxia. In addition, there were a number of sprouts were seen from CIP-expressing cells (3) and it was also seen in hBMECs (1), but few in OVCdk5 under normal conditions.

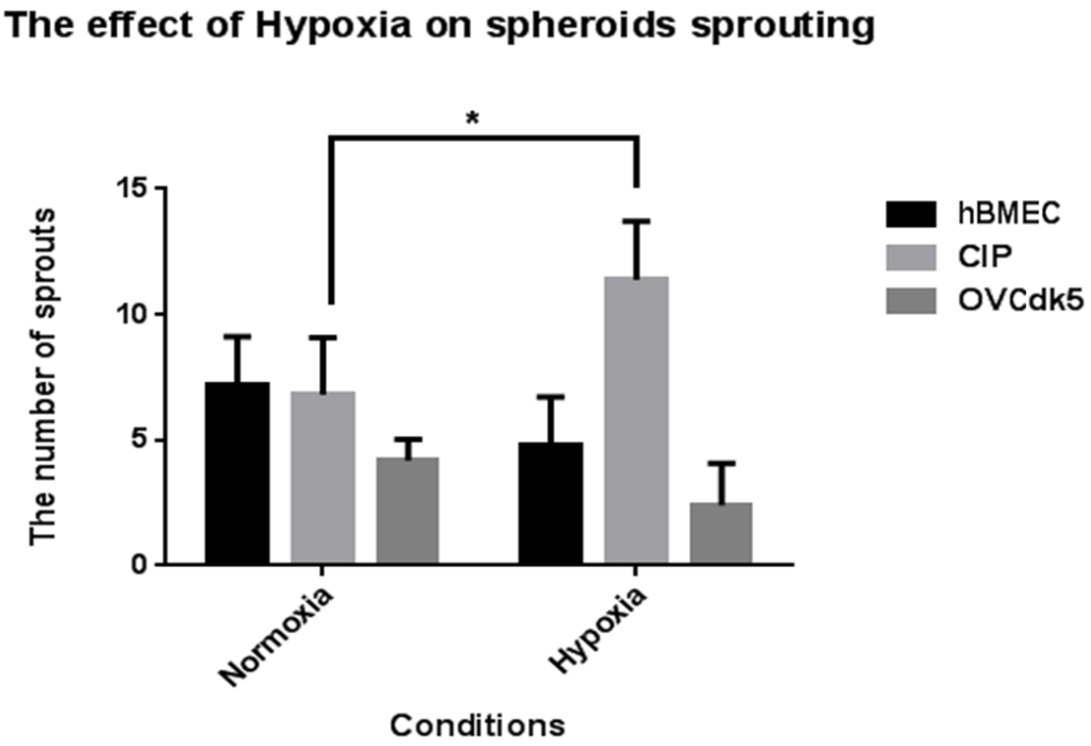

Figure 3-16 The effect of hypoxia on the spheroids sprouting

The effect of 24 hours incubation in hypoxia on hBMECs, CIP-expressing cells and OVCdk5 on spheroid sprouting compared to the normoxic condition.

Two-Way ANOVA test was used to assess the effects of hypoxia and normoxia on a different type of cells and to assess the interaction between them. It showed a significant (*: $p<0.05$) increase in the number of spheroid sprouting in CIP-expressing cells in hypoxia vs normoxia. The experiments were performed in triplicate wells and repeated three times.

3.2.3 Discussion

Angiogenesis has various roles under pathological conditions. Resistance to angiogenesis by hypoxia may be overcome by the use of therapeutic targets directed to areas of ischaemic damage in the brain. This goal can only be implemented if we understand the pathological processes and molecular details of hypoxia-mediated damage and the molecular partners involved. To fulfil this aim, we tested angiogenesis in ECs incubated under hypoxic conditions. When ECs were cultured under stroke-mimicking conditions (hypoxia), there was no migration and/or tube formation due to oxygen deprivation. However, transfecting ECs with the Cdk5 inhibitor peptide (CIP) under hypoxia allowed for migration and tube formation. This suggests 1) The protective role of CIP under hypoxic conditions allows migration and tube formation and 2) Hypoxia-mediated prevention of angiogenesis could be facilitated by Cdk5. Hence, we assume that Cdk5 is involved in hypoxia-mediated damage, and/or activated under hypoxic conditions to facilitate angiogenesis prevention. This phenomenon was previously confirmed by Liebl, who suggested the involvement of Cdk5 in regulating EC migration and angiogenesis (Liebl et al., 2010). The results may promote the use of Cdk5 as a novel target for anti-

angiogenic therapy. Inhibition of the Cdk5-p25 complex formation may enhance Cdk5 availability for p35 binding, hence leading to the activation of the small GTPase Rac1 and results in an organisation of the actin cytoskeleton as well as the formation of focal adhesion or the microtubules necessary for cell migration and angiogenesis (Liebl et al., 2010). Thus, p35 is directly associated with CIP action in inhibiting Cdk5 (or its phosphorylated form), through some form of association (binding) with Cdk5. Evidence suggests that the apoptosis of neurons after a stroke is strongly associated with Cdk5 hyperactivation mediated by its activator p25 (Love, 2003). This, taken together with 1) the increased ratio of p35/p25 in CIP response to hypoxia and 2), the co-localisation of p35 and Cdk5 (which was also evident in CIP-expressing ECs), suggests that CIP inhibits Cdk5 through facilitating its binding and inactivation by p35, thus preventing Cdk5 from p25-binding and hyperactivation, which is implicated in stroke pathology.

3.3 Cell Attachment and Spreading

3.3.1 Introduction

Previous studies have demonstrated the role of Cdk5 in the regulation of cytoskeleton dynamics and motility (Slevin et al., 2006), through the modulation of talin stability and cell migration (Huang et al., 2009). Thus, we investigated the interplay of Cdk5 and p35 with components that control cellular motility.

3.3.2 Results

3.3.2.1 Cytoarchitectural Properties of Cdk5, Activated Cdk5 (pCdk5) and p35

The co-localisation of p35 during spreading, culminated with the formation of focal clusters with Cdk5. Thus, p35 and p-Cdk5 were co-localised at the tips of actin fibres of hBMECs and CIP-expressing cells. These actin tips are linked to the directional movement of the spreading and movement of hBMECs. The co-localisation of p35 and Cdk5 are in favour of the second scenario relating to p35 binding and/or inhibition of Cdk5 to prevent hypoxia-mediated damage.

When activated during in early spreading (pCdk5 and p35), Cdk5 is localised at the tip of actin fibre (Figure 3.17). Figure-3.18 shows the active Cdk5 [pCdk5, $pTyr_{(Ser15)}$] localised at actin tips (arrows) in early spreading. Figure-3.19 shows the pCdk5 co-localisation in late spreading and Figure-3.20 shows the pCdk5 localisation and elongated moving. While Figure-3.21 shows p35 is co-localised with actin stress fibres in early stage moving, and Figure-3.22 shows the cell spreads in filament tips in late spreading cells. Moreover, the p35 localisation and elongated moving are demonstrated in Figure-3.23.

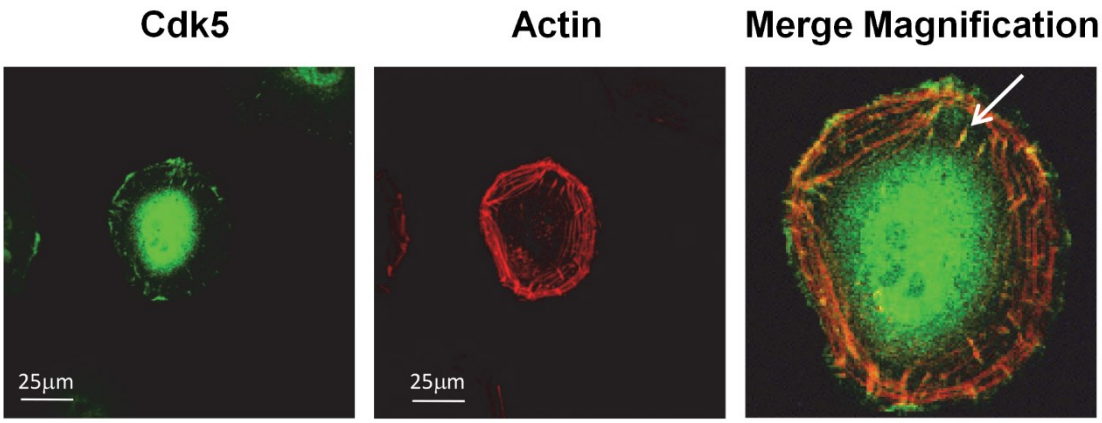

Figure 3-17 Cdk5 localisation with actin in hBMECs

Confocal microscopy showing the Cdk5 localisation and early stage spreading. The merged magnification shows the Cdk5 is located on the tip of the actin fibre (arrow).

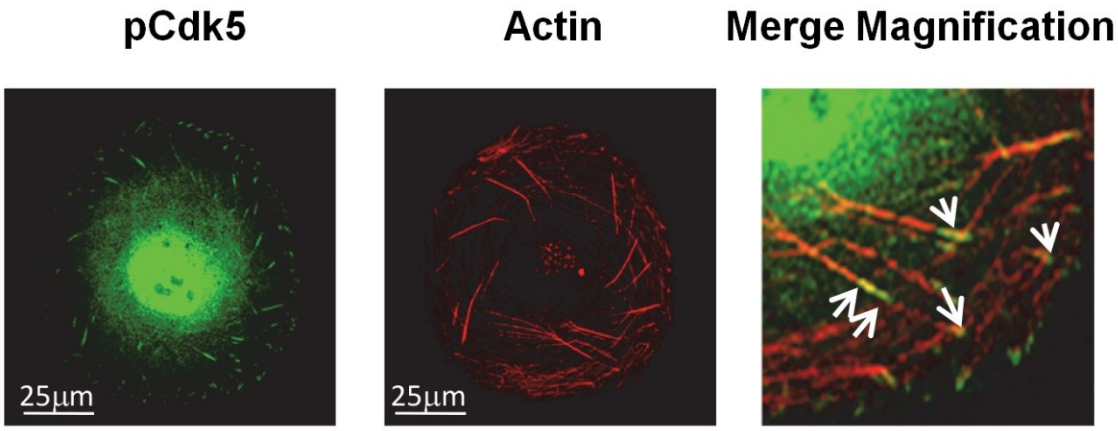

Figure 3-18 Activated Cdk5 (pCdk5) localisation and early spreading

Confocal microscopy showing pCdk5 [pTyr(Ser15)] localisation with actin tips (arrows) and fibres in early spreading in hBMECs.

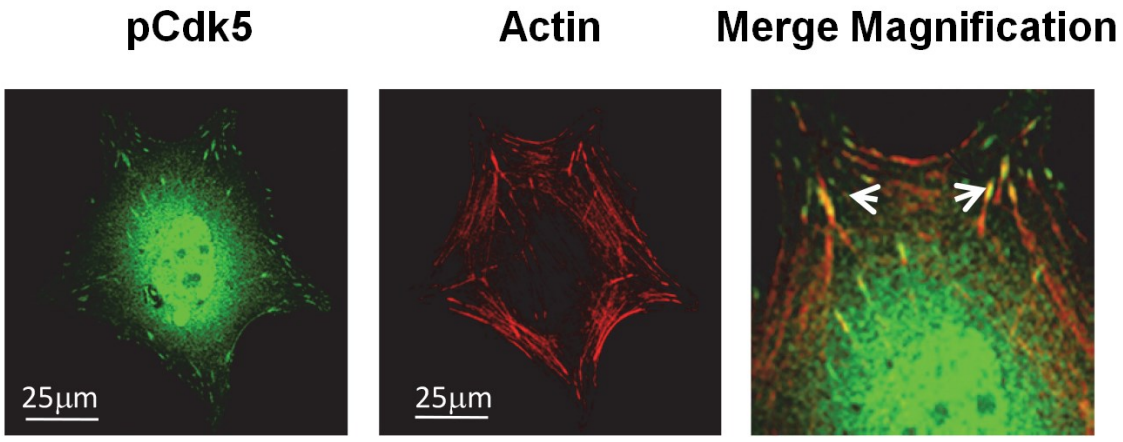

Figure 3-19 pCdk5 Localisation and late spreading

Confocal microscopy showing pCdk5 [pTyr(Ser15)] localisation with actin tips (arrows) and fibres in the late stage of spreading in hBMECs.

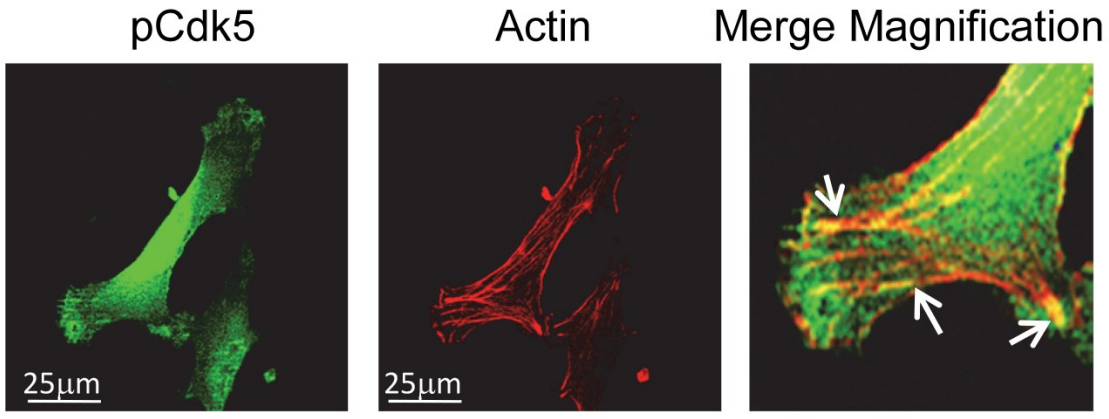

Figure 3-20 pCdk5 Localisation and elongated moving in hBMECs

Confocal microscopy is showing the pCdk5 localisation with actin tips (arrows) and fibre in elongated moving cells.

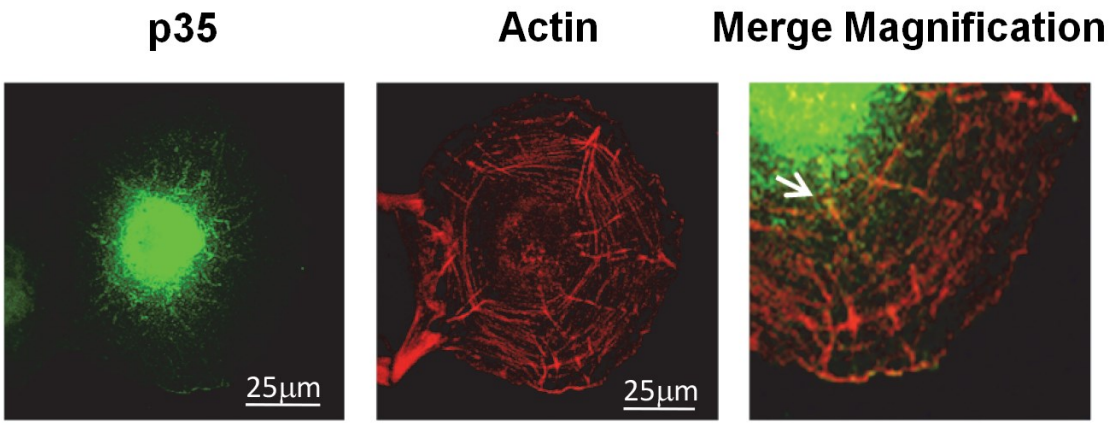

Figure 3-21 p35 localisation and early spreading in hBMECs

Confocal microscopy showing the p35 (green) localisation with actin tips (arrow) and in the early stage of spreading cells.

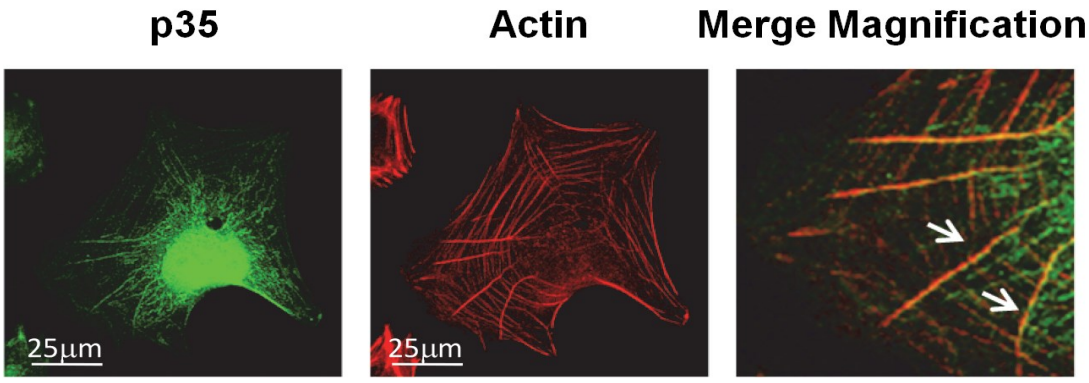

Figure 3-22 p35 localisation and late spreading in hBMECs

Confocal microscopy showing p35 localisation with actin tips (arrows) and in the late stage of spreading cells.

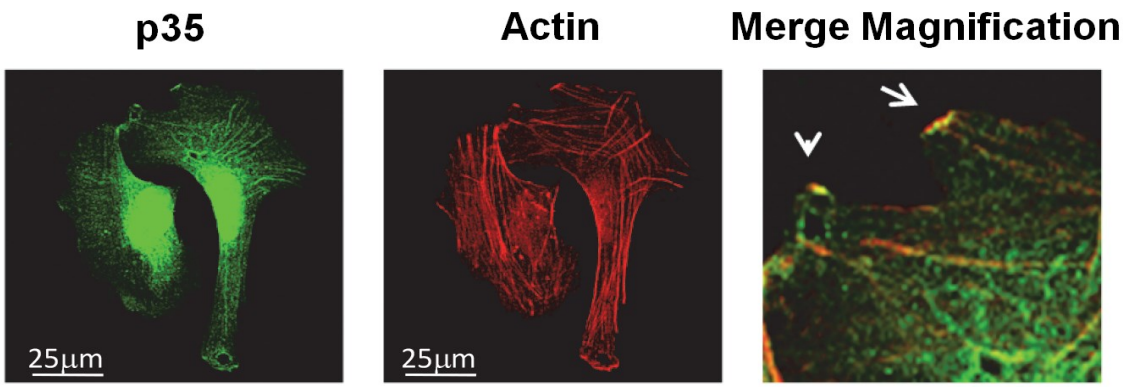

Figure 3-23 p35 localisation and elongated moving

Confocal microscopy showed the p35 localisation with actin tips (arrows) and elongated moving in hBMECs.

The above representative images showing Cdk5 (Figure 3.17), pCDK5 (Figure 3.18, 3.19, 3.20) and p35 (Figure 3.21, 3.22, 3.23) localisation at the tip of actin fibres (arrows) during cell spreads culminating in filament tips (arrows in merge). Immunofluorescence confocal microscope analysis. Objective 65x. Original magnification in the merge, x300. Bars, 25 µm. Each experiment was performed in triplicate.

3.3.2.2 Roscovitine inhibited Cdk5 and p35 clustering with actin fibres and thereby blocking Cdk5 activity and p35 activity

The inhibition of Cdk5 activity with roscovitine resulted in the delocalisation of pCdk5 (Figure 3.24, 3.25) and p35 (Figure 3.26, 3.27) from actin filaments and stress fibres,

producing irregular cytoplasmic bundles with actin (arrows in magnification) in early and late spreading using hBMECs.

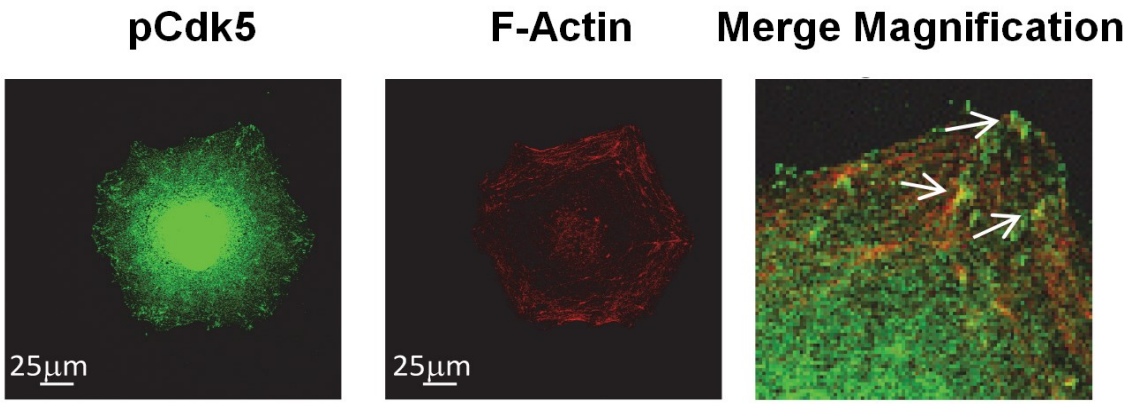

Figure 3-24 Localisation of pCdk5 on F-Actin and merged magnification

Immunofluorescence images showing the cytoplasmic bundles with actin (arrows in magnification) in early spreading hBMECs.

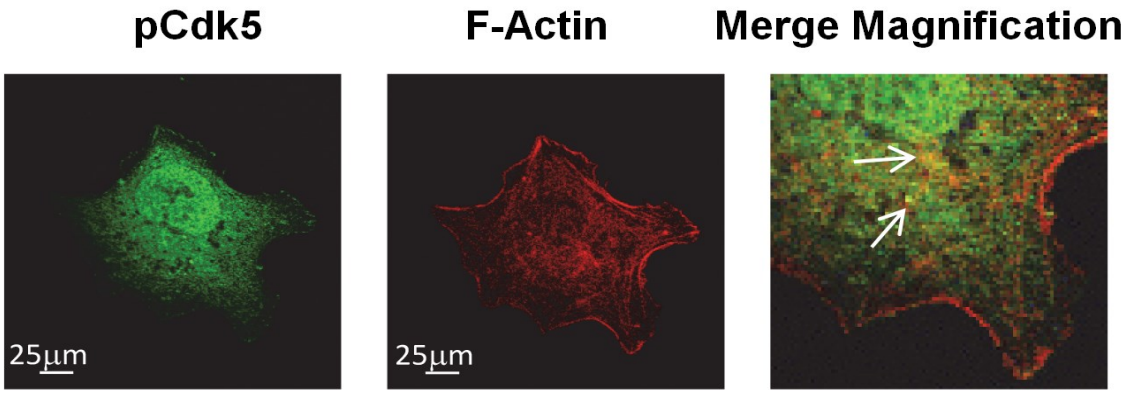

Figure 3-25 Localisation of pCdk5 on F-Actin and merged magnification

Immunofluorescence images showing cytoplasmic bundles with actin (arrows in magnification) in late spreading in hBMECs.

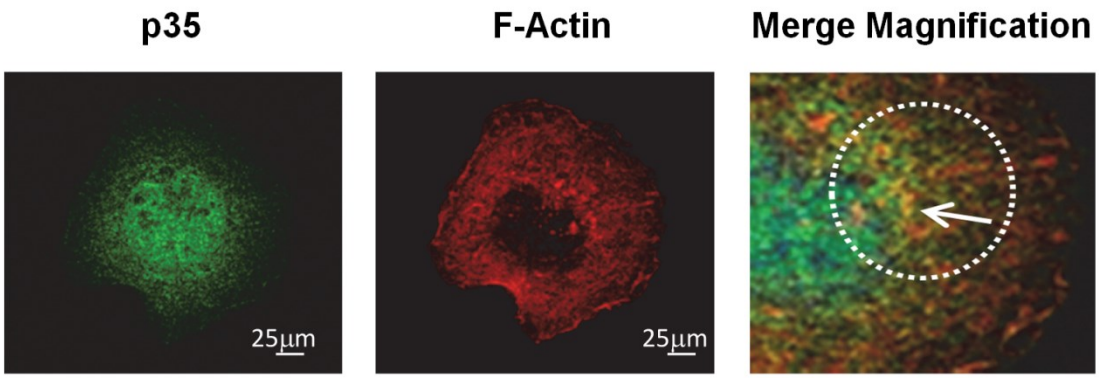

Figure 3-26 Localisation of p35 on F-Actin and merged magnification

Immunofluorescence images showing cytoplasmic bundles with actin (arrows in magnification) in early spreading in hBMECs.

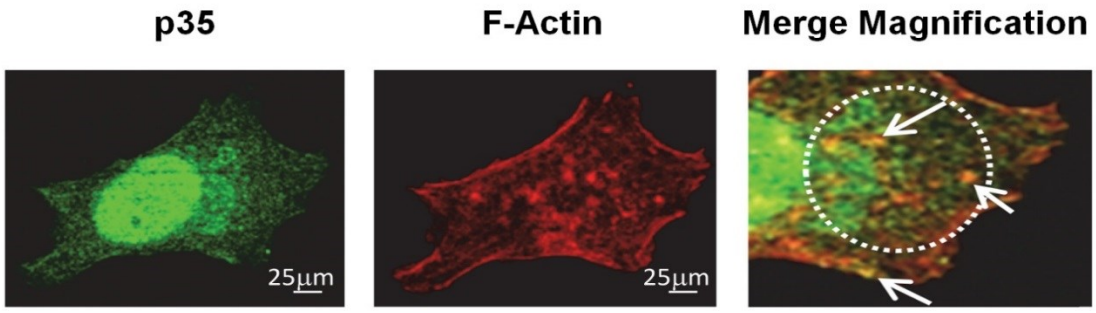

Figure 3-27 Localisation of p35 on F-Actin and merged magnification

Immunofluorescence images showing cytoplasmic bundles with actin (arrows in magnification) in late spreading in hBMECs.

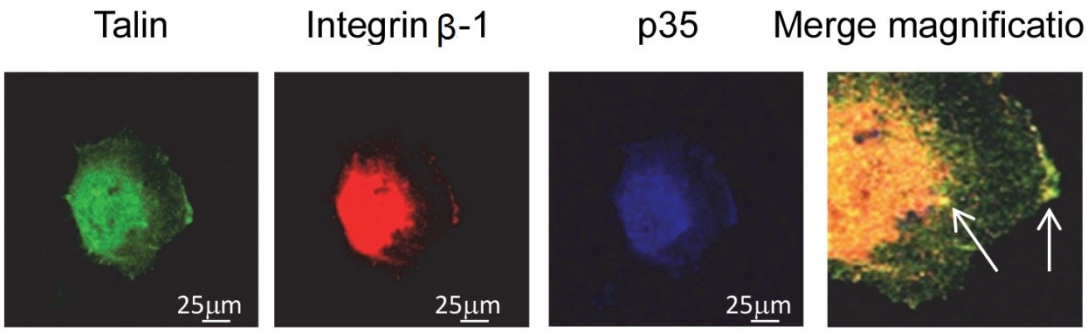

Figure 3-28 Impaired formation of talin tips and their co-localisation with p35 and integrin β-1 by roscovitine in hBMECs

Confocal microscopy showed talin tips and the co-localisation with p35 and integrin β-1 in hBMECs

All of the above representative images showing the inhibition of Cdk5 activity by roscovitine on actin fibres (arrows) in early spreading that resulting in the delocalisation of pCdk5 (Figure 3.24, 3.25), and p35 (Figure 3.26, 3.27) from actin filaments and stress fibres, producing irregular cytoplasmic bundles with actin (arrows in magnification). Roscovitine also impairs formation of talin tips and their co-localisation with p35 and integrin β1 (Figure 3.28). Immunofluorescence confocal microscope analysis. Objective 65x. Original magnification in merge, x200. Bars, 25 μm. Each experiment was performed in triplicate.

3.3.2.3 p-Cdk5, p35/actin intracellular co-localisation during hypoxia

Confocal microscopy showing the images of Cdk5 activity was blocked by roscovitine.

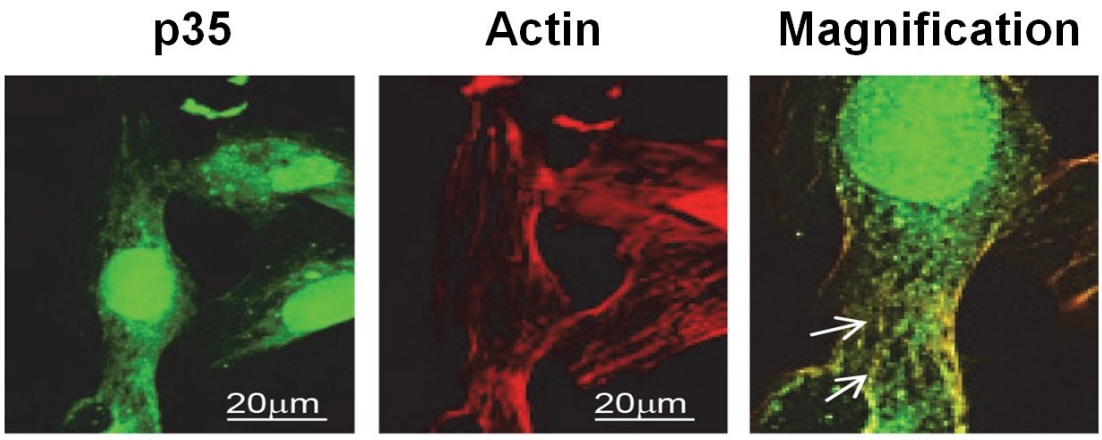

Figure 3-29 p35 and actin intracellular co-localization in hBMECs during hypoxia

Immunofluorescence image shows the effect of hypoxia on p35 intracellular distribution with actin filaments and fibres in hBMECs. Under hypoxia, p35 lost its canonical filament-like structure organisation (arrows in merge magnification,) and localisation at actin fibre tips, showing a more diffuse cytoplasmic distribution.

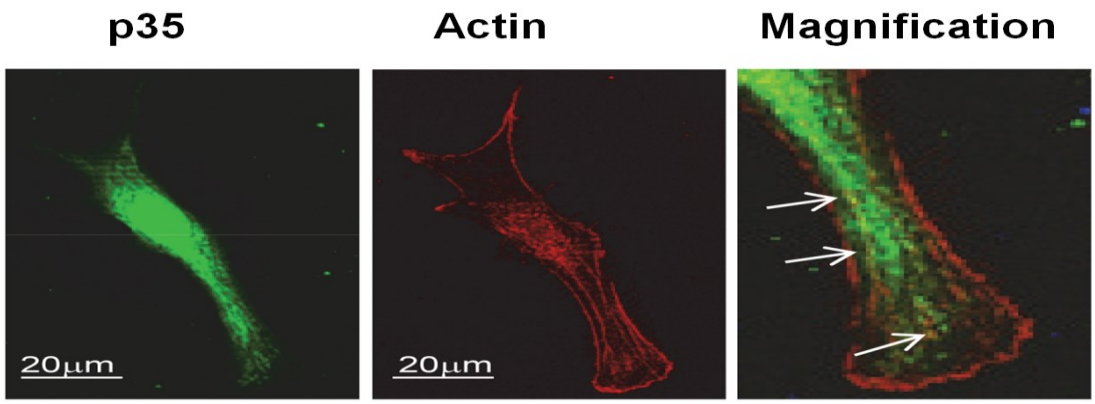

Figure 3-30 Co-localisation of p35 on Actin and merged magnification in CIP expressing cells in hypoxia

Images show the p35 intracellular co-localisation with actin filaments and fibre tips in CIP expressing cells under hypoxia (arrows in magnification image).

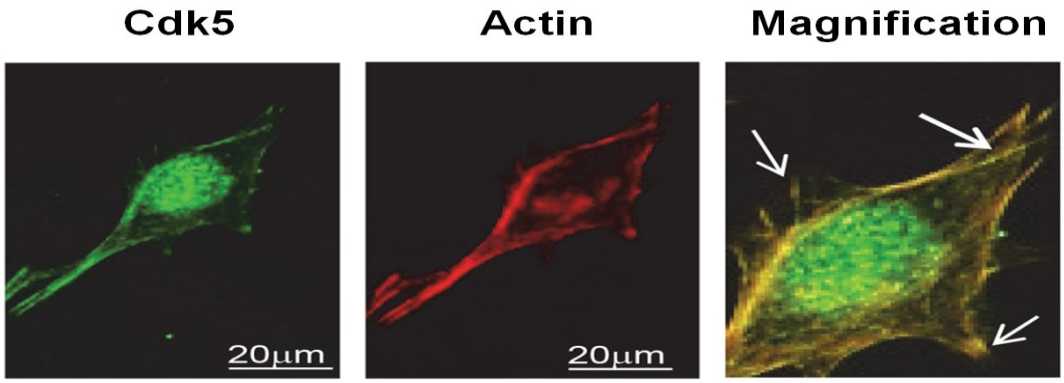

Figure 3-31 Localisation of Cdk5 on Actin and merged magnification in hBMECs control in hypoxia

Images show Cdk5 maintained its intracellular co-localization with actin fibre tips in hBMECs in hypoxia (arrows in merge magnification).

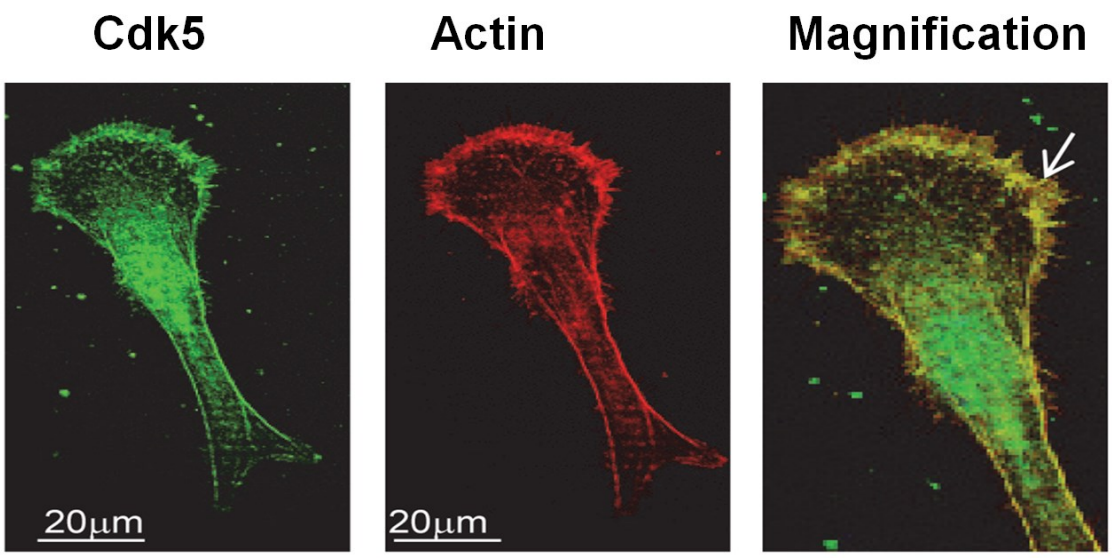

Figure 3-32 Localisation of Cdk5 on Actin and merged magnification in CIP expressing cells in hypoxia

Confocal immunofluorescence Images showing the Cdk5 intracellular localisation with actin filaments and fibres from the effects of hypoxia in CIP expressing cells.

Distribution of actin filaments and fibres in hBMECs in hypoxia. Cdk5 maintained its co-localisation with actin fibre tips (arrows in the merge, Figure 3.31). Compared to

the controls CIP insertion protected p35 (Figure 3.30) and Cdk5 (Figure 3.32) intracellular localisation with actin filaments and fibres from the effects of hypoxia.

3.3.3 Discussion

p35 localisation alongside during spreading culminated with the formation of focal clusters with Cdk5. Thus, p35 and p-Cdk5 were co-localised at the end tips of actin fibres of ECs and CIP-expressing ECs. These actin tips are linked to the directional movement of the spreading and movement of ECs. The co-localisation of p35 and Cdk5 are in favour of the second scenario relating to p35 binding and/or inhibition of Cdk5 to prevent hypoxia-mediated damage. Thus, p35 is directly associated with CIP action in inhibiting Cdk5 (or its phosphorylated form), through some form of association (binding) with Cdk5. The phosphorylated form of active Cdk5 (p-Cdk5) and p35 were previously reported to be associated with integrin β-1 and talin, directed to the formation of microvesicles in late-spreading and elongated cells as well as being localised at the focal tips of actin stress fibres (Qiao et al., 2008; Liebl et al., 2010; He et al., 2011).

Evidence suggests that the apoptosis of neurons after stroke is strongly associated with Cdk5 hyperactivation mediated by its activator p25 (Love, 2003). This, taken together with 1) the increased ratio of p35/p25 in CIP response to hypoxia and 2) the co-localisation of p35 and Cdk5 (which was also evident in CIP-expressing cells), makes us propose that CIP inhibits Cdk5 through facilitating its binding and

inactivation by p35, thus preventing Cdk5 from p25-binding and hyperactivation, which is implicated in stroke conditions.

The aim here was to investigate the role of Cdk5 in the attachment and spreading of ECs (normal vs. CIP-transfected). The cytoskeletal dynamics were investigated using immunofluorescent staining in the presence of roscovitine (an inhibitor of Cdk5).

3.4 Western blotting

3.4.1 Introduction

Following brain ischemia, the rise in neuronal death by Cdk5 hyperactivation is mediated by p25 in hypoxia (Hayashi et al., 1999; Love, 2003). The signal transduction cascade leads to the activation of calpains, a group of calcium-activated cytosolic proteases, that cleave p35 to the more stable p25 peptide, thereby hyperactivating Cdk5 and mediating neuronal apoptosis (Shi et al., 2012; Barros-Miñones et al., 2013). The rationale for co-incubating ECs and CIP-transfected ECs under hypoxia with calcium was due to the role of increased Ca^{2+} in stroke (activation of caspases and proteases such as calpain). Thus, we aimed to mimic or trigger stroke not only by hypoxia but also by increasing the intracellular [Ca^{2+}] content. This would help us explain the effects of Cdk5 and how calpain (a protease that is associated with increased levels of calcium) is involved in stroke-mediated damage.

To examine the signal transduction pathway(s) underpinning Cdk5 action and calpain activation under stroke conditions (hypoxia and elevated calcium), protein targets involved in mediating apoptosis cellular survival and angiogenesis were examined. The role of CIP in protecting hBMECs under hypoxia was also tested. Western blotting techniques were utilised to explain the differences (if any) in the protein expression profiles related to normal and hypoxic conditions within hBMECs, CIP-expressing cells and OVCdk5.

α-tubulin is an intracellular subunit of the tubulin protein that is common in eukaryotes and makes up microtubules which are a component of the cytoskeleton. It is involved in determining cell structure and providing platforms for intracellular transport, including some forms of cell locomotion, the intracellular transport of organelles, and the separation of chromosomes of during mitosis and meiosis (Cooper, 2000; Ndhlovu et al., 2011). In Western blotting, it is essential to correct for protein loading and factors, such as transfer efficiency using normalisation against housekeeping proteins (Ferguson et al., 2005). Therefore, in this study, α-tubulin was used as a loading control for Western blotting.

3.4.2 Results

The results from Ca^{2+}-treated hBMECs suggest that the relative active caspase-3 expression in hBMECs in the presence of Ca^{2+} is higher than CIP-expressing cells in the presence of Ca^{2+}. In normoxia, the p-ERK1/2 expression is similar after 5-min in hBMECs (Ca^{2+}-treated) and CIP-expressing cells (untreated), but higher in CIP-expressing cells treated with Ca^{2+}. And in normoxia, the p-Cdk5 expression is

induced in Ca^{2+}-treated hBMECs and CIP-expressing cells in a time-dependent manner, with levels being higher in control hBMECs.

3.4.2.1 Expressions of p35 and p25 in hypoxia and normoxia

hBMECs and CIP-expressing cells were cultured under hypoxic and normoxic conditions for 24 hours and the relative density of protein expression was analysed using free software Image J. α-tubulin was used as a loading control. These results show that the CIP-expressing cells had a higher p35/p25 ratio compared to the normal cells in hypoxia (B4 versus B3) Fig 3-33.

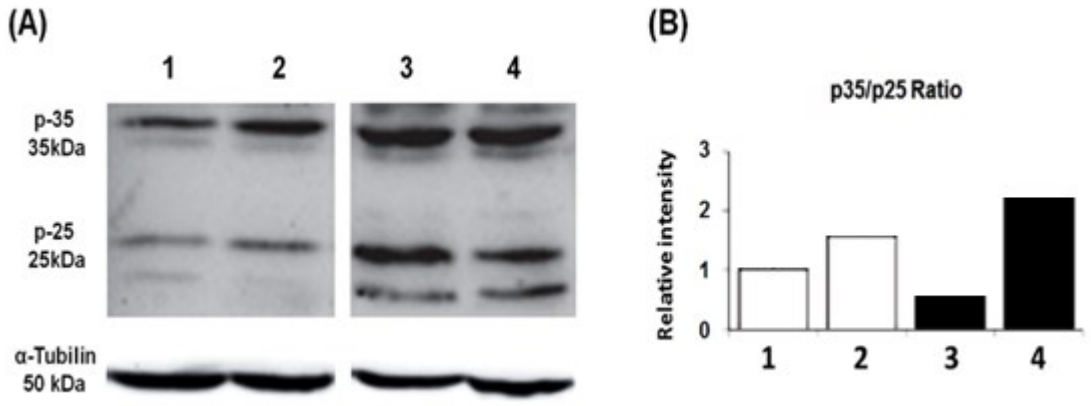

Figure 3-33 Expressions of p35/p25 ratio in hypoxia and normoxia

A) 1: hBMECs (normoxia), 2: CIP-expressing cells (normoxia), 3: hBMECs (hypoxia) and 4: CIP-expressing cells (hypoxia).

B) Calculated results are reported in the graph (B); relative density of p35/p25 protein ratio in control hBMECs and in CIP-expressing cells determined in normoxic and hypoxic conditions. The bar chart represents the relative protein expression compared to the control (=1.0), and the experiment was repeated at least twice.

3.4.2.2 Relative expression of Hsp70 under Normoxic and Hypoxic Conditions

hBMECs were cultured under hypoxic and normal conditions, and the relative density of protein expression was analysed using free software Image-J. The bar chart shows that heat shock protein 70 (HSP70) was up-regulated (increased by 1 fold) in hBMECs under hypoxic conditions. The bars represent the standard deviations, and the experiment was repeated at least twice.

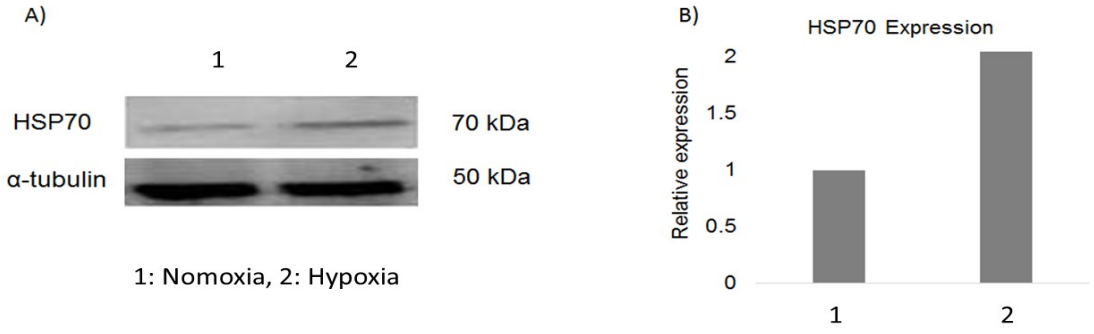

Figure 3-34 Western blot showing that HSP70 was up-regulated weakly under hypoxia compared to the control

A) 1: Normoxia, 2: Hypoxia.

B) The results indicated that the hypoxic condition caused cellular metabolic deprivation, which was effective oxygen deficiency used as this *in vitro* stroke model.

3.4.2.3 The Relative expression of Hsp70 in HBMECs and CIP-expressing cells under normoxic and hypoxic condition

hBMECs and CIP-expressing cells were analysed under hypoxic and normoxic conditions and the relative density of protein expression was analysed using Image-J.

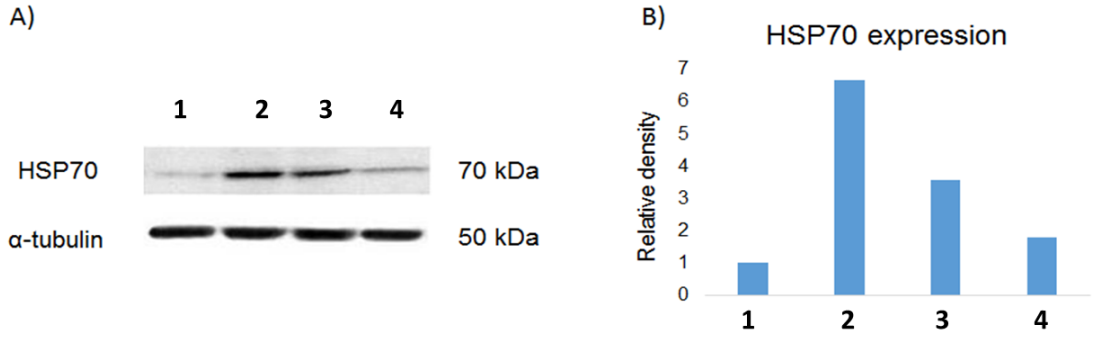

Figure 3-35 Representative Western blot showing the expression of HSP70 in hBMECs and CIP-expressing cells under normoxic and hypoxic conditions

A) 1: hBMECs (normoxia), 2: hBMECs (hypoxia), 3: CIP-expressing cells (normoxia), 4: CIP-expressing cells (hypoxia).

B) The results indicated that the expression of HSP70 was up-regulated in hBMECs, but it was down-regulated in CIP-expressing cells under hypoxic conditions. The bar chart represents the relative protein expression compared to the control (=1.0), and the experiment was repeated at least twice.

3.4.2.4 Expression of p35/p25 in hBMECs, CIP-expressing cells and OVCdk5 in normoxia

hBMECs, CIP-expressing cells and OVCdk5 were cultured under normal conditions (Figure 3.36 A, normoxia) and the relative density of protein expression was analysed using free software Image-J (Figure 3.36 B).

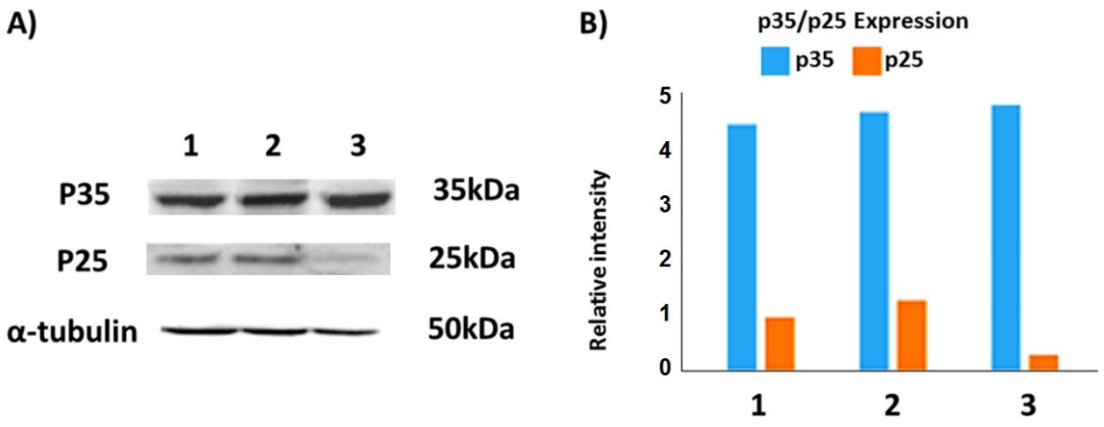

Figure 3-36 Representative Western blot showing p35/p25 expression in hBMECs, CIP-expressing cells and OVCdk5 under normoxic condition

A) 1: hBMECs, 2: OVCdk5 and 3: CIP-expressing cells.

B) In CIP-expressing cells, the levels of p25 showed a decrease compared to control hBMECs. And in OVCdk5, the levels of p25 showed an increase compared to control. The bar chart represents the relative protein expression compared to the control (=1.0), and the experiment was repeated at least twice.

3.4.2.5 Expression of p35/p25 in hBMECs, CIP-expressing Cells and OVCdk5 in hypoxia

hBMECs, CIP-expressing cells and OVCdk5 were cultured under the hypoxic condition for 24 hours and the p35/25 expressions were analysed by Western blotting (Figure 3.37 A). The relative density of protein expression was analysed using Image-J (Figure 3.37 B).

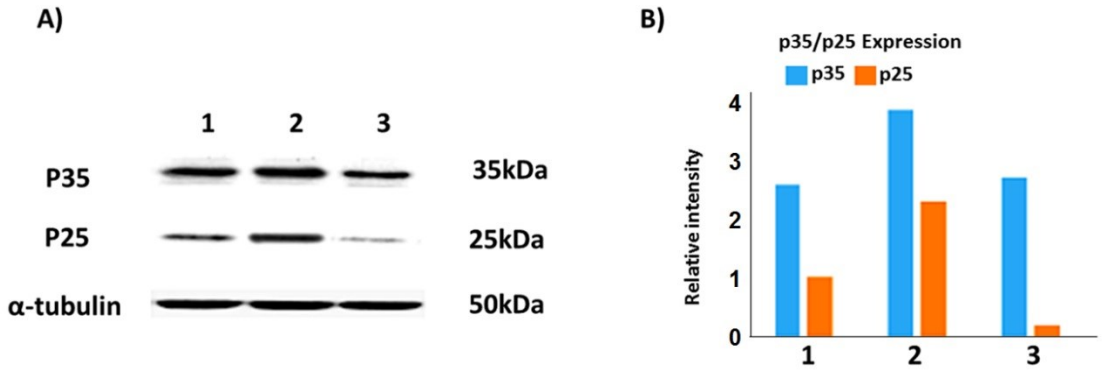

Figure 3-37 Representative Western blot showing p35/p25 expression in hypoxia

A) 1: hBMECs, 2: OVCdk5 and 3: CIP-expressing cells.

B) The Levels of p25 shows the lowest expression in CIP-expressing cells under hypoxic condition, but the p35 expression stays similar level in CIP-expressing cells compared to control cells in hypoxia. The bar chart represents the relative protein expression compared to the control (=1.0), and the experiment was repeated at least twice.

3.4.2.6 Relative active Caspase-3 expression in the presence of Ca^{2+} in different times

hBMECs and CIP-expressing cells were cultured (Figures 3.38A, 3.39A and 3.40A).And the relative density of protein expression was analysed using Image-J (Figure 3.38B, Figure 3.39, Band Figure 3.40B). The untreated cells were used as controls.

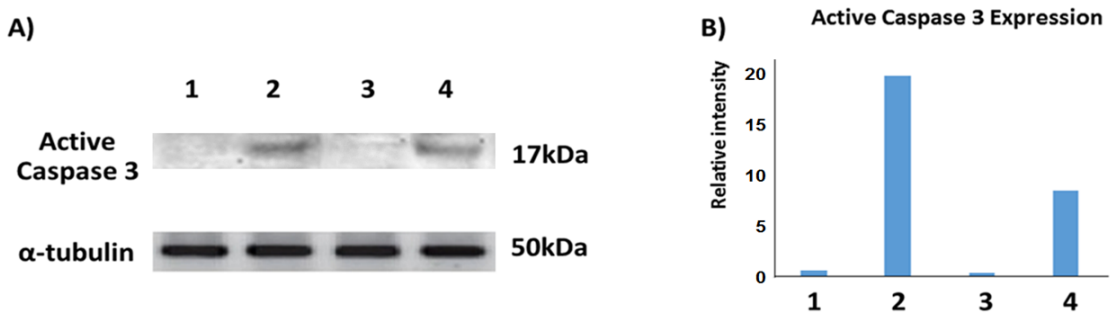

Figure 3-38 Representative Western blot showing the effect of Ca^{2+} on active Caspase-3 expression for 5 mins

A) 1: hBMECs control, 2: hBMECs treated with Ca^{2+} (5μM), 3: CIP-expressing cells in the absence of Ca^{2+} and 4: CIP-expressing cells treated with Ca^{2+} (5μM).

B) hBMECs cells and CIP-expressing cells treated with Ca^{2+} (5μM) for 5 mins. The level of active caspase-3 expression showed an increase in treated hBMEC s (A2 and B2) (19 fold, B2)) and CIP-expressing cells (9 fold, A4 and B4) compared to control (untreated cells A1, B1 and A2, B2) respectively. The bar chart represents the relative protein expression compared to the control (=1.0), and the experiment was repeated at least twice.

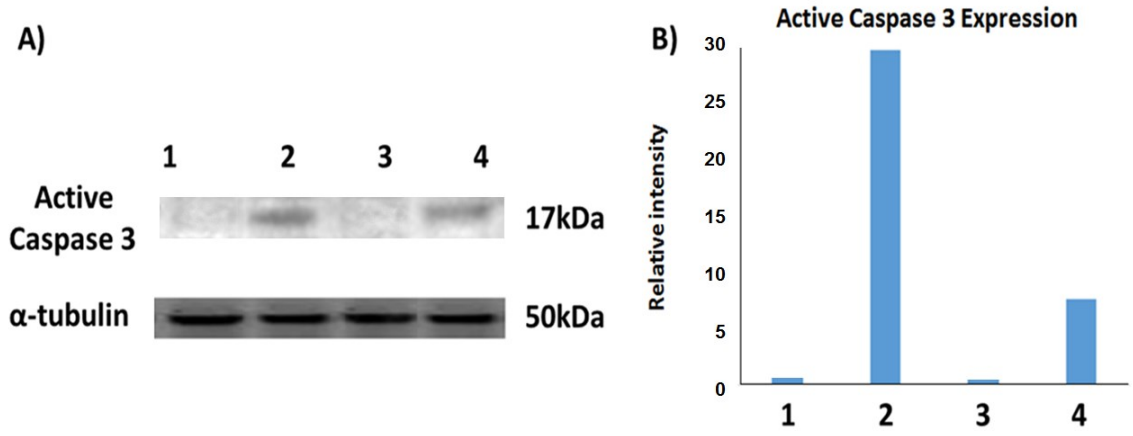

Figure 3-39 Relative active Caspase-3 expressions in the presence of Ca^{2+} for 15 mins

A) 1: hBMECs control, 2: hBMECs treated with Ca^{2+} (5μM), 3: CIP-expressing cells untreated with Ca^{2+} and 4: CIP-expressing cells treated with Ca^{2+} (5μM).

B) The representative Western blot (Figure 3.39A) shows the effect of Ca^{2+} (5μM) on active Caspase-3 expression in hBMECs and CIP-expressing cells treated with Ca^{2+} for 15 mins. Both hBMECs and CIP-expressing cells, the level of active caspase-3 expression was increased (A2, B2 and A4, B4) compared to control (1 and 3) (untreated CIP-expressing cells, A1, B1 and A3, B3). The bar chart represents the relative protein expression compared to the control (=1.0), and the experiment was repeated at least twice.

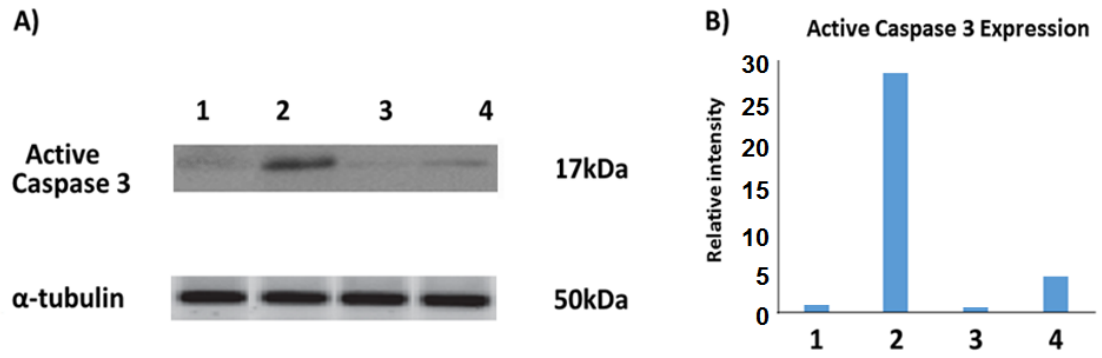

Figure 3-40 Relative active Caspase-3 expressions in the presence of Ca^{2+} for 40 mins

A) 1: hBMECs control, 2: hBMECs treated with Ca^{2+} (5μM), 3: CIP-expressing cells untreated with Ca^{2+} and 4: CIP-expressing cells treated with Ca^{2+} (5μM).

B) Representative Western blot showing the effect of active Caspase-3 expression, hBMECs (B2) and CIP-expressing cells treated with Ca^{2+} (5μM) for 40 mins, again, in treated CIP-expressing cells, the level of active caspase-3 expression showed an increase compared to control (untreated CIP-expressing cells , A4, B4, as did hBMECs (A2, B2 versus A1, B1). The bar chart represents the relative protein expression compared to the control (=1.0), and the experiment was repeated at least twice.

3.4.2.7 p-ERK1/2 expression in hBMECs in the presence of Ca^{2+} in different times

hBMECs and CIP-expressing cells were treated with Ca^{2+} (5μM) for 5, 15 and 40 mins respectively. Untreated cells were used as controls (Figures 3.41A, 3.42A and 3.43A) and the relative density of protein expression was analysed using Image-J (Figures 3.41B, 3.42B and 3.43B).

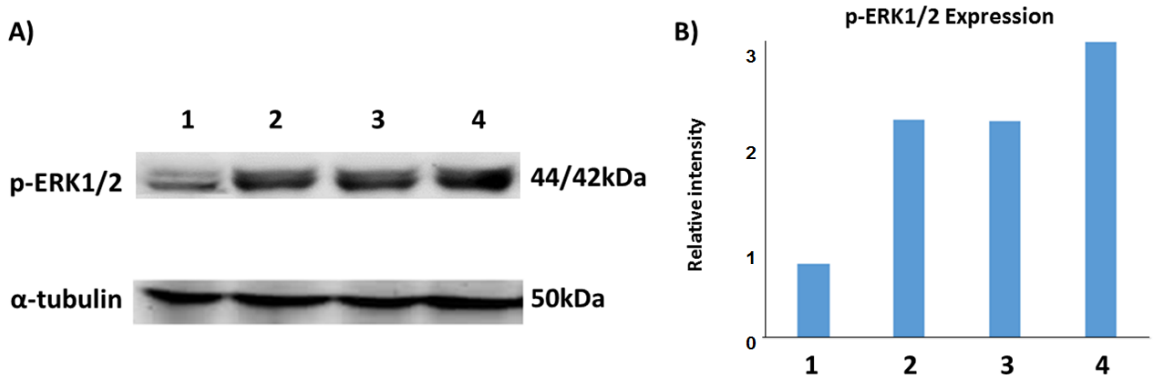

Figure 3-41 Representative Western blot showing the effect of phospho-ERK1/2 in hBMECs and CIP-expressing cells treated with Ca^{2+} for 5 mins.

A) 1: hBMECs control, 2: hBMECs treated with Ca^{2+} (5μM), 3: CIP-expressing cells untreated with Ca^{2+} and 4: CIP-expressing cells treated with Ca^{2+} (5μM).

B) The levels of phospho-ERK1/2 showed an increase both in treated hBMECs (B2) and CIP-expressing cells (B4) compared to control (untreated hBMECs and CIP-expressing cells) (B4 vs B3). The bar chart represents the relative protein expression compared to the control (=1.0), and the experiment was repeated at least twice.

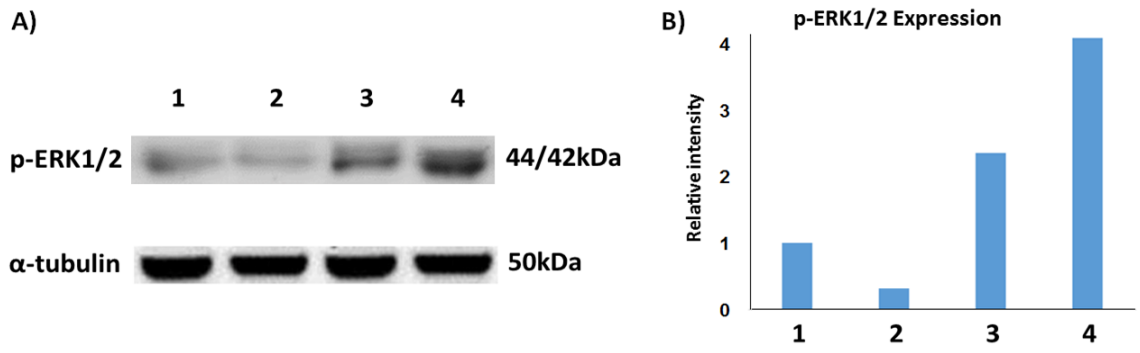

Figure 3-42 Representative Western blot showing the effect of phospho-ERK1/2 in hBMECs and CIP expressing cells treated with Ca^{2+} for 15 mins

A) 1: hBMECs control, 2: hBMECs treated with Ca^{2+} (5μM), 3: CIP-expressing cells untreated with Ca2+ and 4: CIP-expressing cells treated with Ca^{2+} (5μM).

B) In treated CIP-expressing cells, the level of Phospho-ERK1/2 showed an increase compared to control (untreated CIP-expressing cells). But the level of Phospho-ERK1/2 showed a decrease compared to control (untreated hBMECs). The bars represent the standard deviations, and the experiment was repeated at least twice.

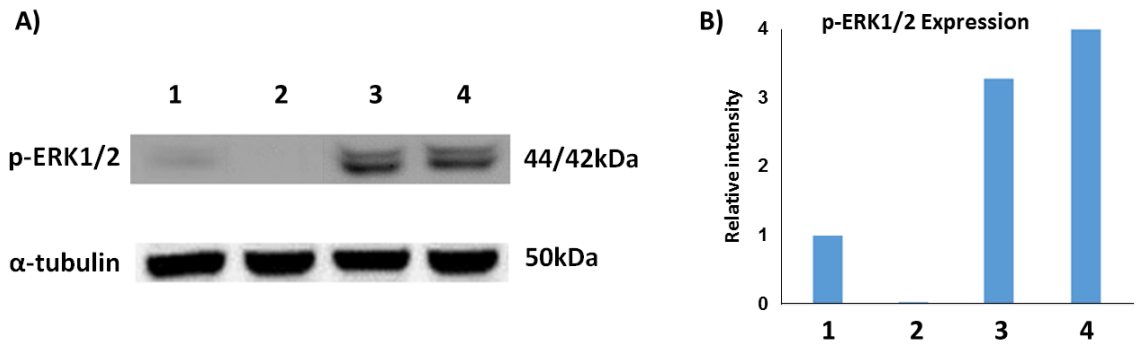

Figure 3-43 Representative Western blot showing the effect of phospho-ERK1/2 in hBMECs and CIP-expressing cells treated with Ca^{2+} for 40 mins

A) 1: hBMECs control, 2: hBMECs treated with Ca^{2+} (5μM), 3: CIP-expressing cells untreated with Ca^{2+} and 4: CIP-expressing cells treated with Ca^{2+} (5μM).

B) In treated CIP-expressing cells, the level of phospho-ERK1/2 showed an increase (A4 and B4) compared to control [untreated CIP-expressing cells (A3 and B3)], but the level of phospho-ERK1/2 showed a decrease (A2 and B2) compared to control (untreated hBMECs, A1 and B1). The bars represent the standard deviations, and the experiment was repeated at least twice.

3.4.2.8 p-Cdk5 Overexpression in hBMECs in Hypoxia

hBMECs were incubated in hypoxic condition for 24 hours, the cells incubated in normoxic condition were used as a control. The relative density of protein expression was analysed using Image-J (Figure 3.44B).

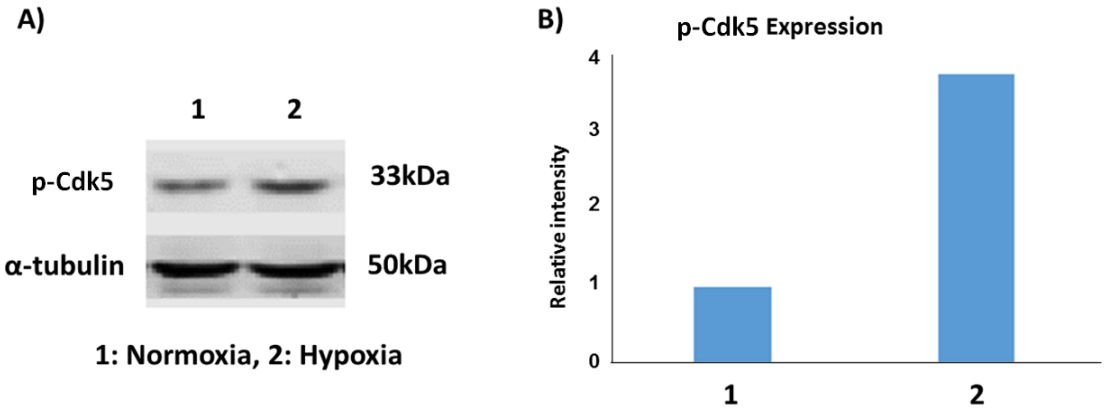

Figure 3-44 Representative Western blot showing the expression of p-Cdk5 in hypoxia samples

Under hypoxic conditions, the level of p-Cdk5 showed an increase of 3.8 fold (B2 vs B1) compared to normoxia control. The bar chart represents the relative protein expression compared to the control (=1.0), and the experiment was repeated at least twice.

3.4.2.9 p35 Expression in hBMECs in Hypoxia

hBMECs were incubated under hypoxic conditions for 24 hours, and the cells incubated under normoxic conditions were used as a control. The relative density of protein expression was analysed using Image-J (Figure 3.45B).

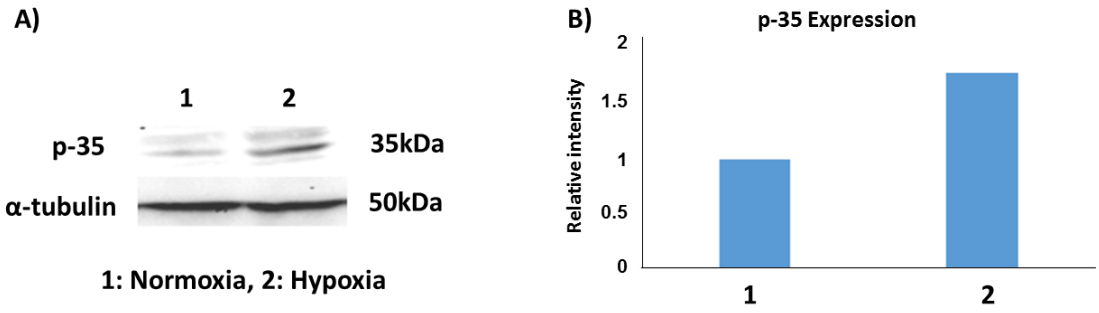

Figure 3-45 Representative Western blot showing the expression of p35 in normoxia and hypoxia samples

In hypoxia, the level of p35 showed an increase (0.8 fold, B2 vs B1) compared to normoxia control. The bar chart represents the relative protein expression compared to the control (=1.0), and the experiment was repeated at least twice.

3.4.2.10 p35 expression in hBMECs and CIP-expressing cells in the presence of calpain

hBMECs and CIP-expressing cells were treated with calpain (10µg/ml) for 30 mins. The relative density of protein expression was analysed using Image-J (Figure 3.46B). The cells untreated with calpain were used as a control.

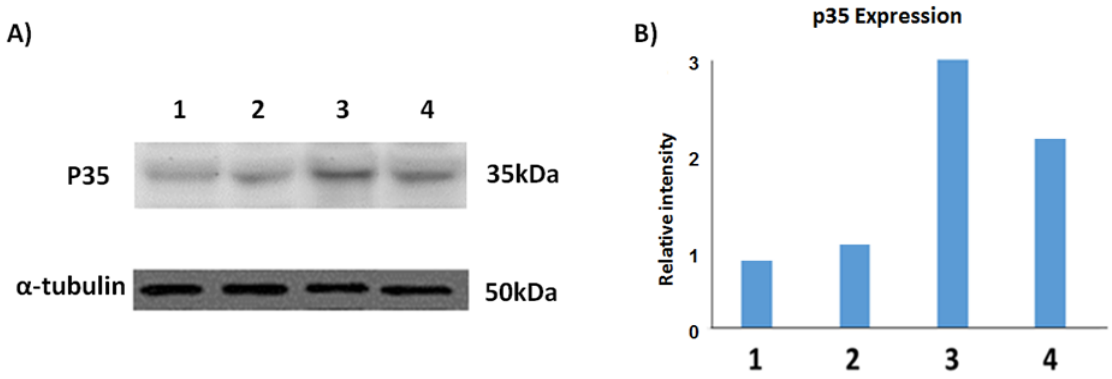

Figure 3-46 Representative Western blot showing the effect on p35 expression, with calpain-treated cells for 30 mins

A) 1: hBMECs control, 2: hBMECs treated with calpain (10µg/ml), 3: CIP-expressing cells untreated control, 4: CIP-expressing cells treated with calpain (10µg/ml).

B) In CIP-expressing cells (B4) treated with calpain, the level of p35 expression showed a 2-fold increase compared to control cells (untreated hBMECs, B1). The bar chart represents the relative protein expression compared to the control (=1.0), and the experiment was repeated at least twice.

3.4.2.11 Capase-3 expression in hBMECs and CIP-expressing cells under hypoxic conditions

hBMECs and CIP-expressing cells were incubated under hypoxic conditions for 24 hours, and the cells incubated in normoxic conditions were used as a control. The relative density of protein expression was analysed using Image-J (Figure 3.47B).

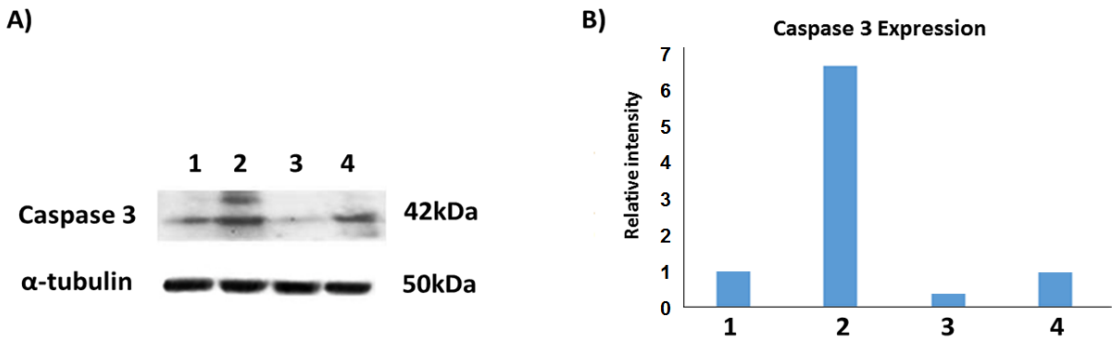

Figure 3-47 Expression of caspase-3 in hBMECs and CIP-expressing cells under normoxic and hypoxic conditions

A) 1: hBMECs (normoxia), 2: hBMECs (hypoxia), 3: CIP-expressing cells (normoxia) and 4: CIP-expressing cells (hypoxia).

B) hBMECs were incubated for 24 hours under hypoxic conditions, the expression of caspase-3 was significantly higher (5.8 fold, A2 and B2) compared to the cells in normoxic conditions. In CIP- expressing cells, the level of caspase-3 expression was higher (1.5 fold, A4 and B4) when exposed to 24 hours of hypoxia compared to CIP-expressing cells under normal conditions, but lower than in the control cells (A2 and B2). The bar chart represents the relative protein expression compared to the control (=1.0), and the experiment was repeated at least twice.

3.4.2.12 p-Cdk5 expression in hBMECs and CIP-expressing cells in the presence of Ca^{2+}

hBMECs and CIP-expressing cells were treated with Ca^{2+} (5μM) for 5, 15 and 40 mins respectively. The untreated cells were used as a control. The relative density of protein expression was analysed using free software Image-J (Figures 3.48B, 3.49B and 3.50B)

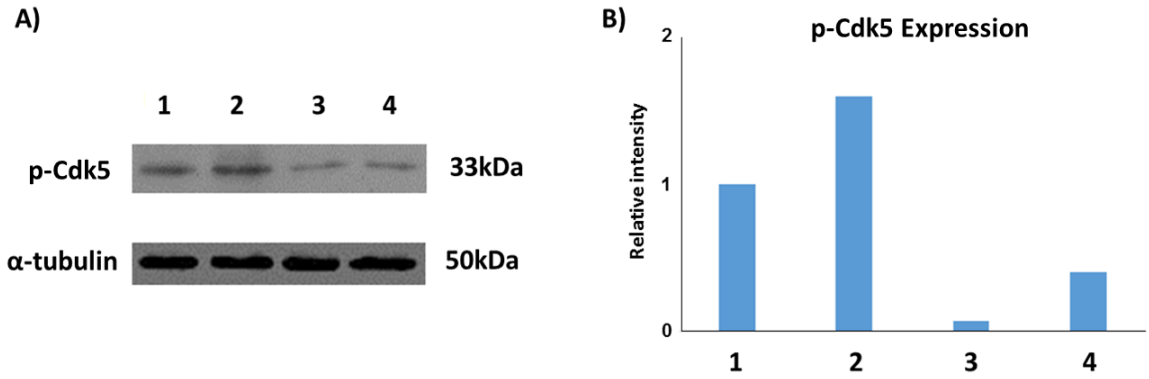

Figure 3-48 Representative Western blot showing the effect of p-Cdk5 expression, with Ca^{2+} treated for 5 mins in hBMECs and CIP-expressing cells

1: hBMECs control, 2: hBMECs treated with Ca^{2+} (5μM), 3: CIP-expressing cells untreated with Ca^{2+} and 4: CIP-expressing cells treated with Ca^{2+} (5μM). The bar chart represents the relative protein expression compared to the control (=1.0), and the experiment was repeated at least twice.

The level of p-Cdk5 expression showed an increase in Ca^{2+}-treated cells compared to untreated cells (A" and B" vs A1 and B1, A4 and B4 vs A3 and B3)

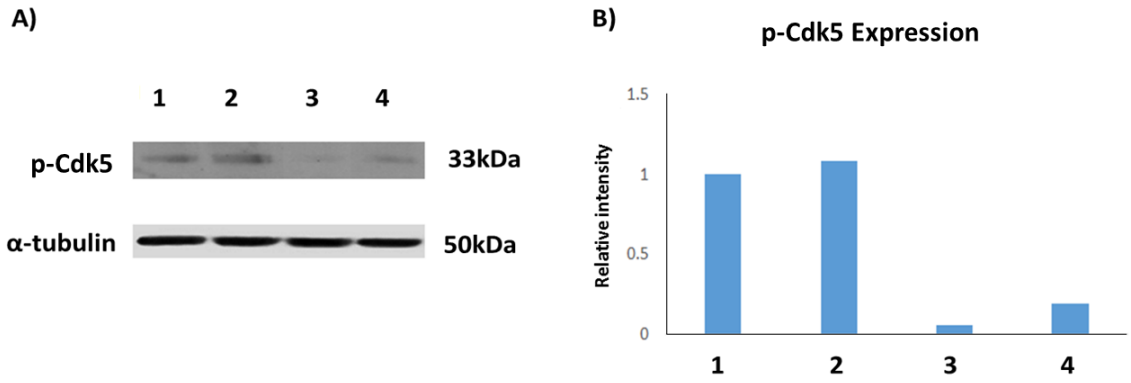

Figure 3-49 Representative Western blot shows the effect of p-Cdk5 expression, with Ca^{2+}-treated cells for 15 mins

1: hBMECs control, 2: hBMECs treated with Ca^{2+} (5μM), 3: CIP-expressing cells untreated with Ca^{2+} and 4: CIP-expressing cells treated with Ca^{2+} (5μM). The bar chart represents the relative protein expression compared to the control (=1.0), and the experiment was repeated at least twice.

The level of p-Cdk5 expression shows an increase in Ca^{2+}-treated cells compared to untreated cells, A2 and B2 vs A1 and B1, A4 and B4 vs A3 and B3.

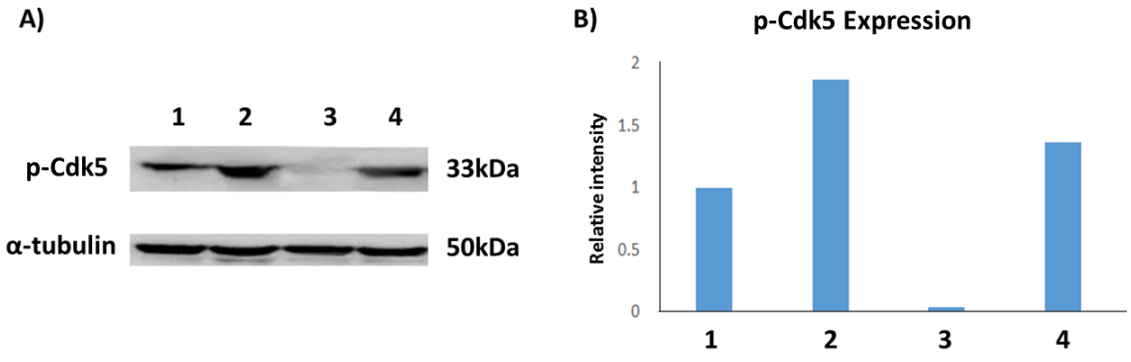

Figure 3-50 Representative Western blot showing the effect of p-Cdk5 expression, with Ca^{2+} treated cells for 40 mins

A) 1: hBMECs control, 2: hBMECs treated with Ca^{2+} (5μM), 3: CIP-expressing cells untreated with Ca^{2+} and 4: CIP-expressing cells treated with Ca^{2+} (5μM).

B) The level of p-Cdk5 expression shows an increase in Ca^{2+}-treated CIP-expressing cells compared to untreated CIP-expressing cells (A4 and B4 vs A3 and B3). The bars represent the standard deviations, and the experiment was repeated at least twice.

3.4.2.13 p-CDK5 Expression in cells treated with Ca^{2+} in different times

hBMECs, CIP-expressing cells and OVCdk5 were cultured and treated with the Ca^{2+} (5μM) calcium ionophore A23187 for 5, 15 and 40 mins respectively. The cells not with Ca^{2+}were used as controls (Figures 3.53A, 3.54A and 3.55A). The relative density of protein expression was analysed using Image-J (Figures 3.51B, 3.52B and 3.53B).

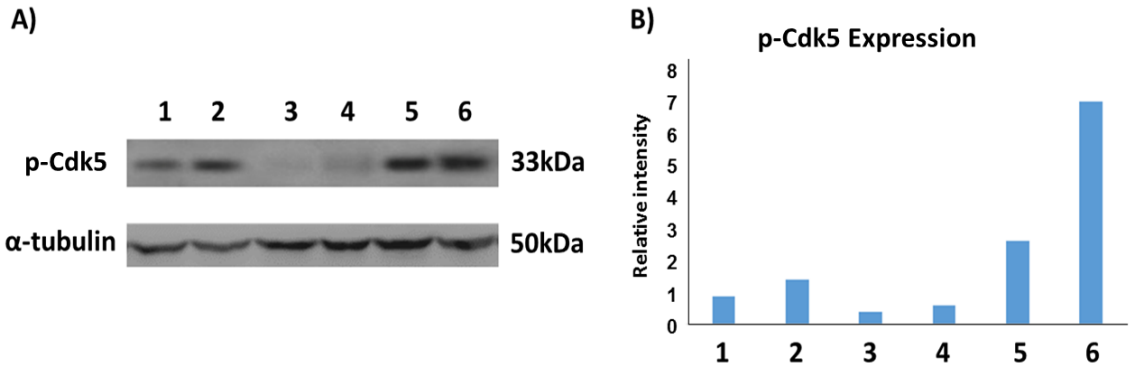

Figure 3-51 Representative Western blot showing the effect of Ca^{2+} on p-Cdk5 expression in hBMECs, CIP-expressing cells and OVCdk5 treated with Ca^{2+} for 5 mins

A) 1: hBMECs control, 2: hBMECs treated with Ca^{2+} (5μM), 3: CIP-expressing cells untreated with Ca^{2+}, 4: CIP-expressing cells treated with Ca^{2+} (5μM), 5: OVCdk5 untreated with Ca^{2+} and 6: OVCdk5 treated with Ca^{2+} (5μM).

B) In treated hBMECs and CIP-expressing cells, the level of p-Cdk5 expression showed a slight increase compared to untreated cells (A2 and B2 vs A1 and B1, A4 and B4 vs A3 and B3), but in treated OVCdk5, the level of p-Cdk5 was greatly increased compared to untreated cells (A6 and B6 vs A5 and B5). The bar chart represents the relative protein expression compared to the control (=1.0), and the experiment was repeated at least twice.

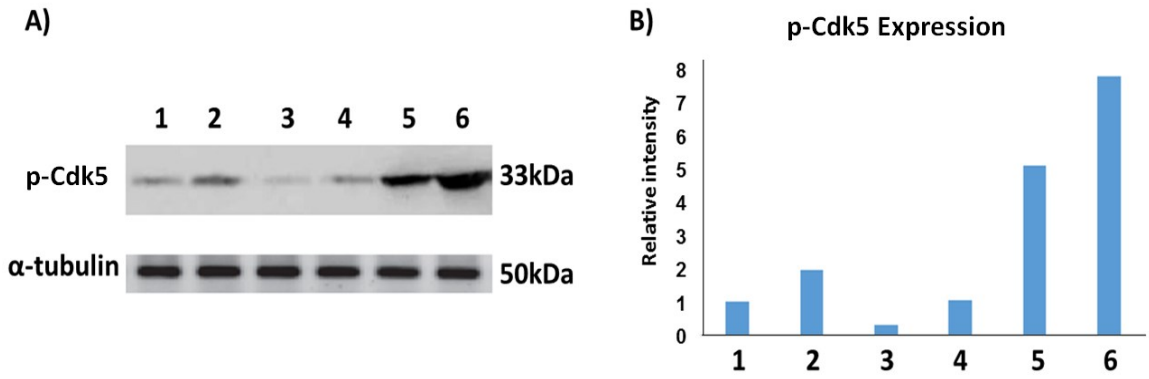

Figure 3-52 Representative Western blot shows the effect of Ca^{2+} treatment on p-Cdk5 expression in hBMECs, CIP-expressed cells and OVCdk5 for 15 mins

A) 1: hBMECs control, 2: hBMECs treated with Ca^{2+} (5μM), 3: CIP-expressing cells untreated with Ca^{2+}, 4: CIP-expressing cells treated with Ca^{2+} (5μM), 5: Overexpressing Cdk5 transfectants untreated with Ca^{2+} and 6: OVCdk5 treated with Ca^{2+} (5μM).

B) In treated cells, the level of p-Cdk5 expression showed a slight increase compared to untreated cells (A2 and B2 vs A1 and B1), but there was a large increase in OVCdk5 (A5 and B5) and a small increase between treated OVCdk5 cells and untreated cells (A6 and B6 vs A5 and B5). The bar chart represents the relative protein expression compared to the control (=1.0), and the experiment was repeated at least twice.

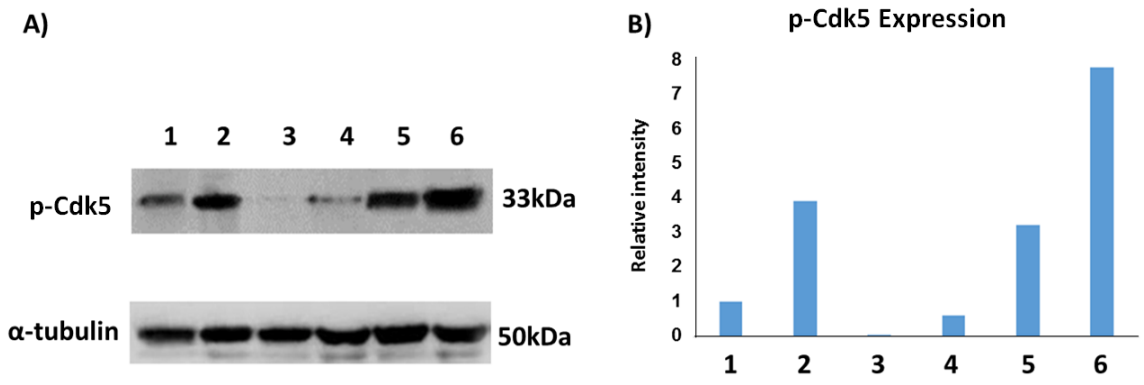

Figure 3-53 Representative Western blot showing the effect of Ca^{2+} treatment on p-Cdk5 expression for 40 mins

A) 1: hBMECs control, 2: hBMECs treated with Ca^{2+} (5μM), 3: CIP-expressing cells untreated with Ca^{2+} and 4: CIP-expressing cells treated with Ca^{2+} (5μM), 5: OVCdk5 untreated with Ca^{2+} and 6: OVCdk5 treated with Ca^{2+} (5μM).

B) In treated hBMECs and CIP-expressing cells, the level of p-Cdk5 expression showed a slight increase compared to untreated cells (A2 and B2 vs A1 and B1, A4 and B4 vs A3 and B3), but in treated OVCdk5 cells, the level of p-Cdk5 showed a large increase compared to untreated cells (A6 and B6 vs A5 and B5). The bar chart represents the relative protein expression compared to the control (=1.0), and the experiment was repeated at least twice.

3.4.2.14 P35 Expression in cells treated with Ca^{2+} in different times

hBMECs and CIP-expressing cells were cultured and treated with Ca^{2+} (5μM) for 5, 15 and 40 mins respectively (Figures 3.54A, 3.55A and 3.56A).The relative density of protein expression was analysed using Image-J (Figures 3.56B, 3.57B and 3.58B). The untreated cells were used as controls.

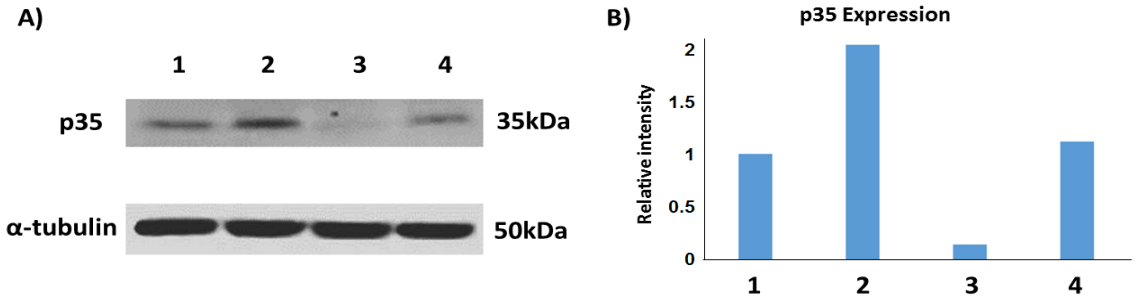

Figure 3-54 Representative Western blot showing the effect on p35 expression of Ca^{2+} for 5 mins

A) 1: hBMECs control, 2: hBMECs treated with Ca^{2+} (5μM), 3: CIP expressing cells untreated with Ca^{2+} and 4: CIP-expressing cells treated with Ca^{2+} (5μM).

B) hBMECs were treated with Ca^{2+} (5μM) for 5 mins. In Ca^{2+}-treated CIP-expressing cells, the level of p35 expression showed a 5-fold increase compared to the untreated CIP-expressing cells. The bars represent the standard deviations, and the experiment was repeated at least twice.

The effect of cells play no roles of p35 activity. It was unable to show clear changes in expression and break down the level in calcium-treated samples, however, in the same samples, phosphorylation of Cdk5 was changed by Ca^{2+}. Although it could not show p25, as it is very difficult to see p25 level. Struggling throughout the project

to see changes in the amount of the protein but indirectly it has been shown that caspase and p-Cdk5 particularly substrate.

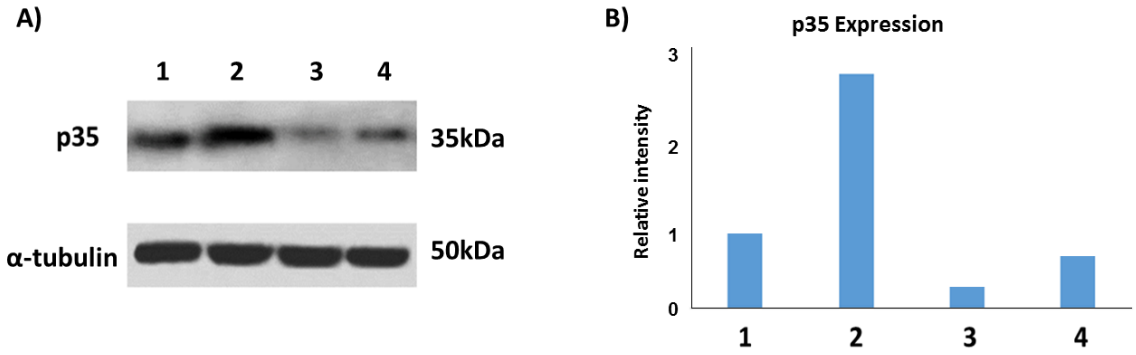

Figure 3-55 Representative Western blot showing the effect of p35 expression, with Ca^{2+} treated cells for 15 mins

A) 1: hBMECs control, 2: hBMECs treated with Ca^{2+} (5μM), 3: CIP-expressing cells untreated with Ca^{2+} and 4: CIP-expressing cells treated with Ca^{2+} (5μM).

B) There is 1.8 fold increase in p35 expression in hBMECs treated with Ca^{2+} (5μM), but there is a slight increase in CIP-expressing cells treated with Ca^{2+} (A2 and B2 vs A1 and B1, A4 and B4 vs A3 and B3). The bar chart represents the relative protein expression compared to the control (=1.0), and the experiment was repeated at least twice.

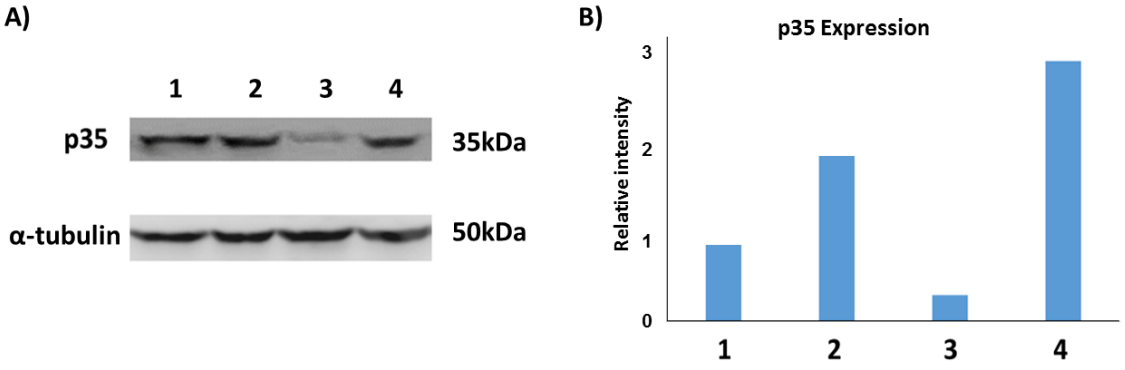

Figure 3-56 Representative Western blot showing the effect of p35 expression in hBMECs treated with Ca^{2+} for 40 mins

A) 1: hBMECs control, 2: hBMECs treated with Ca^{2+} (5μM), 3: CIP expressing cells untreated with Ca^{2+} and 4: CIP expressing cells treated with Ca^{2+} (5μM).

B) In Ca^{2+} treated CIP-expressing cells, the level of p35 expression showed about an 8-fold increase compared to the untreated cells (A4 and B4 vs A3 and B3), but there was no significant difference between the hBMECs (A2 and B2 vs A1 and B1). The bar chart represents the relative protein expression compared to the control (=1.0), and the experiment was repeated at least twice.

3.4.2.15 p35 Expression in hBMECs treated with Ca^{2+} and calpain

hBMECs were cultured and treated with Ca^{2+} (5μM) and calpain (10μg/ml) respectively for 30 mins. The untreated hBMECs were used as controls (Figure 3.57A) and the relative density of protein expression was analysed using Image-J (Figure 3.57B). α-tubulin was used as a loading control.

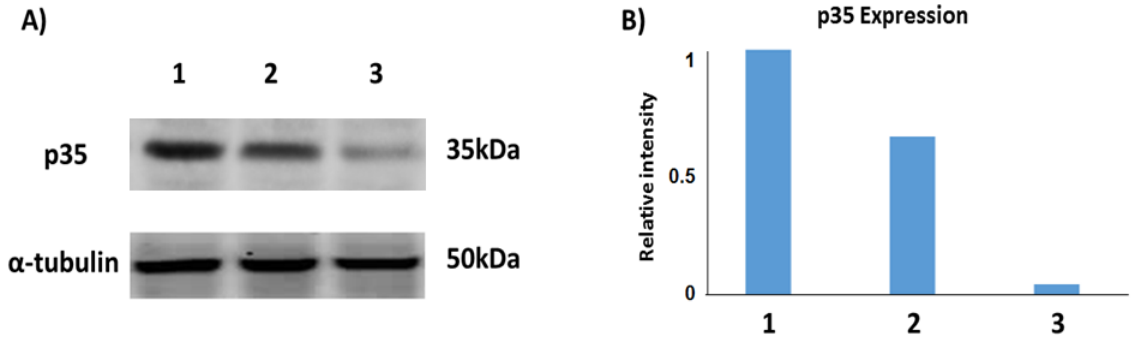

Figure 3-57 p35 expression in hBMECs treated with calpain and Ca^{2+} for 30 mins

A) 1: hBMECs control, 2: hBMECs treated with calpain (10µg/ml) and 3: hBMECs treated with Ca^{2+} (5µM).

B) Representative Western blot showing the p35 expression in hBMECs treated with calpain (10µg/ml) and Ca^{2+} (5µM) for 30 mins. The calpain- treated cells had a 0.45-fold decrease in p35 expression (A2 and B2 vs A1 and B1). The level of p35 expression showed a 5-fold decrease in Ca^{2+}-treated cells compared to controls (A3 and B3 vs A1 and B1). The bar chart represents the relative protein expression compared to the control (=1.0), and the experiment was repeated at least twice.

3.4.3 Discussion

The protein expression profiles of ECs under hypoxic conditions show an up-regulation of HSP-70 and caspase-3 (key proteins involved in apoptosis) and a downregulation of p35. This suggests that hypoxia induces apoptosis through HSP-70- and caspase-3-mediated pathways and that these pathways are dependent on the down-regulation and/or inhibition of p35. The evidence from this study suggests that CIP-expressing ECs reverse the actions of hypoxia through promoting p35 expression and reducing HSP-70 and caspase-3 and/or inhibiting their activity. This

implies that CIP exhibited resistance to hypoxia through 1) blocking apoptosis and 2) mediating p35-mediated pathways and/or by increasing the ratio of p35/p25 in response to hypoxia. Hence, two scenarios exist for CIP action (inhibition of Cdk5) under hypoxia: 1) inhibition of Cdk5 blocks the mechanism of apoptosis and/or 2) due to its high levels, p35 binds to and/or inhibits Cdk5 hypoxia-mediated damage.

Ca^{2+}-treatment at 5μM induces caspase-3 expression in ECs and CIP-expressing ECs under normoxia with this being time-dependent (decreases with time). Caspase-3 activation has been shown to trigger necrosis and apoptosis, and to exacerbate cerebral oedema and neuronal death after intracerebral haemorrhage (Wang et al., 2013). It was previously demonstrated that increases in intracellular calcium are involved in the activation of one or more families of proteases and possibly other degradative enzymes (Criddle et al., 2004) and that this is associated with cell death (Orrenius et al., 2003). Calcium overload was also suggested as one of the mechanisms for neuronal degeneration after an excitotoxic insult (Bano and Nicotera, 2007). CIP protects ECs from Ca^{2+}-induced caspase-3 expression suggesting a mechanism in which CIP blocks apoptosis and/or caspase-3 expression under normal conditions. CIP-expressing cells induce p-ERK 1/2 expression 40 mins after Ca^{2+} incubation in normal conditions and immediately (with a time-dependent increase), under conditions of increased [Ca^{2+}]. This is the second mechanism of CIP protection by enhancing the cellular proliferation marker (p-ERK1/2). ERK activity has been associated with neurodegenerative diseases and brain injury following ischaemia in animal models (Cagnol and Chambard, 2010).

Under conditions of increased [Ca^{2+}], ECs have reduced p-ERK1/2 levels, providing a mechanism for enhanced cellular damage. The increase in p-Cdk5 is a sign of EC protection under increased [Ca^{2+}], with CIP-expressing cells promoting its expression 40 mins after the elevation of Ca^{2+}. This phenomenon is also true in OVCdk5 cells treated with Ca^{2+}. CIP protection, through p-Cdk5, means a third mechanism for CIP protection. Also, it means that p-Cdk5 is the form of Cdk5 involved in mediating cellular protection under stroke conditions. Thus, in combined elevated Ca^{2+} and hypoxic conditions, p-35 expression coincides with the results from the p-Cdk5, which leads us to conclude that it is the p35-Cdk5 that is driving the cellular protective response to elevated Ca^{2+} levels. The results from the downregulation of p-35 expression under hypoxia and upregulation in the presence of CIP means that the protection of p-35/Cdk5 is also present in hypoxia and therefore stroke (since hypoxia and elevated Ca^{2+} represent two states of the stroke condition) (Aarts et al., 2003). The reduction of p-25 in presence of CIP means that CIP is preventing the conversion of p35 into p25 by calpain-dependent proteolysis of p25, thus inactivating the pathological role and the mislocalisation of Cdk5 by releasing it from p-25 and binding it to p35. Without CIP, Cdk5-p25 kinase hyperphosphorylated tau disrupts the cytoskeleton and promotes the apoptosis of primary neurons (Polster and Fiskum, 2004).

Chapter 4 Discussion

Stroke is one of the major causes of death and disability in developing countries. It takes place when the blood supply to a fraction of the brain is abruptly interrupted or severely reduced by, for instance, a blood clot. This is known as an ischaemic stroke. Hence, a detailed understanding of the mechanisms involved in the pathogenesis of stroke can provide a platform for therapeutic intervention and the adaptation of strategies to prevent the disease.

A number of studies indicate that deregulation of a set of cell cycle kinases has been implicated in neural death following an ischaemic insult and in neurodegenerative disorders. Here, it was highlighted Cdk5 and its two activators, the p35/p25 peptides, may act as potential critical players in neural survival, via support of revascularisation/angiogenesis. Below, the particular novel findings of the work and current literature and further hypotheses are highlighted.

4.1 A Role for Cdk5 in Cellular Attachment and Spreading

This study demonstrates that Cdk5 activation through its major substrate, p35, provides a key trigger for the initiation and maintenance of *in vitro* brain ECs angiogenesis and that this interaction and signalling cascade are crucial for ensuring correct cytoskeletal arrangement. While the activation of Cdk5 through p35 is associated with cytoprotection (Shi et al., 2012), as evident in this study, Cdk5 hyper-activation mediated by the cleaved p35 fragment, p25, and initiated via calpains is associated with neuronal cytoskeletal derangement, neuronal apoptosis

and cell death during ischaemic brain insult, similar to other observations (Love, 2003).

Cdk5 activity is regulated by synthesis and degradation of p35. p35, the activator of Cdk5, is a short-lived protein with a half-life of 20 to 30 minutes. A balance of synthesis and degradation controls the amount of the p35 protein. It can be degraded by the ubiquitin-proteasome pathway. The Cdk5/p35 complex is involved in multiple cellular functions such as differentiation, migration and angiogenesis (Kanungo et al., 2009; Liebl et al., 2010). In addition, previous work has shown that the incorporation of the inactive form of Cdk5 to developing neurones inhibited neurite outgrowth, and this could be relevant to stroke recovery (Lai et al., 2014).

It has been investigated the interplay of Cdk5 and p35 with classical molecular players of the control of mechanical forces and motility in EC. It was found a specific time/spatial interaction of active (phosphorylated) Cdk5 (p-Cdk5) and p35 with integrin β1 and talin, directed to the formation of microvesicles in late-spreading and elongated/moving cells. This observation was also evident where p35, Cdk5 and pCdk5 were localised at the focal tips of actin stress fibres (Huang et al., 2009; Liebl et al., 2010; He et al., 2011). Inhibition of this interaction, by roscovitine or in DN-mutants in our cellular model blocked cell protrusion and stable adhesions. Notably, the p35 localisation alongside actin fibres during spreading was time-dependent, hence longer time incubation leads to higher levels of localisation and culminated with the formation of focal clusters with Cdk5.

Under pathological conditions of cell stress or injury, calcium influx activates calpain, which in turn cleaves p35 to generate p25. This study was conducted to evaluate the ratio of p35/p25 in normoxic and hypoxic conditions. The degradation of p35 accompanied by the increase in abundance of p25 during hypoxic conditions suggest increased Cdk5/p25 ratio in cells under stress. The Cdk5/p25 complex contributes directly to cell death and pathogenesis of stroke (Kanungo et al., 2009). p25 in this scenario is responsible for the negative activation of Cdk5 and thus its subsequent involvement in the cellular death, opposing the actions of the Cdk5/p35 complex in directing cellular proliferation. Hence, the ratio of p35/p25 in cells determines the availability and ratio of Cdk5/p35 over Cdk5/p25 and thus promotion of either cellular proliferation or apoptosis.

4.2 Cdk5 Directly Promoted Cellular Migration and Angiogenesis

The results from this current study demonstrate that Cdk5 stimulated angiogenesis through cellular migration. It was suggested that Cdk5 and its activator proteins (e.g. p35) mediate migration through the phosphorylation of a variety of targets (Paterson and Courtneidge, 2017). The role of the p35 proteins is attributed to their presence within the plasma membrane at the cytoplasmic projection regions to assist cell motility as previously shown (Kanungo et al., 2009). Cdk5 may mediate migration through the phosphorylated regulation of Smurf1 binding to talin head (TH), thereby controlling TH turnover and adhesion stability leading to cell migration (Schaefer et al., 2012).

Upon talin proteolysis by Cdk5 phosphorylation, talin head ubiquitination and degradation are inhibited, thereby limiting focal adhesion turnover (promoting focal adhesion disassembly) and stabilising lamellipodia at the leading edges that, in turn, leads to cell migration mediated Smurf1-induced ubiquitination and degradation (Xie et al., 2013). A study by Demelash *et al*. also confirmed the presence of p35 in nuclear, cytoplasmic, and membranous locations using primary lung cancer cells as a model (Demelash et al., 2012). This study suggests that Cdk5 promotes the expression and upregulation of the *p35* gene(s) hence the presence of p35 within the nucleus. It was previously reported that the expression of the *p35*gene, as well as other genes involved in cellular migration, was regulated by neurogenic bHLH genes (Ge et al., 2006).

Here, the Cdk5-dependent hBMECs migration was preserved during hypoxia in those overexpressing Cdk5, but not in normal cells. Such a protective role of Cdk5 has previously in hypoxia *in vitro* (Kang et al., 2015). This effect of Cdk5 may be attributable to its ability to induce the expression of actin, microtubules and intermediate filament cytoskeletal components, which modulate cell adhesion, transport and intracellular signalling (Dhavan and Tsai, 2001).

Indeed, a study by Dhavan and Tsai suggests the involvement of Cdk5 and its activator, p35 in promoting neuronal migration and neurite outgrowth in actin polymerisation by PAK1, downregulation by PAK1 hyperphosphorylation through Cdk5 in a RAC-dependent manner using neuronal cells (Dhavan and Tsai, 2001; He et al., 2016). The latter process is complex and involves the contribution from the Rho family of GTPases and the PAK kinases. Furthermore, Cdk5 may indirectly

promote migration via the associated inhibition of p35-Cdk5 with β-catenin and N-cadherin (Dhavan and Tsai, 2001; Nguyen et al., 2002), which are implicated in neuronal adhesion and aggregation (Takeichi et al., 1990; Chalasani et al., 2005). Also shown here is that calpain decreased ECs migration; this may be due to the minor role of p25 in the regulation of Cdk5 during endothelial migration, although our current experimental data cannot really explain the mechanisms of this finding.

4.3 Inhibition Studies to Elucidate Mechanisms of Cdk5 Migration

When the Notch signalling inhibitor; DAPT was used, ECs and OVCdk5 migration were significantly reduced, as previously reported (Chen et al., 2015). DAPT has been shown to suppress Cdk5 activity and to modulate the distribution of cytoskeletal proteins in rat cortical neurons (Kanungo et al., 2008; Inestrosa et al., 2011). Hence, it was suggested that the inhibition of migration is due to the disruption of Cdk5/p35 interaction linked somehow through Notch signalling pathways (Kanungo et al., 2008; Pozo and Bibb, 2016). The latter also demonstrated the role of Cdk5 in forming a component in modulating Notch signalling and the role it may play in cytoskeletal protein arrangements and hence, neuronal development and survival. Furthermore, Cdk5 as well as acting through Notch was shown to phosphorylate integrin β-1, talin (Bosutti et al., 2013), neurofilaments and tau protein, involved in organisation/dynamics, cell spreading and subsequent cell migration (Ackerley et al., 2003; Shea et al., 2004; Compagnucci et al., 2016;). Thus, DAPT attenuation of Cdk5 activity may have led

to the reduced phosphorylation state of cytoskeletal proteins and their subsequent distribution.

FGF-2 in our cell migration assays also promoted Cdk5-dependent hBMECs migration. FGF-2 enhances cell differentiation and thus leads to cellular migration (Slevin and Krupinski, 2009), however, in this case, the increased Cdk5-dependent hBMECs migration may also be attributed to the effect of FGF-2 in upregulating the activity of Cdk5 (Ding et al., 2011). Although the impact of FGF-2 on Cdk5 activity was not measured in this current study, the latter may have important therapeutic implications when used *in vivo* to enhance the Cdk5 action and hence cellular survival under stroke conditions and/or CNS development to recover from the chronic effects of stroke.

4.4 The Pathophysiological Role of Cdk5-Possible Activators/Inhibitors under Hypoxia

The results in this thesis show that under normal conditions Cdk5 induces cell migration. The latter is reduced under the hypoxic condition similar to control. The overexpression of p35 in our ECs in hypoxia was previously confirmed by Mitsios *et al*., where Cdk5 and p35/p25 were shown to be concomitantly overexpressed in ECs in hypoxic regions of stroke tissue (Mitsios et al., 2007).

The latter phenomenon suggests that the balance of signalling between these pathways defines cellular fate in relation to angiogenesis or cell protection after

stroke (Slevin and Krupinski, 2009). The increase in the expression of p35 by overexpressed Cdk5 might provide some protection of the latter cells under hypoxic conditions. Overexpressed Cdk5 means there is more available to bind p35 and so competing against p25, so in effect, less aberrant p25 binding would occur. Overexpressed Cdk5 was demonstrated to have an effect on increasing the stability of p35 by 2 to 3 fold (Patrick et al., 1998; Corbel et al., 2015). The molecular mechanisms that underlie the higher ratio of p35/p25 association with OVCdk5 in hypoxia remain unknown.

4.5 CIP Inhibited Calpain-dependent Cdk5/p25-mediated Effects

It has been shown previously that excessive activation of calpain contributes to ischaemic neurodegeneration, neurotrauma and necrotic death (Liebl et al., 2010). Cdk5 hyper-activation mediated by the cleaved p35 fragment, p25, and initiated via calpain was shown to be associated with neuronal cytoskeletal derangement, neuronal apoptosis, and cell death during ischaemic brain insult (Love, 2003). This study confirms that the calcium-activated proteolytic enzyme, calpain is associated with an increased in the level and expression of p25 (the truncated product of p35) and abnormal Cdk5 activation by p25, as previously demonstrated (Amini et al., 2013).

The Ca^{2+}-activated protease calpain decreases the p35 availability and in this way contribute to the balance between cellular apoptosis and/or death in the normal situation. The results suggest a transient decrease in the expression of Cdk5

provoked by Ca^{2+} suggesting that calpain may play a role in this decrease. The Ca^{2+}-induced rise p-ERK expression followed a similar time course as that of Cdk5, which disappeared after 40 minutes of incubation in Ca^{2+}. In CIP overexpressing cells, the duration of increased p-ERK expression was prolonged, as was the reduction in Cdk5, suggesting a role of CIP in promoting p-ERK expression, activation of calpain and reduction in Cdk5 expression.

It has been demonstrated that the ratio of p35/p25 in CIP-expressing cells was up-regulated in response to hypoxia and exhibited resistance to hypoxia, which is involved in cell protection and angiogenesis. The results were as consistent with previous studies reporting the altered balance of p25/p35-Cdk5 signalling in favour of p35 *in vitro* in hBMECs during hypoxic conditions (Bosutti et al., 2013). Hence, the co-expression of CIP with p25 can reduce p25 mediated activation of Cdk5.

The results confirmed the role of CIP in increasing p35 bio-availability under hypoxic conditions while decreasing p25, as compared to normal controls. The CIP, Cdk5/p25 inhibitory peptide, is a derivative fragment of p35, which binds with high affinity to Cdk5. CIP competes with p25 for Cdk5 causing an inhibition of Cdk5/p25 activity without affecting the Cdk5/p35 ratio *in vitro*. The effects of CIP on inducing neuronal regeneration and inhibiting neuronal apoptosis have been demonstrated (Zheng et al., 2002; Zheng et al., 2005), but its protective effect in ECs has not been reported. It is suggested that CIP could protect ECs from hypoxia; the mechanism may involve the inhibition of the activity of Cdk5/p25. The 15 minutes incubation period may be insufficient for the expression of p-Cdk5 by CIP. The disorganised tube formation in our p-Cdk5 cells upon the inhibition of the p-35-Cdk5 axis may be

due to the decrease in the activity of the small GTPase Rac1, as previously suggested, leading to the disorganisation of the actin cytoskeleton (Liebl et al., 2010).

Linked to brain damage and neurodegeneration, it is believed that Cdk5/p25 directly phosphorylates the tau protein, which enhances cytoskeletal derangement (Lloret et al., 2015) and its endogenous activators, p35 and p25, regulate its activity. It was reported that forced expression of CIP inhibits Cdk5/p25 activity, preventing the phosphorylation of tau in neurons, thereby reversing the actions of calpain (Zheng et al., 2005; KOSARAJU, 2013). Therefore, it was suggested a possible additional function/use of CIP may be to act indirectly to reduce tau phosphorylation that could lead to a decrease in the neurofibrillary tangles and/or enhanced tube formation. Indeed, the use of the Cdk5 inhibitory peptide, CIP, in our case may reverse the process of neurodegeneration and neurofibrillary tangles triggered by calpain leading to an increase in the levels p35 and cellular survival signals, including Cdk5-mediated regulation of endothelial cell migration and angiogenesis (Liebl et al., 2010).

Furthermore, it has been shown that CIP reduces the expression of Heat shock protein 70 (HSP70, 70 kDa) and caspase-3 thus promoting cellular survival against apoptosis *in vitro*. Heat shock proteins are molecular chaperones, which guide protein folding and are involved in cellular transport. They can be upregulated in response to cellular stress, but some are also constitutively expressed (Conway, 2003). HSP70 was shown to bind to and enhance the degradation of Cdk5-hyperphosphorylated tau (Mietelska-Porowska et al., 2014). Thus, the down-

regulation of expression of the HP70 by CIP can be protective against tau protein phosphorylation by Cdk5 and thus promote EC migration (Kesavapany et al., 2007). Caspases, also known as interleukin 1β-converting enzyme (ICE)-like proteases, play key biological roles in inflammation and mammalian apoptosis (Loppnow et al., 2013), while CIP has a neuroprotective role in dissociating Cdk5 from p25, promoting the binding of Cdk5 to p35 (Ji et al., 2017).

The most intensively studied apoptotic caspase is caspase-3, which normally exists in the cytosolic fraction of cells as an inactive precursor that is activated by proteolysis during apoptotic cell death (Kavanagh et al., 2014). Caspase-3 can be activated by multiple apoptotic signals and has been shown to promote hypoxia-dependent cellular apoptosis (Hua et al., 2005). Caspase-3 expression, enzymatic activity and cleavage of its substrates inhibition were found to reduce DNA fragmentation and brain tissue loss (Han et al., 2002; Toulmond et al., 2004; McIlwain et al., 2013).

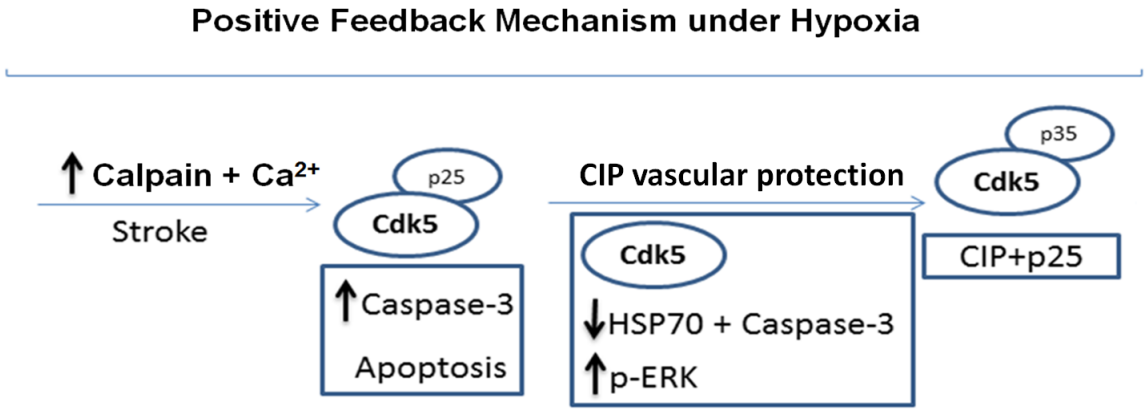

Figure 4-1 A schematic representation displaying a model for the mechanism of hypoxia-induced toxicity through calpain cleavage of the Cdk5-p35 complex

Hence, it is logical to believe that the reduction of caspase-3 expression through CIP can be protective against stroke-induced hypoxia and may display a therapeutic potential. P-ERK was demonstrated to have a long-term role in promoting vascular cell survival, and these findings indicate the protective role of CIP in reversing the activity of the Cdk5-p25 cytotoxic pathway. The involvement of ERK in the early growth response (EGR-1)-induced expression of p35, may explain the protective role of the latter in promoting cellular survival in CIP cells under hypoxia (Dhavan and Tsai, 2001; Sun et al., 2013). Hence, this study suggests that CIP mediates its protective role through decreasing the expression of HSP70 and caspase-3 and enhancing the expression of ERK (Figure 4.1).

Specifically, regarding EC/angiogenesis, after stroke, the presence of CIP appears to abrogate hypoxia and calpain-induced apoptosis at the same time allowing

vascularization to continue. Hence, during the remodelling phase of stroke, a more effective production of functional/patent microvessels within the penumbra region and sub-core of the infarct, following the release of growth factors and cytokines during the inflammatory phase, could lead to greater functional brain tissue recovery and reduce patient disability. Therefore a proposal for the use of CIP or a derivative of CIP as a therapeutic protection agent after stroke may be a viable possibility.

Chapter 5 Conclusions

- Findings from this study suggest that Cdk5 promotes an increase in the ratio p35/ p25 similar to that induced by CIP, thereby indicating CIP may have a protective role under hypoxic-stroke-mimicking conditions and could help therapeutically in reducing cellular/vascular apoptosis whilst improving tissue remodelling and angiogenesis.
- Cell morphological studies indicate the role of Cdk5 in sprout formation which under hypoxic conditions and in the presence of DAPT inhibitor is inhibited. This confirms a pre-angiogenic role for normal Cdk5 signalling pathways.
- Cdk5 promoted tube formation. Hence the overexpression of Cdk5 under hypoxic conditions may lead to cellular cytoskeletal rearrangement and aid the process of angiogenesis. However, an imbalance between the later mechanisms leads to Cdk5/p25 dependent apoptosis.
- CIP may determine the cellular fate and/or the degree of cell protection. Hence, this indicated the critical role of the p35/Cdk5 pathway in controlling cell dynamics of brain EC and general protection of brain cells against apoptosis under hypoxic conditions. CIP may be a potential therapeutic for acute stroke treatment with multiple positive attributes, therefore. Activation of p35/Cdk5 signalling at the expense of p25-Cdk5 plays a protective role in hypoxic conditions and positively contributes to preserving cell motility and the proper spatial and temporal control of cytoskeletal dynamics, which is essential for successful angiogenesis - mechanisms linking Cdk5 to cell attachment and movement have been described here.

- Taken together we suggest that the protective roles of CIP are mediated through the down-regulation of HSP-70 and caspase-3 (key proteins involved in apoptosis) and up-regulation of p-ERK (a marker for cellular survival and proliferation).

Chapter 6 Future prospects

The results from the present study indicate a protective role of CIP via promoting endothelial cell survival through enhancing the expression of ERK and reducing the caspase-3 and HSP70. Hence, CIP can display a potential therapeutic for individuals suffering a stroke.

Further studies are needed to account for the role of CIP as well as Cdk5 in stroke and adapt strategies to modulate their role *in vivo*.

Future studies could be employed to target specific substrates of Cdk5 linked to apoptosis, such as tau, p53, caspase 3 and Bax, thereby inhibiting their interaction with Cdk5, hence bypassing their cytotoxic pathways.

Future studies may also employ animal stroke models/studies to target both CIP and Cdk5 in real time *in vivo*. Kinase inhibitors (such as roscovitine) are not specific inhibitors of Cdk5-p25 but also of Cdk5-p35 and other Cdks, leading to potential side effects and reduced therapeutic efficacy. In order to overcome this problem, several peptides consisting of amino acid residues of p35, such as CIP (a peptide of 125 amino acid residues), p10 and p5, have been generated and can specifically reduce Cdk5-p25 hyperactivity. Stroke recovery would be monitored using MRI imaging platforms and recovery measurements as well as histology.

Nanoparticle-mediated drug loading, delivery and/or release strategies might be used to deliver CIP and/or active analogues to specific stroke tissues in a

nanoparticle-guided manner (e.g. superparamagnetic iron oxide). Studies could also be aimed at inhibiting the activity of the Cdk5-p25 complex. Previous studies have used truncated peptides of p35; P5, which is a 24-residue mimetic peptide of the p35 C-terminal and a more readily diffusible peptide through the blood-brain barrier. It can specifically inhibit p25-Cdk5 activity similar to CIP but was found ineffective for inhibiting the normal endogenous p35-Cdk5 activity. Strategies could also be targeted at blocking the cleavage of p35 to p25 by calpain to reduce its cytotoxic effects *in vivo*.

Chapter 7 Appendices

1. CIP Sequence 378bp

TGCCTGGGTGAGTTTCTCTGCCGCCGGTGCTACCGCCTGAAGCACCTGTCC

CCCACGGACCCCGTGCTCTGGCTGCGCAGCGTGGACCGCTCGCTGCTTCTG

CAGGGCTGGCAGGACCAGGGCTTCATCACGCCGGCCAACGTGGTCTTCCTC

TACATGCTCTGCAGGGATGTTATCTCCTCCGAGGTGGGCTCGGATCACGAGC

TCCAGGCCGTCCTGCTGACATGCCTGTACCTCTCCTACTCCTACATGGGCAA

CGAGATCTCCTACCCGCTCAAGCCCTTCCTGGTGGAGAGCTGCAAGGAGGC

CTTTTGGGACCGTTGCCTCTCTGTCATCAACCTCATGAGCTCAAAGATGCTGC

AGATAAATGCC

2. Construction of pcDNA3-CIP-GFP expression vectors

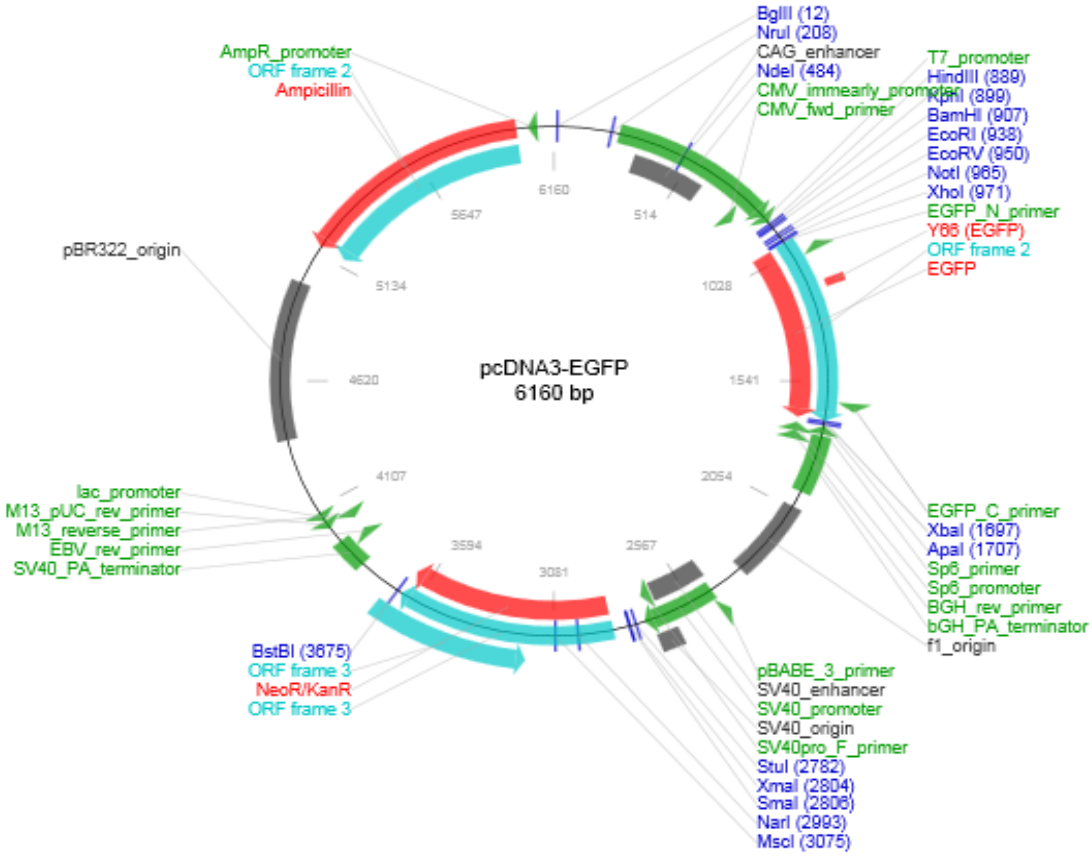

CIP DNA fragments were gained by PCR from pLV-CIP plasmids, the primers were 5'-TTAG GATCCTTGCCTGGGTGAGTTTC-3' and 5'-GTCGGATCCTCATGGGTCGGCATTTATC-3'. PCR product digested by *BamH I* (Invitrogen) was inserted into pcDNA3-GFP vectors by T4 ligation reaction. After transformation positive clones were screened by PCR, finally verified DNA sequence and reading frame through sequencing.

Transfecting hBMEC and selecting stable expression cell clones Using TransIT-2020 (Mirus) pcDNA3-CIP-GFP was transfected into hBMECs in 6-well plates. 260

μL of DNA complex including 2.5 μg plasmids and 7.5 μL TransIT-2020 reagents in EBM-2 medium was added to 80% confluence cells of each well. After transfection 24 hrs, cells were trypsinized and seeded in 48-well plates at different dilutions in EGM-2 medium containing 500 μg/ml Geneticin (GIBCO). The transfected cells were selected under the drug medium for next 4 weeks. Resistant clones were transferred into 6-well plates and were detected GFP fluorescent signals under fluorescence microscopy and the level of CIP mRNA by RT-PCR. All RT-PCR reagents were from Invitrogen, the RNAs of cell clones were isolated by TRIzol; RT reaction was carried out following Company's protocol including using 2.5 μg of RNA, 1 μl of SuperScript II and 1 μl of 50 μM random primer in 20 μl volume. 5 μl of cDNA was used for PCR reaction, CIP primers were the same as PCR clone primers, 18S rRNA as a housekeeping gene, primers were 5'-TAGAGGGACAAGTGGCGTTC-3' and 5'-TGTACAAAGGGCAGGGACTT-3'.

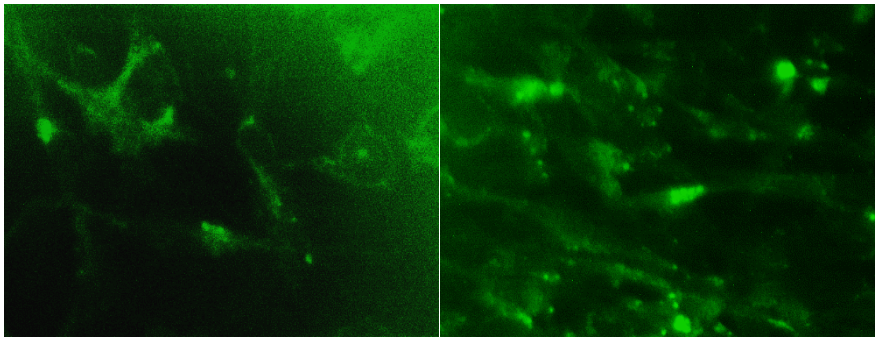

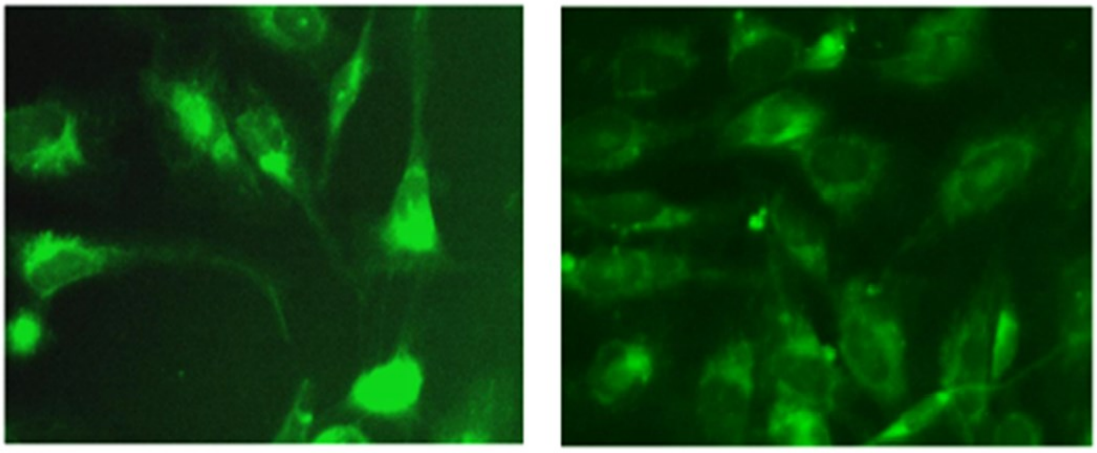

Expression of GFP fluorescent marker in CIP-17 clone transferred with pcDNA-GFP-CIP

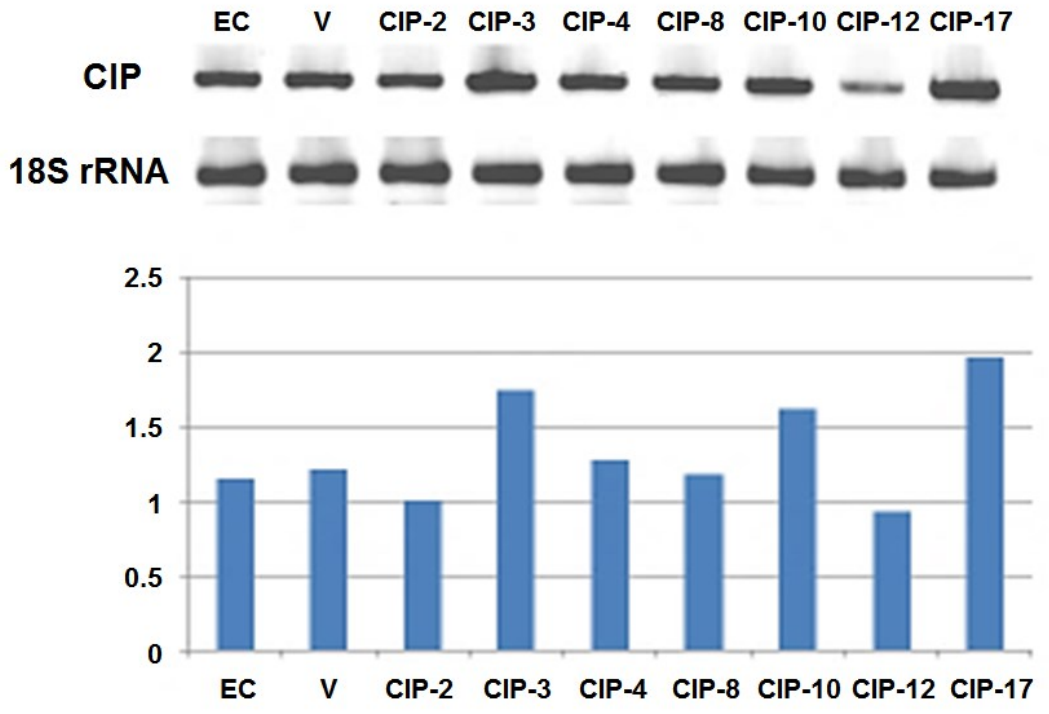

The levels of CIP mRNA in hBMEC clones transferred with pcDNA-GFP-CIP using RT-PCR

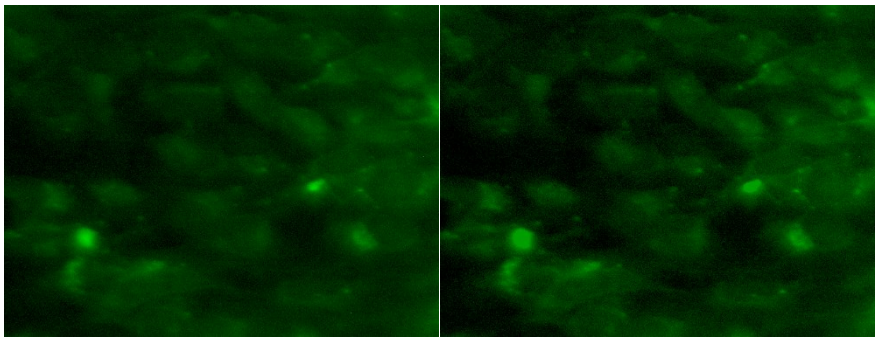

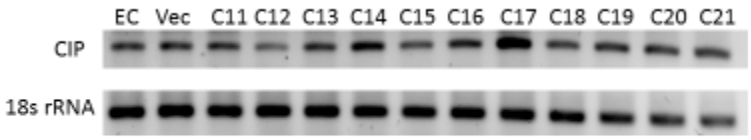
EC Vec C11 C12 C13 C14 C15 C16 C17 C18 C19 C20 C21
CIP
18s rRNA

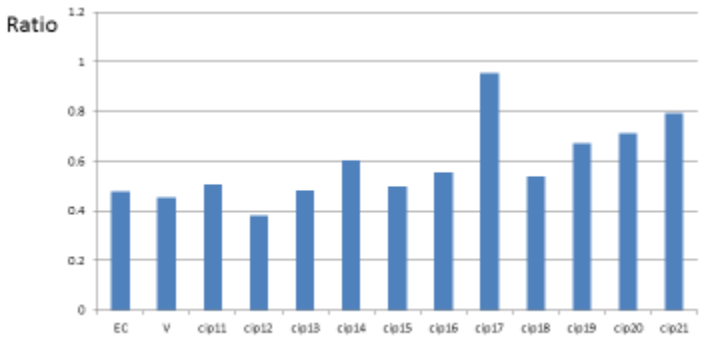
Ratio
1.2
1
0.8
0.6
0.4
0.2
0
EC
V
cip11
cip12
cip13
cip14
cip15
cip16
cip17
cip18
cip19
cip20
cip21

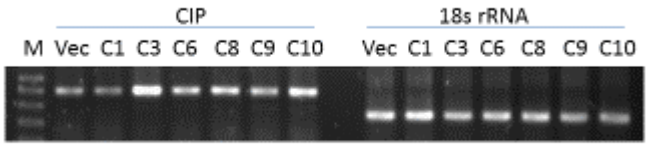
CIP
18s rRNA
M Vec C1 C3 C6 C8 C9 C10
Vec C1 C3 C6 C8 C9 C10

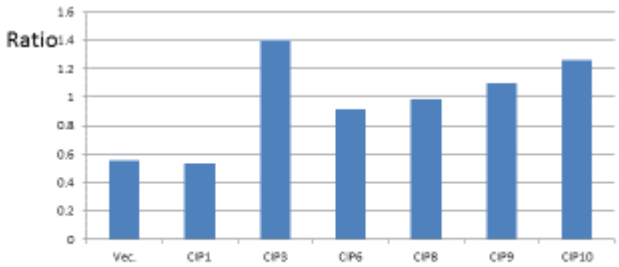
Ratio
1.6
1.4
1.2
1
0.8
0.6
0.4
0.2
0
Vec.
CIP1
CIP3
CIP6
CIP8
CIP9
CIP10

3. Chamber Used for Hypoxia Assay.

Chapter 8 REFERENCES

Aarts, M., Iihara, K., Wei, W.-L., Xiong, Z.-G., Arundine, M., Cerwinski, W., MacDonald, J. F. and Tymianski, M. (2003) 'A key role for TRPM7 channels in anoxic neuronal death.' *Cell*, 115(7) pp. 863-877.

Ackerley, S., Thornhill, P., Grierson, A. J., Brownlees, J., Anderton, B. H., Leigh, P. N., Shaw, C. E. and Miller, C. C. (2003) 'Neurofilament heavy chain side arm phosphorylation regulates axonal transport of neurofilaments.' *The Journal of Cell Biology*, 161(3) pp. 489-495.

Alway, D. and Cole, J. W. (2009) *Stroke Essentials for Primary Care: A Practical Guide.* Springer Science & Business Media.

Amini, M., Ma, C.-l., Farazifard, R., Zhu, G., Zhang, Y., Vanderluit, J., Zoltewicz, J. S., Hage, F., Savitt, J. M. and Lagace, D. C. (2013) 'Conditional disruption of calpain in the CNS alters dendrite morphology, impairs LTP, and promotes neuronal survival following injury.' *Journal of Neuroscience*, 33(13) pp. 5773-5784.

Andersen, J. P., Vestergaard, A. L., Mikkelsen, S. A., Mogensen, L. S., Chalat, M. and Molday, R. S. (2016) 'P4-ATPases as Phospholipid Flippases—Structure, Function, and Enigmas.' *Frontiers in Physiology*, 7

Andersen, M. H., Becker, J. C. and thor Straten, P. (2005) 'Regulators of apoptosis: suitable targets for immune therapy of cancer.' *Nature Reviews Drug Discovery*, 4(5) pp. 399-409.

Aronowski, J., Cho, K.-H., Strong, R. and Grotta, J. C. (1999) 'Neurofilament proteolysis after focal ischemia; when do cells die after experimental stroke?' *Journal of Cerebral Blood Flow & Metabolism*, 19(6) pp. 652-660.

Asada, A., Yamamoto, N., Gohda, M., Saito, T., Hayashi, N. and Hisanaga, S. i. (2008) 'Myristoylation of p39 and p35 is a determinant of cytoplasmic or nuclear localization of active cycline-dependent kinase 5 complexes.' *Journal of Neurochemistry*, 106(3) pp. 1325-1336.

Auerbach, R., Lewis, R., Shinners, B., Kubai, L. and Akhtar, N. (2003) 'Angiogenesis assays: a critical overview.' *Clinical Chemistry*, 49(1) pp. 32-40.

Avraham, H. K., Lee, T.-H., Koh, Y., Kim, T.-A., Jiang, S., Sussman, M., Samarel, A. M. and Avraham, S. (2003) 'Vascular endothelial growth factor regulates focal adhesion assembly in human brain microvascular endothelial cells through activation of the focal adhesion kinase and related adhesion focal tyrosine kinase.' *Journal of Biological Chemistry*, 278(38) pp. 36661-36668.

Baeten, K. M. and Akassoglou, K. (2011) 'Extracellular matrix and matrix receptors in blood–brain barrier formation and stroke.' *Developmental Neurobiology*, 71(11) pp. 1018-1039.

Bano, D. and Nicotera, P. (2007) 'Ca2+ signals and neuronal death in brain ischemia.' *Stroke*, 38(2) pp. 674-676.

Barber, P. A., Demchuk, A. M., Hirt, L. and Buchan, A. M. (2003) 'Biochemistry of ischemic stroke.' *Advances in Neurology*, 92 pp. 151-164.

Barros-Miñones, L., Martín-de-Saavedra, D., Perez-Alvarez, S., Orejana, L., Suquía, V., Goñi-Allo, B., Hervias, I., López, M. G., Jordan, J. and Aguirre, N. (2013) 'Inhibition of calpain-regulated p35/cdk5 plays a central role in sildenafil-induced protection against chemical hypoxia produced by malonate.' *Biochimica et Biophysica Acta (BBA)-Molecular Basis of Disease*, 1832(6) pp. 705-717.

Belayev, L., Lu, Y. and Bazan, N. G. (2012) 'Brain ischemia and reperfusion: cellular and molecular mechanisms in stroke injury.' *Basic Neurochemistry. Elsevier*, pp. 621-642.

Bonaventura, A., Liberale, L., Vecchié, A., Casula, M., Carbone, F., Dallegri, F. and Montecucco, F. (2016) 'Update on Inflammatory Biomarkers and Treatments in Ischemic Stroke.' *International Journal of Molecular Sciences*, 17(12) p. 1967.

Bornstein, N. M. (2009) *Stroke: practical guide for clinicians.* Karger Medical and Scientific Publishers.

Bosutti, A., Qi, J., Pennucci, R., Bolton, D., Matou, S., Ali, K., Tsai, L.-H., Krupinski, J., Petcu, E. B. and Montaner, J. (2013) 'Targeting p35/Cdk5 signalling via CIP-peptide promotes angiogenesis in hypoxia.' *PLoS One*, 8(9) p. e75538.

Brunner, L. S., Smeltzer, S. C. C., Bare, B. G., Hinkle, J. L. and Cheever, K. H. (2010) *Brunner & Suddarth's textbook of medical-surgical nursing.* Vol. 1. Lippincott Williams & Wilkins.

Budd, S. L. (1998) 'Mechanisms of neuronal damage in brain hypoxia/ischemia: focus on the role of mitochondrial calcium accumulation.' *Pharmacology & therapeutics*, 80(2) pp. 203-229.

Cagnol, S. and Chambard, J. C. (2010) 'ERK and cell death: Mechanisms of ERK-induced cell death–apoptosis, autophagy and senescence.' *FEBS journal*, 277(1) pp. 2-21.

Cao, Y. (2010) 'Therapeutic angiogenesis for ischemic disorders: what is missing for clinical benefits?' *Discovery Medicine*, 9(46) pp. 179-184.

Caplan, L. R. (2009) *Caplan's stroke: a clinical approach.* Elsevier Health Sciences.

Caplan, L. R. (2010) 'Stroke.' *ReadHowYouWant.com*,

Carmeliet, P., Moons, L., Luttun, A., Vincenti, V., Compernolle, V., De Mol, M., Wu, Y., Bono, F., Devy, L. and Beck, H. (2001) 'Synergism between vascular endothelial growth factor and placental growth factor contributes to angiogenesis and plasma extravasation in pathological conditions.' *Nature Medicine*, 7(5) pp. 575-583.

Carvajal, F. J., Mattison, H. A. and Cerpa, W. (2016) 'Role of NMDA Receptor-Mediated Glutamatergic Signaling in Chronic and Acute Neuropathologies.' *Neural Plasticity*, 2016

Chalasani, K., John, K., Yeo, S., Chitnis, A. and Brewster, R. (2005) *Role of N-Cadherin-mediated cell adhesion in regulating neurogenesis.* Vol. 283: Academic Press Inc Elsevier Science 525 B ST, Str 1900, San Diego, CA 92101-4495 USA.

Chang, K.-H., Vincent, F. and Shah, K. (2012) 'Deregulated Cdk5 triggers aberrant activation of cell cycle kinases and phosphatases inducing neuronal death.' *Journal of Cell Science*, 125(21) pp. 5124-5137.

Chang, K.-H., Multani, P. S., Sun, K.-H., Vincent, F., De Pablo, Y., Ghosh, S., Gupta, R., Lee, H.-P., Lee, H.-g. and Smith, M. A. (2011) 'Nuclear envelope dispersion triggered by deregulated Cdk5 precedes neuronal death.' *Molecular Biology of the Cell*, 22(9) pp. 1452-1462.

Chang, K. H., De Pablo, Y., Lee, H. p., Lee, H. g., Smith, M. A. and Shah, K. (2010) 'Cdk5 is a major regulator of p38 cascade: relevance to neurotoxicity in Alzheimer's disease.' *Journal of Neurochemistry*, 113(5) pp. 1221-1229.

Chappell, J. C., Wiley, D. M. and Bautch, V. L. (2011) *Regulation of blood vessel sprouting.* Vol. 22: Elsevier.

Chen, G., Wu, G.-Y., Zhang, L., Jiu-Chao, Y., Hana, Y., Ning-Xin, M. and Lee, G. (2015) Chemical reprogramming of human glial cells into neurons for brain and spinal cord repair. Google Patents.

Chen, J., Jin, K., Chen, M., Pei, W., Kawaguchi, K., Greenberg, D. A. and Simon, R. P. (1997) 'Early detection of DNA strand breaks in the brain after transient focal ischemia: implications for the role of DNA damage in apoptosis and neuronal cell death.' *Journal of Neurochemistry*, 69(1) pp. 232-245.

Chen, W., Li, Y., Li, J., Han, Q., Ye, L. and Li, A. (2011) 'Myricetin affords protection against peroxynitrite-mediated DNA damage and hydroxyl radical formation.' *Food and chemical toxicology*, 49(9) pp. 2439-2444.

Chillakuri, C. R., Sheppard, D., Lea, S. M. and Handford, P. A. (2012) *Notch receptor–ligand binding and activation: Insights from molecular studies.* Vol. 23: Elsevier.

Chiong, M., Wang, Z., Pedrozo, Z., Cao, D., Troncoso, R., Ibacache, M., Criollo, A., Nemchenko, A., Hill, J. and Lavandero, S. (2011) 'Cardiomyocyte death: mechanisms and translational implications.' *Cell Death & Disease*, 2(12) p. e244.

Chodobski, A., Zink, B. J. and Szmydynger-Chodobska, J. (2011) 'Blood–brain barrier pathophysiology in traumatic brain injury.' *Translational stroke research*, 2(4) pp. 492-516.

Chopp, M., Li, Y. and Zhang, J. (2008) 'Plasticity and remodeling of brain.' *Journal of the neurological sciences*, 265(1) pp. 97-101.

Clark, W. M. and Zivin, J. A. (1997) 'Antileukocyte adhesion therapy preclinical trials and combination therapy.' *Neurology*, 49(5 Suppl 4) pp. S32-S38.

Collen, A., Maas, A., Kooistra, T., Lupu, F., Grimbergen, J., Haas, F. J., Biesma, D. H., Koolwijk, P., Koopman, J. and van Hinsbergh, V. W. (2001) 'Aberrant fibrin formation and cross-linking of fibrinogen Nieuwegein, a variant with a shortened Aα-chain, alters endothelial capillary tube formation.' *Blood*, 97(4) pp. 973-980.

Compagnucci, C., Piemonte, F., Sferra, A., Piermarini, E. and Bertini, E. (2016) 'The cytoskeletal arrangements necessary to neurogenesis.' *Oncotarget*, 7(15) p. 19414.

Contreras-Vallejos, E., Utreras, E. and Gonzalez-Billault, C. (2012) 'Going out of the brain: non-nervous system physiological and pathological functions of Cdk5.' *Cellular signalling*, 24(1) pp. 44-52.

Conway, E. M. (2003) 'Angiogenesis: a link to thrombosis in athero-thrombotic disease.' *Pathophysiology of Haemostasis and Thrombosis*, 33(5-6) pp. 241-248.

Conway, E. M., Collen, D. and Carmeliet, P. (2001) 'Molecular mechanisms of blood vessel growth.' *Cardiovascular Research*, 49(3) pp. 507-521.

Cooper, G. M. (2000) 'Microtubules.' *The Cell*, (2nd edition; A Molecular Approach)

Corbel, C., Zhang, B., Le Parc, A., Baratte, B., Colas, P., Couturier, C., Kosik, K. S., Landrieu, I., Le Tilly, V. and Bach, S. (2015) 'Tamoxifen inhibits CDK5 kinase activity by interacting with p35/p25 and modulates the pattern of tau phosphorylation.' *Chemistry & biology*, 22(4) pp. 472-482.

Crews, L., Patrick, C., Achim, C. L., Everall, I. P. and Masliah, E. (2009) 'Molecular pathology of neuro-AIDS (CNS-HIV).' *International journal of molecular sciences*, 10(3) pp. 1045-1063.

Criddle, D. N., Raraty, M. G., Neoptolemos, J. P., Tepikin, A. V., Petersen, O. H. and Sutton, R. (2004) 'Ethanol toxicity in pancreatic acinar cells: mediation by nonoxidative fatty acid metabolites.' *Proceedings of the National Academy of Sciences of the United States of America*, 101(29) pp. 10738-10743.

D'amelio, M., Cavallucci, V. and Cecconi, F. (2010) 'Neuronal caspase-3 signaling: not only cell death.' *Cell Death & Differentiation*, 17(7) pp. 1104-1114.

Del Zoppo, G., Ginis, I., Hallenbeck, J. M., Iadecola, C., Wang, X. and Feuerstein, G. Z. (2000) 'Inflammation and stroke: putative role for cytokines, adhesion molecules and iNOS in brain response to ischemia.' *Brain Pathology*, 10(1) pp. 95-112.

Demelash, A., Rudrabhatla, P., Pant, H. C., Wang, X., Amin, N. D., McWhite, C. D., Naizhen, X. and Linnoila, R. I. (2012) 'Achaete-scute homologue-1 (ASH1) stimulates migration of lung cancer cells through Cdk5/p35 pathway.' *Molecular Biology of the Cell*, 23(15) pp. 2856-2866.

Dhavan, R. and Tsai, L.-H. (2001) 'A decade of CDK5.' *Nature Reviews Molecular Cell Biology*, 2(10) pp. 749-759.

Dietrich, W. D., Busto, R. and Bethea, J. R. (1999) 'Postischemic hypothermia and IL-10 treatment provide long-lasting neuroprotection of CA1 hippocampus following transient global ischemia in rats.' *Experimental Neurology*, 158(2) pp. 444-450.

Ding, V. M., Boersema, P. J., Foong, L. Y., Preisinger, C., Koh, G., Natarajan, S., Lee, D.-Y., Boekhorst, J., Snel, B. and Lemeer, S. (2011) 'Tyrosine phosphorylation profiling in FGF-2 stimulated human embryonic stem cells.' *PLoS One*, 6(3) p. e17538.

Dirnagl, U., Iadecola, C. and Moskowitz, M. A. (1999) 'Pathobiology of ischaemic stroke: an integrated view.' *Trends in Neurosciences*, 22(9) pp. 391-397.

Elmore, S. (2007) 'Apoptosis: a review of programmed cell death.' *Toxicologic pathology*, 35(4) pp. 495-516.

Fassbender, K., Rossol, S., Kammer, T., Daffertshofer, M., Wirth, S., Dollman, M. and Hennerici, M. (1994) 'Proinflammatory cytokines in serum of patients with acute cerebral ischemia: kinetics of secretion and relation to the extent of brain damage and outcome of disease.' *Journal of the Neurological Sciences*, 122(2) pp. 135-139.

Ferguson, R. E., Carroll, H. P., Harris, A., Maher, E. R., Selby, P. J. and Banks, R. E. (2005) 'Housekeeping proteins: a preliminary study illustrating some limitations as useful references in protein expression studies.' *Proteomics*, 5(2) pp. 566-571.

Feuerstein, G., Wang, X. and Barone, F. (1998) 'Inflammatory mediators of ischemic injury: cytokine gene regulation in stroke.' *Cerebrovascular Disease: Pathophysiology, Diagnosis and Management*, pp. 507-531.

Fischer, A., eacute, Sananbenesi, F., Spiess, J. and Radulovic, J. (2003) 'Cdk5: a novel role in learning and memory.' *Neurosignals*, 12(4-5) pp. 200-208.

Fisher, M. (2009) 'Stroke: Investigation and management.' *Amsterdam: Elsevier Health Sciences*,

Fu, X., Choi, Y.-K., Qu, D., Yu, Y., Cheung, N. S. and Qi, R. Z. (2006) 'Identification of nuclear import mechanisms for the neuronal Cdk5 activator.' *Journal of Biological Chemistry*, 281(51) pp. 39014-39021.

Ge, W., He, F., Kim, K. J., Blanchi, B., Coskun, V., Nguyen, L., Wu, X., Zhao, J., Heng, J. I.-T. and Martinowich, K. (2006) 'Coupling of cell migration with neurogenesis by proneural bHLH factors.' *Proceedings of the National Academy of Sciences*, 103(5) pp. 1319-1324.

Gillardon, F., Kiprianova, I., Sandkühler, J., Hossmann, K.-A. and Spranger, M. (1999) 'Inhibition of caspases prevents cell death of hippocampal CA1 neurons, but not impairment of hippocampal long-term potentiation following global ischemia.' *Neuroscience*, 93(4) pp. 1219-1222.

Gillessen, T., Budd, S. L. and Lipton, S. A. (2013) 'Excitatory Amino Acid Neurotoxicity.'

Glading, A., Lauffenburger, D. A. and Wells, A. (2002) 'Cutting to the chase: calpain proteases in cell motility.' *Trends in Cell Biology*, 12(1) pp. 46-54.

Goldstein, L. B. (2011) *A primer on stroke prevention and treatment: An overview based on AHA/ASA guidelines.* John Wiley & Sons.

Gomez-Villafuertes, R., Torres, B., Barrio, J., Savignac, M., Gabellini, N., Rizzato, F., Pintado, B., Gutierrez-Adan, A., Mellström, B. and Carafoli, E. (2005) 'Downstream regulatory element antagonist modulator regulates Ca2+ homeostasis and viability in cerebellar neurons.' *The Journal of Neuroscience*, 25(47) pp. 10822-10830.

Gorgui, J., Gorshkov, M., Khan, N. and Daskalopoulou, S. S. (2014) 'Hypertension as a risk factor for ischemic stroke in women.' *Canadian Journal of Cardiology*, 30(7) pp. 774-782.

Greenberg, D. A. and Jin, K. (2005) 'From angiogenesis to neuropathology.' *Nature*, 438(7070) pp. 954-959.

Guan, J.-S., Su, S. C., Gao, J., Joseph, N., Xie, Z., Zhou, Y., Durak, O., Zhang, L., Zhu, J. J. and Clauser, K. R. (2011) 'Cdk5 is required for memory function and hippocampal plasticity via the cAMP signaling pathway.' *PLoS One*, 6(9) p. e25735.

Gusev, E. and Skvortsova, V. I. (2003a) 'Hemodynamic Events Associated with Acute Focal Brain Ischemia and Reperfusion. Ischemic Penumbra.' *In Brain Ischemia*. Springer, pp. 9-19.

Gusev, E. and Skvortsova, V. I. (2003b) 'Microglial activation, cytokine production, and local inflammation in focal brain ischemia.' *In Brain ischemia*. Springer, pp. 115-145.

Gwag, B. J., Won, S. J. and Kim, D. Y. (2002) 'Excitotoxicity, oxidative stress, and apoptosis in ischemic neuronal death.' *New concepts in cerebral ischemia*, pp. 79-112.

Haarmann, A., Deiss, A., Prochaska, J., Foerch, C., Weksler, B., Romero, I., Couraud, P.-O., Stoll, G., Rieckmann, P. and Buttmann, M. (2010) 'Evaluation of soluble junctional adhesion molecule-A as a biomarker of human brain endothelial barrier breakdown.' *PLoS One*, 5(10) p. e13568.

Han, B. H., Xu, D., Choi, J., Han, Y., Xanthoudakis, S., Roy, S., Tam, J., Vaillancourt, J., Colucci, J. and Siman, R. (2002) 'Selective, reversible caspase-3 inhibitor is

neuroprotective and reveals distinct pathways of cell death after neonatal hypoxic-ischemic brain injury.' *Journal of Biological Chemistry*, 277(33) pp. 30128-30136.

Hawasli, A. H., Benavides, D. R., Nguyen, C., Kansy, J. W., Hayashi, K., Chambon, P., Greengard, P., Powell, C. M., Cooper, D. C. and Bibb, J. A. (2007) 'Cyclin-dependent kinase 5 governs learning and synaptic plasticity via control of NMDAR degradation.' *Nature Neuroscience*, 10(7) pp. 880-886.

Hayashi, T., Warita, H., Abe, K. and Itoyama, Y. (1999) 'Expression of cyclin-dependent kinase 5 and its activator p35 in rat brain after middle cerebral artery occlusion.' *Neuroscience letters*, 265(1) pp. 37-40.

He, H., Deng, K., Siddiq, M. M., Pyie, A., Mellado, W., Hannila, S. S. and Filbin, M. T. (2016) 'Cyclic AMP and Polyamines Overcome Inhibition by Myelin-Associated Glycoprotein through eIF5A-Mediated Increases in p35 Expression and Activation of Cdk5.' *Journal of Neuroscience*, 36(10) pp. 3079-3091.

He, L., Zhang, Z., Yu, Y., Ahmed, S., Cheung, N. S. and Qi, R. Z. (2011) 'The neuronal p35 activator of Cdk5 is a novel F-actin binding and bundling protein.' *Cellular and Molecular Life Sciences*, 68(9) pp. 1633-1643.

Heiss, W.-D. (2000) 'Ischemic Penumbra: Evidence From Functional Imaging in Man.' *Journal of Cerebral Blood Flow & Metabolism*, 20(9) pp. 1276-1293.

Hoeben, A., Landuyt, B., Highley, M. S., Wildiers, H., Van Oosterom, A. T. and De Bruijn, E. A. (2004) 'Vascular endothelial growth factor and angiogenesis.' *Pharmacological Reviews*, 56(4) pp. 549-580.

Hu, X., De Silva, T. M., Chen, J. and Faraci, F. M. (2017) 'Cerebral vascular disease and neurovascular injury in ischemic stroke.' *Circulation research*, 120(3) pp. 449-471.

Hua, F., Cornejo, M. G., Cardone, M. H., Stokes, C. L. and Lauffenburger, D. A. (2005) 'Effects of Bcl-2 levels on Fas signaling-induced caspase-3 activation: molecular genetic tests of computational model predictions.' *The Journal of Immunology*, 175(2) pp. 985-995.

Huang, C., Rajfur, Z., Yousefi, N., Chen, Z., Jacobson, K. and Ginsberg, M. H. (2009) 'Talin phosphorylation by Cdk5 regulates Smurf1-mediated talin head ubiquitylation and cell migration.' *Nature Cell Biology*, 11(5) pp. 624-630.

Ikeda, T., Ikenoue, T., Xia, X. Y. and Xia, Y. X. (2000) 'Important role of 72-kd heat shock protein expression in the endothelial cell in acquisition of hypoxic-ischemic tolerance in the immature rat.' *American Journal of Obstetrics and Gynecology*, 182(2) pp. 380-386.

Inestrosa, N., Tapia-Rojas, C., Griffith, T., Carvajal, F., Benito, M., Rivera-Dictter, A., Alvarez, A., Serrano, F., Hancke, J. and Burgos, P. (2011) 'Tetrahydrohyperforin prevents cognitive deficit, Aβ deposition, tau phosphorylation and synaptotoxicity in the APPswe/PSEN1ΔE9 model of Alzheimer's disease: a possible effect on APP processing.' *Translational psychiatry*, 1(7) p. e20.

Ji, Y.-B., Zhuang, P.-P., Ji, Z., Wu, Y.-M., Gu, Y., Gao, X.-Y., Pan, S.-Y. and Hu, Y.-F. (2017) 'TFP5 peptide, derived from CDK5-activating cofactor p35, provides neuroprotection in early-stage of adult ischemic stroke.' *Scientific Reports*, 7

Jin, J., Lao, A., Katsura, M., Caputo, A., Schweizer, F. and Sokolow, S. (2014) 'Involvement of the sodium–calcium exchanger 3 (NCX3) in ziram-induced calcium dysregulation and toxicity.' *Neurotoxicology*, 45 pp. 56-66.

Jin, R., Yang, G. and Li, G. (2010) 'Inflammatory mechanisms in ischemic stroke: role of inflammatory cells.' *Journal of leukocyte biology*, 87(5) pp. 779-789.

Johannes Binder, K. S. (2012) 'Stroke.' *Oxford: Oxford University Press*, Book

Joshi, G., Chi, Y., Huang, Z. and Wang, Y. (2014) 'Aβ-induced Golgi fragmentation in Alzheimer's disease enhances Aβ production.' *Proceedings of the National Academy of Sciences*, 111(13) pp. E1230-E1239.

Kalogeris, T., Bao, Y. and Korthuis, R. J. (2014) 'Mitochondrial reactive oxygen species: a double edged sword in ischemia/reperfusion vs preconditioning.' *Redox biology*, 2 pp. 702-714.

Kamei, H., Saito, T., Ozawa, M., Fujita, Y., Asada, A., Bibb, J. A., Saido, T. C., Sorimachi, H. and Hisanaga, S.-i. (2007) 'Suppression of calpain-dependent cleavage of the CDK5

activator p35 to p25 by site-specific phosphorylation.' *Journal of Biological Chemistry*, 282(3) pp. 1687-1694.

Kang, Y., Tierney, M., Ong, E., Zhang, L., Piermarocchi, C., Sacco, A. and Paternostro, G. (2015) 'Combinations of Kinase Inhibitors Protecting Myoblasts against Hypoxia.' *PloS one*, 10(6) p. e0126718.

Kanungo, J., Zheng, Y. L., Amin, N. D. and Pant, H. C. (2008) 'The Notch signaling inhibitor DAPT down-regulates cdk5 activity and modulates the distribution of neuronal cytoskeletal proteins.' *Journal of Neurochemistry*, 106(5) pp. 2236-2248.

Kanungo, J., Zheng, Y.-l., Amin, N. D. and Pant, H. C. (2009) 'Targeting Cdk5 activity in neuronal degeneration and regeneration.' *Cellular and Molecular Neurobiology*, 29(8) pp. 1073-1080.

Kaufmann, A. M., Firlik, A. D., Fukui, M. B., Wechsler, L. R., Jungries, C. A. and Yonas, H. (1999) 'Ischemic Core and Penumbra in Human Stroke.' *Stroke*, 30(1) pp. 93-99.

Kavanagh, E., Rodhe, J., Burguillos, M., Venero, J. and Joseph, B. (2014) 'Regulation of caspase-3 processing by cIAP2 controls the switch between pro-inflammatory activation and cell death in microglia.' *Cell death & disease*, 5(12) p. e1565.

Kesavapany, S., Zheng, Y. L., Amin, N. and Pant, H. C. (2007) 'Peptides derived from Cdk5 activator p35, specifically inhibit deregulated activity of Cdk5.' *Biotechnology Journal*, 2(8) pp. 978-987.

Kim, J. Y., Kawabori, M. and Yenari, M. A. (2014) 'Innate inflammatory responses in stroke: mechanisms and potential therapeutic targets.' *Current medicinal chemistry*, 21(18) pp. 2076-2097.

Kimura, T., Ishiguro, K. and Hisanaga, S.-i. (2014) 'Physiological and pathological phosphorylation of tau by Cdk5.' *Frontiers in Molecular Neuroscience*, 7 p. 65.

Koh, J.-Y., Goldberg, M. P., Hartley, D. M. and Choi, D. W. (1990) 'Non-NMDA receptor-mediated neurotoxicity in cortical culture.' *The Journal of Neuroscience*, 10(2) pp. 693-705.

KOSARAJU, V. K. (2013) *BIOINFORMATICS ANALYSIS OF CYCLIN-DEPENDENT KINASE 5: INSIGHTS TO DRUG DISCOVERY.* NATIONAL UNIVERSITY OF SINGAPORE.

Koumura, A., Nonaka, Y., Hyakkoku, K., Oka, T., Shimazawa, M., Hozumi, I., Inuzuka, T. and Hara, H. (2008) 'A novel calpain inhibitor,((1S)-1 ((((1S)-1-benzyl-3-cyclopropylamino-2, 3-di-oxopropyl) amino) carbonyl)-3-methylbutyl) carbamic acid 5-methoxy-3-oxapentyl ester, protects neuronal cells from cerebral ischemia-induced damage in mice.' *Neuroscience*, 157(2) pp. 309-318.

Krupinski, J., Lopez, E., Marti, E. and Ferrer, I. (2000) 'Expression of caspases and their substrates in the rat model of focal cerebral ischemia.' *Neurobiology of Disease*, 7(4) pp. 332-342.

Lai, T. W., Zhang, S. and Wang, Y. T. (2014) 'Excitotoxicity and stroke: identifying novel targets for neuroprotection.' *Progress in neurobiology*, 115 pp. 157-188.

Lakhan, S. E., Kirchgessner, A. and Hofer, M. (2009) 'Inflammatory mechanisms in ischemic stroke: therapeutic approaches.' *Journal of translational medicine*, 7(1) p. 97.

Lee, M.-s., Kwon, Y. T., Li, M., Peng, J., Friedlander, R. M. and Tsai, L.-H. (2000) 'Neurotoxicity induces cleavage of p35 to p25 by calpain.' *Nature*, 405(6784) pp. 360-364.

Leker, R. R. and Shohami, E. (2002) 'Cerebral ischemia and trauma—different etiologies yet similar mechanisms: neuroprotective opportunities.' *Brain Research Reviews*, 39(1) pp. 55-73.

Li, S., Wong, A. H. and Liu, F. (2014) 'Ligand-gated ion channel interacting proteins and their role in neuroprotection.' *Frontiers in cellular neuroscience*, 8

Liebl, J., Weitensteiner, S. B., Vereb, G., Takács, L., Fürst, R., Vollmar, A. M. and Zahler, S. (2010) 'Cyclin-dependent kinase 5 regulates endothelial cell migration and angiogenesis.' *Journal of Biological Chemistry*, 285(46) pp. 35932-35943.

Liu, C., Zhai, X., Zhao, B., Wang, Y. and Xu, Z. (2017) 'Cyclin I-like (CCNI2) is a cyclin-dependent kinase 5 (CDK5) activator and is involved in cell cycle regulation.' *Scientific reports*, 7 p. 40979.

Liu, X.-q., Sheng, R. and Qin, Z.-h. (2009) 'The neuroprotective mechanism of brain ischemic preconditioning.' *Acta Pharmacologica Sinica*, 30(8) pp. 1071-1080.

Lloret, A., Fuchsberger, T., Giraldo, E. and Vina, J. (2015) 'Molecular mechanisms linking amyloid β toxicity and Tau hyperphosphorylation in Alzheimer′ s disease.' *Free Radical Biology and Medicine*, 83 pp. 186-191.

Loppnow, H., Guzik, K. and Pryjma, J. (2013) 'The role of caspases in modulation of cytokines and other molecules in apoptosis and inflammation.'

Losordo, D. W. and Dimmeler, S. (2004) 'Therapeutic angiogenesis and vasculogenesis for ischemic disease part I: angiogenic cytokines.' *Circulation*, 109(21) pp. 2487-2491.

Love, S. (2003) 'Neuronal expression of cell cycle-related proteins after brain ischaemia in man.' *Neuroscience Letters*, 353(1) pp. 29-32.

Ma, Y., Zechariah, A., Qu, Y. and Hermann, D. M. (2012) 'Effects of vascular endothelial growth factor in ischemic stroke.' *Journal of neuroscience research*, 90(10) pp. 1873-1882.

McIlwain, D. R., Berger, T. and Mak, T. W. (2013) 'Caspase functions in cell death and disease.' *Cold Spring Harbor perspectives in biology*, 5(4) p. a008656.

Mehta, J. and Dhalla, N. S. (2013) *Biochemical basis and therapeutic implications of angiogenesis.* Springer.

Mendoza, M. C., Er, E. E. and Blenis, J. (2011) 'The Ras-ERK and PI3K-mTOR pathways: cross-talk and compensation.' *Trends in biochemical sciences*, 36(6) pp. 320-328.

Mietelska-Porowska, A., Wasik, U., Goras, M., Filipek, A. and Niewiadomska, G. (2014) 'Tau protein modifications and interactions: their role in function and dysfunction.' *International Journal of Molecular Sciences*, 15(3) pp. 4671-4713.

Mirabelli-Badenier, M., Braunersreuther, V., Viviani, G. L., Dallegri, F., Quercioli, A., Veneselli, E., Mach, F. and Montecucco, F. (2011) 'CC and CXC chemokines are pivotal

mediators of cerebral injury in ischaemic stroke.' *Thrombosis and Haemostasis*, 105(3) pp. 409-420.

Mitsios, N., Pennucci, R., Krupinski, J., Sanfeliu, C., Gaffney, J., Kumar, P., Kumar, S., Juan-Babot, O. and Slevin, M. (2007) 'Expression of Cyclin-Dependent Kinase 5 mRNA and Protein in the Human Brain Following Acute Ischemic Stroke.' *Brain Pathology*, 17(1) pp. 11-23.

Morrison, R. S., Kinoshita, Y., Johnson, M. D., Ghatan, S., Ho, J. T. and Garden, G. (2003) 'Neuronal survival and cell death signaling pathways.' *In Molecular and Cellular Biology of Neuroprotection in the CNS*. Springer, pp. 41-86.

Multhoff, G., Radons, J. and Vaupel, P. (2014) 'Critical role of aberrant angiogenesis in the development of tumor hypoxia and associated radioresistance.' *Cancers*, 6(2) pp. 813-828.

Munoz-Chapuli, R., Quesada, A. and Medina, M. A. (2004) 'Angiogenesis and signal transduction in endothelial cells.' *Cellular and Molecular Life Sciences*, 61(17) pp. 2224-2243.

Ndhlovu, M., Preuß, B. E., Dengjel, J., Stevanovic, S., Weiner, S. M. and Klein, R. (2011) 'Identification of α-tubulin as an autoantigen recognized by sera from patients with neuropsychiatric systemic lupus erythematosus.' *Brain, Behavior, and Immunity*, 25(2) pp. 279-285.

Nguyen, M., Mushynski, W. and Julien, J. (2002) 'Cycling at the interface between neurodevelopment and neurodegeneration.' *Cell death and differentiation*, 9(12) p. 1294.

Northington, F. J., Chavez-Valdez, R. and Martin, L. J. (2011) 'Neuronal cell death in neonatal hypoxia-ischemia.' *Annals of neurology*, 69(5) pp. 743-758.

Obermeier, B., Daneman, R. and Ransohoff, R. M. (2013) 'Development, maintenance and disruption of the blood-brain barrier.' *Nature Medicine*, 19(12) pp. 1584-1596.

Ohshima, T., Ogura, H., Tomizawa, K., Hayashi, K., Suzuki, H., Saito, T., Kamei, H., Nishi, A., Bibb, J. A. and Hisanaga, S. i. (2005) 'Impairment of hippocampal long-term

depression and defective spatial learning and memory in p35−/−mice.' *Journal of Neurochemistry*, 94(4) pp. 917-925.

Olsen, T. S., Larsen, B., Herning, M., Skriver, E. B. and Lassen, N. (1983) 'Blood flow and vascular reactivity in collaterally perfused brain tissue. Evidence of an ischemic penumbra in patients with acute stroke.' *Stroke*, 14(3) pp. 332-341.

Ooboshi, H., Ibayashi, S., Shichita, T., Kumai, Y., Takada, J., Ago, T., Arakawa, S., Sugimori, H., Kamouchi, M. and Kitazono, T. (2005) 'Postischemic gene transfer of interleukin-10 protects against both focal and global brain ischemia.' *Circulation*, 111(7) pp. 913-919.

Orrenius, S., Zhivotovsky, B. and Nicotera, P. (2003) 'Regulation of cell death: the calcium–apoptosis link.' *Nature Reviews Molecular Cell Biology*, 4(7) pp. 552-565.

Panickar, K. S., Nonner, D., White, M. G. and Barrett, J. N. (2008) 'Overexpression of Cdk5 or non-phosphorylatable retinoblastoma protein protects septal neurons from oxygen–glucose deprivation.' *Neurochemical Research*, 33(9) pp. 1852-1858.

Pantoni, L., Sarti, C. and Inzitari, D. (1998) 'Cytokines and cell adhesion molecules in cerebral ischemia experimental bases and therapeutic perspectives.' *Arteriosclerosis, Thrombosis and Vascular Biology*, 18(4) pp. 503-513.

Paterson, E. K. and Courtneidge, S. A. (2017) 'Invadosomes are coming: new insights into function and disease relevance.' *The FEBS Journal*,

Patrick, G. N., Zhou, P., Kwon, Y. T., Howley, P. M. and Tsai, L.-H. (1998) 'p35, the neuronal-specific activator of cyclin-dependent kinase 5 (Cdk5) is degraded by the ubiquitin-proteasome pathway.' *Journal of Biological Chemistry*, 273(37) pp. 24057-24064.

Patrick, G. N., Zukerberg, L., Nikolic, M., de La Monte, S., Dikkes, P. and Tsai, L.-H. (1999) 'Conversion of p35 to p25 deregulates Cdk5 activity and promotes neurodegeneration.' *Nature*, 402(6762) pp. 615-622.

Pignataro, G., Simon, R. P. and Xiong, Z.-G. (2007) 'Prolonged activation of ASIC1a and the time window for neuroprotection in cerebral ischaemia.' *Brain*, 130(1) pp. 151-158.

Pignataro, G., Esposito, E., Cuomo, O., Sirabella, R., Boscia, F., Guida, N., Di Renzo, G. and Annunziato, L. (2011) 'The NCX3 isoform of the Na+/Ca2+ exchanger contributes to neuroprotection elicited by ischemic postconditioning.' *Journal of Cerebral Blood Flow & Metabolism*, 31(1) pp. 362-370.

Polster, B. M. and Fiskum, G. (2004) 'Mitochondrial mechanisms of neural cell apoptosis.' *Journal of Neurochemistry*, 90(6) pp. 1281-1289.

Popp, A. J. (2011) *Guide to the Primary Care of Neurological Disorders.* New York: Thieme.

Portt, L., Norman, G., Clapp, C., Greenwood, M. and Greenwood, M. T. (2011) 'Anti-apoptosis and cell survival: a review.' *Biochimica et Biophysica Acta (BBA)-Molecular Cell Research*, 1813(1) pp. 238-259.

Potthoff, M. J., Arnold, M. A., McAnally, J., Richardson, J. A., Bassel-Duby, R. and Olson, E. N. (2007) 'Regulation of skeletal muscle sarcomere integrity and postnatal muscle function by Mef2c.' *Molecular and Cellular Biology*, 27(23) pp. 8143-8151.

Pottorf, W. J., Johanns, T. M., Derrington, S. M., Strehler, E. E., Enyedi, A. and Thayer, S. A. (2006) 'Glutamate-induced protease-mediated loss of plasma membrane Ca2+ pump activity in rat hippocampal neurons.' *Journal of Neurochemistry*, 98(5) pp. 1646-1656.

Pozo, K. and Bibb, J. A. (2016) 'The Emerging Role of Cdk5 in Cancer.' *Trends in Cancer*, 2(10) pp. 606-618.

Qiao, F., Gao, C. Y., Tripathi, B. K. and Zelenka, P. S. (2008) 'Distinct functions of Cdk5 (Y15) phosphorylation and Cdk5 activity in stress fiber formation and organization.' *Experimental Cell Research*, 314(19) pp. 3542-3550.

Rajdev, S., Hara, K., Kokubo, Y., Mestril, R., Dillmann, W., Weinstein, P. R. and Sharp, F. R. (2000) 'Mice overexpressing rat heat shock protein 70 are protected against cerebral infarction.' *Annals of Neurology*, 47(6) pp. 782-791.

Ramesh, G., MacLean, A. G. and Philipp, M. T. (2013) 'Cytokines and chemokines at the crossroads of neuroinflammation, neurodegeneration, and neuropathic pain.' *Mediators of inflammation*, 2013

Rastogi, R. P. and Sinha, R. P. (2010) 'Apoptosis: molecular mechanisms and pathogenicity.' *Excli Journal*, pp. 155-181.

Rodríguez-Yáñez, M., Castellanos, M., Blanco, M., Mosquera, E. and Castillo, J. (2006) 'Vascular protection in brain ischemia.' *Cerebrovascular Diseases*, 21(Suppl. 2) pp. 21-29.

Sacilotto, N., Chouliaras, K. M., Nikitenko, L. L., Lu, Y. W., Fritzsche, M., Wallace, M. D., Nornes, S., García-Moreno, F., Payne, S. and Bridges, E. (2016) 'MEF2 transcription factors are key regulators of sprouting angiogenesis.' *Genes & Development*, 30(20) pp. 2297-2309.

Sahlgren, C. M., Pallari, H. M., He, T., Chou, Y. H., Goldman, R. D. and Eriksson, J. E. (2006) 'A nestin scaffold links Cdk5/p35 signaling to oxidant-induced cell death.' *The EMBO Journal*, 25(20) pp. 4808-4819.

Sato, S., Xu, J., Okuyama, S., Martinez, L. B., Walsh, S. M., Jacobsen, M. T., Swan, R. J., Schlautman, J. D., Ciborowski, P. and Ikezu, T. (2008) 'Spatial learning impairment, enhanced CDK5/p35 activity, and downregulation of NMDA receptor expression in transgenic mice expressing tau-tubulin kinase 1.' *The Journal of Neuroscience*, 28(53) pp. 14511-14521.

Schaefer, A., Nethe, M. and Hordijk, P. (2012) 'Ubiquitin links to cytoskeletal dynamics, cell adhesion and migration.' *The Biochemical journal*, 442(1) p. 13.

Shah, K. and Lahiri, D. K. (2014) 'Cdk5 activity in the brain–multiple paths of regulation.' *J Cell Sci*, 127(11) pp. 2391-2400.

Sharp, F. R., Zhan, X. and Liu, D.-Z. (2013) 'Heat shock proteins in the brain: role of Hsp70, Hsp 27, and HO-1 (Hsp32) and their therapeutic potential.' *Translational stroke research*, 4(6) pp. 685-692.

Shea, T. B., Yabe, J. T., Ortiz, D., Pimenta, A., Loomis, P., Goldman, R. D., Amin, N. and Pant, H. C. (2004) 'Cdk5 regulates axonal transport and phosphorylation of neurofilaments in cultured neurons.' *Journal of Cell Science*, 117(6) pp. 933-941.

Shi, L.-L., Yang, W.-N., Chen, X.-L., Zhang, J.-S., Yang, P.-B., Hu, X.-D., Han, H., Qian, Y.-H. and Liu, Y. (2012) 'The protective effects of tanshinone IIA on neurotoxicity induced by β-amyloid protein through calpain and the p35/Cdk5 pathway in primary cortical neurons.' *Neurochemistry International*, 61(2) pp. 227-235.

Shi, Y. and Wardlaw, J. M. (2016) 'Update on cerebral small vessel disease: a dynamic whole-brain disease.' *Stroke and Vascular Neurology*, 1(3) pp. 83-92.

Shirley, R., Ord, E. N. and Work, L. M. (2014) 'Oxidative stress and the use of antioxidants in stroke.' *Antioxidants*, 3(3) pp. 472-501.

Shuaib, A. and Hussain, M. S. (2008) 'The past and future of neuroprotection in cerebral ischaemic stroke.' *European Neurology*, 59(1-2) pp. 4-14.

Shukla, V., Shakya, A. K., Perez-Pinzon, M. A. and Dave, K. R. (2017) 'Cerebral ischemic damage in diabetes: an inflammatory perspective.' *Journal of neuroinflammation*, 14(1) p. 21.

Sisalli, M. J., Annunziato, L. and Scorziello, A. (2015) 'Novel cellular mechanisms for neuroprotection in ischemic preconditioning: a view from inside organelles.' *Frontiers in Neurology*, 6 p. 115.

Slevin, M. and Krupinski, J. (2009) 'Cyclin-dependent kinase-5 targeting for ischaemic stroke.' *Current Opinion in Pharmacology*, 9(2) pp. 119-124.

Slevin, M., Kumar, P., Gaffney, J., Kumar, S. and Krupinski, J. (2006) 'Can angiogenesis be exploited to improve stroke outcome? Mechanisms and therapeutic potential.' *Clinical Science*, 111(3) pp. 171-183.

Slevin, M., Matou, S., Zeinolabediny, Y., Corpas, R., Weston, R., Liu, D., Boras, E., Di Napoli, M., Petcu, E., Sarroca, S., Popa-Wagner, A., Love, S., Font, M. A., Potempa, L. A., Al-Baradie, R., Sanfeliu, C., Revilla, S., Badimon, L. and Krupinski, J. (2015) 'Monomeric C-reactive protein--a key molecule driving development of Alzheimer's disease associated with brain ischaemia?' *Scientific Report*, 5 p. 13281.

Sokolow, S., Manto, M., Gailly, P., Molgó, J., Vandebrouck, C., Vanderwinden, J.-M., Herchuelz, A. and Schurmans, S. (2004) 'Impaired neuromuscular transmission and skeletal muscle fiber necrosis in mice lacking Na/Ca exchanger 3.' *The Journal of Clinical Investigation*, 113(2) pp. 265-273.

Spera, P. A., Ellison, J. A., Feuerstein, G. Z. and Barone, F. C. (1998) 'IL-10 reduces rat brain injury following focal stroke.' *Neuroscience Letters*, 251(3) pp. 189-192.

Sprick, M. R. and Walczak, H. (2004) 'The interplay between the Bcl-2 family and death receptor-mediated apoptosis.' *Biochimica et Biophysica Acta (BBA)-Molecular Cell Research*, 1644(2) pp. 125-132.

Sun, D.-B., Xu, M.-J., Chen, Q.-M. and Hu, H.-T. (2017) 'Significant elevation of serum caspase-3 levels in patients with intracerebral hemorrhage.' *Clinica Chimica Acta*,

Sun, K.-H., Lee, H.-g., Smith, M. A. and Shah, K. (2009) 'Direct and indirect roles of cyclin-dependent kinase 5 as an upstream regulator in the c-Jun NH2-terminal kinase cascade: relevance to neurotoxic insults in Alzheimer's disease.' *Molecular Biology of the Cell*, 20(21) pp. 4611-4619.

Sun, K.-H., de Pablo, Y., Vincent, F., Johnson, E. O., Chavers, A. K. and Shah, K. (2008) 'Novel genetic tools reveal Cdk5's major role in Golgi fragmentation in Alzheimer's disease.' *Molecular Biology of the Cell*, 19(7) pp. 3052-3069.

Sun, K. H., De Pablo, Y., Vincent, F. and Shah, K. (2008) 'Deregulated Cdk5 promotes oxidative stress and mitochondrial dysfunction.' *Journal of Neurochemistry*, 107(1) pp. 265-278.

Sun, L., Liu, Y., Lin, S., Shang, J., Liu, J., Li, J., Yuan, S. and Zhang, L. (2013) 'Early growth response gene-1 and hypoxia-inducible factor-1α affect tumor metastasis via regulation of tissue factor.' *Acta Oncologica*, 52(4) pp. 842-851.

Sundaram, J. R., Poore, C. P., Sulaimee, N. H. B., Pareek, T., Asad, A., Rajkumar, R., Cheong, W. F., Wenk, M. R., Dawe, G. S. and Chuang, K.-H. (2013) 'Specific inhibition of p25/Cdk5 activity by the Cdk5 inhibitory peptide reduces neurodegeneration in vivo.' *The Journal of Neuroscience*, 33(1) pp. 334-343.

Takacs, E., Nyilas, R., Szepesi, Z., Baracskay, P., Karlsen, B., Røsvold, T., Bjørkum, A. A., Czurko, A., Kovacs, Z. and Kekesi, A. K. (2010) 'Matrix metalloproteinase-9 activity increased by two different types of epileptic seizures that do not induce neuronal death: a possible role in homeostatic synaptic plasticity.' *Neurochemistry International*, 56(6) pp. 799-809.

Takeichi, M., Inuzuka, H., Shimamura, K., Matsunaga, M. and Nose, A. (1990) 'Cadherin-mediated cell-cell adhesion and neurogenesis.' *Neuroscience Research Supplements*, 13 pp. S92-S96.

Tanaka, T., Ohshima, T., Rajan, P., Amin, N. D., Cho, A., Sreenath, T., Pant, H. C., Brady, R. O. and Kulkarni, A. B. (2001) 'Neuronal cyclin-dependent kinase 5 activity is critical for survival.' *The Journal of Neuroscience*, 21(2) pp. 550-558.

Tarkowski, E., Rosengren, L., Blomstrand, C., Wikkelsö, C., Jensen, C., Ekholm, S. and Tarkowski, A. (1995) 'Early intrathecal production of interleukin-6 predicts the size of brain lesion in stroke.' *Stroke*, 26(8) pp. 1393-1398.

Tarricone, C., Dhavan, R., Peng, J., Areces, L. B., Tsai, L.-H. and Musacchio, A. (2001) 'Structure and regulation of the CDK5-p25 nck5a complex.' *Molecular Cell*, 8(3) pp. 657-669.

Tedgui, A. and Mallat, Z. (2001) 'Anti-inflammatory mechanisms in the vascular wall.' *Circulation Research*, 88(9) pp. 877-887.

Timsit, S. and Menn, B. (2012) 'Cyclin-Dependent Kinase Inhibition With Roscovitine: Neuroprotection in Acute Ischemic Stroke.' *Clinical Pharmacology & Therapeutics*, 91(2) pp. 327-332.

Toulmond, S., Tang, K., Bureau, Y., Ashdown, H., Degen, S., O'Donnell, R., Tam, J., Han, Y., Colucci, J. and Giroux, A. (2004) 'Neuroprotective effects of M826, a reversible caspase-3 inhibitor, in the rat malonate model of Huntington's disease.' *British Journal of Pharmacology*, 141(4) pp. 689-697.

Tripathi, B. K. and Zelenka, P. S. (2010) 'Cdk5: A regulator of epithelial cell adhesion and migration.' *Cell Adhesion & Migration*, 4(3) pp. 333-336.

Vila, N., Castillo, J., Dávalos, A. and Chamorro, Á. (2000) 'Proinflammatory cytokines and early neurological worsening in ischemic stroke.' *Stroke*, 31(10) pp. 2325-2329.

Walker, K. R. and Tesco, G. (2013) 'Molecular mechanisms of cognitive dysfunction following traumatic brain injury.' *Frontiers in aging neuroscience*, 5 p. 29.

Wang, H., Wu, M., Zhan, C., Ma, E., Yang, M., Yang, X. and Li, Y. (2012) 'Neurofilament proteins in axonal regeneration and neurodegenerative diseases.' *Neural regeneration research*, 7(8) p. 620.

Wang, H., Zhang, C., Lu, D., Shu, X., Zhu, L., Qi, R., So, K.-F., Lu, D. and Xu, Y. (2013) 'Oligomeric proanthocyanidin protects retinal ganglion cells against oxidative stress-induced apoptosis.' *Neural Regeneration Research*, 8(25) p. 2317.

Wang, W.-Y., Tan, M.-S., Yu, J.-T. and Tan, L. (2015) 'Role of pro-inflammatory cytokines released from microglia in Alzheimer's disease.' *Annals of translational medicine*, 3(10)

Wang, Y., Zhang, J., Han, M., Liu, B., Gao, Y., Ma, P., Zhang, S., Zheng, Q. and Song, X. (2016) 'SMND-309 promotes neuron survival through the activation of the PI3K/Akt/CREB-signalling pathway.' *Pharmaceutical Biology*, pp. 1-9.

Wei, F. Y., Tomizawa, K., Ohshima, T., Asada, A., Saito, T., Nguyen, C., Bibb, J. A., Ishiguro, K., Kulkarni, A. B. and Pant, H. C. (2005) 'Control of cyclin-dependent kinase 5 (Cdk5) activity by glutamatergic regulation of p35 stability.' *Journal of Neurochemistry*, 93(2) pp. 502-512.

Williams, J. E., Perry, L. and Watkins, C. (2010) *Acute stroke nursing.* Wiley Online Library.

Wright, M. F. (2013) *Mechanisms of Intracellular Calcium Homeostasis in the Developing and Mature Bovine Corpora Lutea An In-Depth Study to Promote Scientific Literacy through the Use of Primary Literature in an Introductory Biology Course.* West Virginia University.

Xie, Y., Avello, M., Schirle, M., McWhinnie, E., Feng, Y., Bric-Furlong, E., Wilson, C., Nathans, R., Zhang, J. and Kirschner, M. W. (2013) 'Deubiquitinase FAM/USP9X interacts with the E3 ubiquitin ligase SMURF1 protein and protects it from ligase

activity-dependent self-degradation.' *Journal of Biological Chemistry*, 288(5) pp. 2976-2985.

Yin, Y., She, H., Li, W., Yang, Q., Guo, S. and Mao, Z. (2012) 'Modulation of neuronal survival factor MEF2 by kinases in Parkinson's disease.' *Frontiers in Physiology*, 3 p. 171.

Zhang, H.-H., Zhang, X.-Q., Wang, W.-Y., Xue, Q.-S., Lu, H., Huang, J.-L., Gui, T. and Yu, B.-W. (2012) 'Increased synaptophysin is involved in inflammation-induced heat hyperalgesia mediated by cyclin-dependent kinase 5 in rats.' *PLoS One*, 7(10) p. e46666.

Zhang, L., Liu, W., Szumlinski, K. K. and Lew, J. (2012) 'p10, the N-terminal domain of p35, protects against CDK5/p25-induced neurotoxicity.' *Proceedings of the National Academy of Sciences*, 109(49) pp. 20041-20046.

Zhang, R. L., Zhang, Z. G. and Chopp, M. (2005) 'Neurogenesis in the adult ischemic brain: generation, migration, survival, and restorative therapy.' *The Neuroscientist*, 11(5) pp. 408-416.

Zhang, Y. (2016) 'Biotechnology and Medical Science: Proceedings of the 2016 International Conference on Biotechnology and Medical Science.' 16-17 April 2016,

Zhang, Y., She, F., Li, L., Chen, C., Xu, S., Luo, X., Li, M., He, M. and Yu, Z. (2013) 'p25/CDK5 is partially involved in neuronal injury induced by radiofrequency electromagnetic field exposure.' *International journal of radiation biology*, 89(11) pp. 976-984.

Zheng, Y. l., Li, B. S., Amin, N. D., Albers, W. and Pant, H. C. (2002) 'A peptide derived from cyclin-dependent kinase activator (p35) specifically inhibits Cdk5 activity and phosphorylation of tau protein in transfected cells.' *European Journal of Biochemistry*, 269(18) pp. 4427-4434.

Zheng, Y. L., Kesavapany, S., Gravell, M., Hamilton, R. S., Schubert, M., Amin, N., Albers, W., Grant, P. and Pant, H. C. (2005) 'A Cdk5 inhibitory peptide reduces tau hyperphosphorylation and apoptosis in neurons.' *The EMBO Journal*, 24(1) pp. 209-220.

Zhou, C., Yamaguchi, M., Kusaka, G., Schonholz, C., Nanda, A. and Zhang, J. H. (2004) 'Caspase inhibitors prevent endothelial apoptosis and cerebral vasospasm in dog model of experimental subarachnoid hemorrhage.' *Journal of Cerebral Blood Flow & Metabolism*, 24(4) pp. 419-431.

Zhou, R., Yang, Z., Tang, X., Tan, Y., Wu, X. and Liu, F. (2013) 'Propofol protects against focal cerebral ischemia via inhibition of microglia-mediated proinflammatory cytokines in a rat model of experimental stroke.' *PLoS One*, 8(12) p. e82729.